NOTICE

The quality of this microform is heavily dependent upon the quality of the original thesis submitted for microfilming. Every effort has been made to ensure the highest quality of reproduction possible.

If pages are missing, contact the university which granted the degree.

Some pages may have indistinct print especially if the original pages were typed with a poor typewriter ribbon or if the university sent us an inferior photocopy.

Reproduction in full or in part of this microform is governed by the Canadian Copyright Act, R.S.C. 1970, c. C-30, and subsequent amendments.

AVIS

La qualité de cette microforme dépend grandement de la qualité de la thèse soumise au microfilmage. Nous avons tout fait pour assurer une qualité supérieure de reproduction.

S'il manque des pages, veuillez communiquer avec l'université qui a conféré le grade.

La qualité d'impression de certaines pages peut laisser à désirer, surtout si les pages originales ont été dactylographiées à l'aide d'un ruban usé ou si l'université nous a fait parvenir une photocopie de qualité inférieure.

La reproduction, même partielle, de cette microforme est soumise à la Loi canadienne sur le droit d'auteur, SRC 1970, c. C-30, et ses amendements subséquents.

BEHAVIOR OF CONFINED CONCRETE UNDER ECCENTRIC LOADING

By
Amir H. Salamat

A Thesis Submitted

In Partial Fulfillment
of the Requirements for the Degree of
Master of Applied Sciences

Department of Civil Engineering
Faculty of Engineering
University of Ottawa

ISBN 0-315-68082-2

UNIVERSITÉ D'OTTAWA
UNIVERSITY OF OTTAWA

Abstract

Concrete in a triaxial stress condition exhibits different stress-strain characteristics than that of concrete under uniaxial stress. Lateral pressure, either in the form of externally applied active pressure or internally generated passive pressure results in a triaxial state of stress when combined with axial stress.

Core concrete in a reinforced concrete column is in a triaxial state of stress when passive lateral pressure is generated by the reinforcement cage. Transverse reinforcement, in the form of closely spaced spirals or ties provides lateral confinement pressure as concrete expands due to Poisson's effect. Previous research has indicated that spacing, volumetric ratio and arrangement of lateral steel play dominant roles on concrete confinement. However, most of the previous research was conducted on column tests under concentric compression. Currently there is little information available on the effect of strain gradient on concrete confinement.

The objective of the research program reported in this thesis was to establish characteristics of confined concrete under a strain gradient. Both experimental and analytical research were conducted. Twelve large scale columns were tested under monotonically increasing eccentric compression.

The level of eccentricity was the main variable. Columns with different tie spacings and reinforcement arrangements were subjected to different levels of eccentric loading. The results indicated that the eccentricity of loading did not affect the behavior of confined concrete significantly.

The experimental results were compared against analytical results based on three previously proposed models for confined concrete. The analytical results confirmed the experimental findings. Models developed for concentric loading produced good estimates of column response under eccentric loading.

Acknowledgements

I wish to express my appreciation to Dr. M. Saatcioglu for his guidance, advice and financial support throughout this research program.

I also wish to thank the technical staff of the machine shop and Structural Laboratory of Civil Engineering Department and Mr. Jaber Alsiwat for their assistance during the experimental part of this project.

Dedication

To my wife for her patience and moral support who became sad when I was sad and enjoyed life when I was happy.

To my parents who encouraged me and gave me their best support from the bottom of their heart.

To my sister and brother and my beautiful niece whose thoughts drove me through with hope.

Contents

List of Figures

List of Tables

Notation

A_b	=	bound concrete area under compression.
A_c	=	concrete area under compression.
A_{si}, A_s''	=	area of lateral steel tie.
B	=	core size measured center to center of tie perimeter.
b_c	=	width of concrete core.
c	=	the distance from the extreme concrete compression fiber to the neutral axis.
C_c	=	concrete contribution to the load carrying capacity of the section.
C	=	the distance between laterally supported longitudinal bars.
d	=	the distance from the center of tension steel to the extreme concrete compression fiber.
E,e	=	eccentricity of applied load.
f, f_c	=	concrete stress.
f'_{cc}, f_{cc}	=	confined concrete strength.
f'_{ccexp}	=	experimentally obtained confined concrete stress.
$f'_{ccanaly}$	=	analytically obtained confined concrete stress.
f_{cp}, f_p, f'_{co}	=	strength of concrete in plain specimen.
f'_c, u_{cyl}	=	ultimate strength of plain concrete obtained from standard cylinder test. and size.
f_l	=	average pressure on core concrete.
f_{le}	=	effective pressure on core concrete.
f_y	=	yield strength of longitudinal steel.
f_{yi} ,f_{yh}, f'_s	=	yield strength of lateral tie.
K	=	ratio of strength of confined concrete to the strength of plain concrete.
k_1	=	coefficient that relates lateral pressure to increase in concrete strength.
k_2	=	reduction factor to change average pressure to effective pressure in concrete.

K_s	=	ratio of strength of confined concrete to the strength of plain concrete in the specimens of similar size and shape.
n	=	number of laterally supported longitudinal bars.
q''	=	effectiveness factor of transverse reinforcement in concrete confinement.
s, S	=	tie spacing.
s_l	=	maximum center to center distance between longitudinal bars supported by the corner of a tie or hoop.
s_o	=	longitudinal spacing at which lateral steel is not effective in concrete confinement.
P	=	experimentally applied load on column section in kN.
P_{occ}	=	theoritical load carrying capacity of core concrete in kN.
Z	=	slope of descending branch of the confined concrete curve.
Z_{exp}	=	experimentally calculated slope of descending branch of the confined concrete curve.
Z_{analy}	=	analytically calculated slope of descending branch of the confined concrete curve.
α, γ	=	rectangular stress block parameters for confined concrete.
ϵ, ϵ_c	=	average longitudinal strain in concrete.
ϵ_{cc}, ϵ_{s1}	=	minimum average longitudinal strain corresponding to the maximum stress in concrete.
ϵ_{cs}, ϵ_{s2}, ϵ_1	=	maximum average longitudinal strain corresponding to the maximum stress in concrete.
ϵ_{oo}, ϵ_{01}	=	strain corresponding to the maximum stress in plain concrete.
ϵ_{cf}	=	average longitudinal strain of confined concrete corresponding to 80% of peak stress on the falling branch of the curve.
ϵ_{o85}	=	average longitudinal strain of plain concrete corresponding to 85% of peak stress on the falling branch of the curve.
ϵ_{s85}, ϵ_{85}	=	average longitudinal strain of confined concrete corresponding to 85% of peak stress on the falling branch of the curve.

ρ_{gross} = ratio of area of longitudinal steel to gross area of column.

ρ_s = ratio of volume of tie steel to volume of concrete core measured center to center of outer tie.

ρ = ratio of the area of lateral reinforcement to the area bounded by tie spacing and core dimension b_c.

Chapter 1

Introduction

1.1 General

Structural damage observed during recent earthquakes has attracted the attention of structural engineers and researchers to the behavior of reinforced concrete columns under ground motions.

Earthquake resistant structures are expected to have adequate ductility and energy absorption capacity to dissipate the energy induced by earthquakes. A frame structure is considered to have adequate ductility if it can sustain large inelastic deformations without a significant loss of strength. This can be achieved by promoting the formation of plastic hinges in flexural rather than compression members. Therefore columns in a building structure are designed to have load carrying capacities higher than those of the adjoining beams. However, the experience with recent earthquakes has shown that following this design procedure does not always prevent the formation of hinges in compression members, especially in the lower storey columns.

The difficulty associated with preventing plastic hinges in columns makes it necessary to come up with design and detailing procedures that will improve the behavior of columns in the inelastic range. Column ductility can best be achieved by confining the core concrete by means of closely spaced circular or rectangular hoops, cross ties and spirals. While the confinement steel is a requirement in the current building codes [30,31] for earthquake resistant construction, many aspects of the confinement mechanism are not well understood, and the code requirements are often questioned. Until recently, researchers concentrated on the spacing and volumetric ratio of lateral steel as the governing parameters of confinement. Research during the last decade has shown that the arrangement of lateral reinforcement, which includes the distribution of longitudinal reinforcement, also plays a major role on concrete confinement. Furthermore, the level of axial force at which the inelastic deformation cycles take place, and the resultant eccentricity of loading has been shown to affect the confinement action. While these factors may have significant effects on concrete confinement, they are not properly addressed in the building codes. There appears to be lack of experimental data and rational analytical tools to explain the mechanism of concrete confinement under eccentric loading. Also the interaction of eccentricity as a confinement parameter with other confinement parameters needs to be studied. The research reported in this thesis is directed towards establishing the importance of eccentricity of applied load on column confinement.

1.2 Research Needs

It has been established by previous research [15,21,22,23,25] that concrete confinement by reinforcement improves both the ductility and strength of concrete under concentric compression. Concrete has a tendency to expand

laterally under axial compression due to the Poisson's effect. The presence of confinement reinforcement provides external pressure on the concrete, which counteracts the lateral expansion and associated internal cracking. This permits the concrete to develop higher stresses and strains. The ability of concrete to sustain higher strains improves deformability of the member, which in turn improves its seismic resistance.

Most of the previous studies on concrete confinement were based on uniform distribution of strain across the section. This implies that in the case of columns, the axial forces on columns were assumed to be concentric. However columns are subjected to combined axial force and bending under gravity and/or earthquake loading. Therefore the column section is under a strain gradient rather than a uniform strain. During a strong earthquake the eccentric loading may well be in the inelastic range, exceeding the material strength levels generally used for ordinary design. Although some efforts have been made recently [19,25] to take the effect of strain gradient into consideration within the inelastic range, not enough experimental data is currently available, and the research findings are conflicting in many ways. While Sargin et al. [20], and Sheikh and Yeh [25] claim that strain gradient increases ductility of confined concrete, others [10,12,21] use stress-strain relationships developed for concentric loading in predicting member response in flexure, implying the effect is negligible. Therefore there is a need to conduct experimental and analytical research to establish the importance of strain gradient on the stress-strain characteristics of confined concrete.

1.3 Objective and Scope

The primary objective of this investigation is to establish the importance of strain gradient on column confinement experimentally. The experimental research consists of large scale reinforced concrete columns with different tie spacings and reinforcement arrangements, tested under different levels of eccentricity. The objective also includes verification of previously proposed confinement models analytically, in terms of their applicability to columns under eccentric loading. The analytical models selected for comparison include two models developed on the basis of concentrically tested specimens and a model modified for eccentricity effects.

The following outlines the scope of the research program:

- Review of the previous research,
- Design and construction of twelve large scale columns,
- Instrumentation and testing of columns under eccentrically increasing monotonic loading,
- Evaluation of test data and presentation of test results,
- Preparation of computer software to compute internal forces from recorded test data,
- Statistical analysis of test data and comparisons of experimentally obtained concrete stress-strain relationships with those obtained from an analytical model,
- Analytical predictions of moment-curvature relationships for each column specimen using three previously proposed confinement models, and comparison with respective test data,

- Presentation and discussion of results.

1.4 Previous Research

Most of the previous research on concrete confinement was conducted on concentrically loaded specimens. The pioneering work on concrete confinement was done by *Richart et al.* in 1928 [16]. The work involved a large number of concrete cylinders tested under axial compression, while also subjecting them to different levels of hydrostatic fluid pressure. Their results produced a relationship between the lateral pressure and axial strength, which is still used in the current building codes. The research conducted by Richart et al. was later extended to cover cylinders confined by spirals without any longitudinal reinforcement. It was reported that there was a striking similarity between the active lateral pressure provided by hydrostatic pressure and the passive pressure provided by hoop steel. Their research was limited to circular concrete sections.

Confinement of concrete by rectilinear reinforcement was investigated by *Chan* [2] in 1955, and *Roy and Sozen* [17] in 1963. The main variables considered were the volumetric ratio of lateral steel, and tie spacing. Their conclusion was that the ductility of concrete was improved due to confinement, but the strength was not. Based on these research findings and others reported by *Bertero et al.* [1] and *Soliman and Yu* [27], *Kent and Park* [8] proposed an analytical model in 1971 which did not recognize the increase in concrete strength caused by confinement.

The effect of longitudinal reinforcement and the resultant tie arrangement on concrete confinement was first discussed in 1975 by *Park and Paulay* [12]. *Vallenas, Bertero and Popov* [29] proposed a new confinement model in

1977 which included the volumetric ratio of longitudinal reinforcement as a parameter. The strength enhancement as well as ductility improvement due to confinement were incorporated in their model. However, it was *Sheikh and Uzumeri* [23] who demonstrated the improvements obtained by the use of proper tie arrangement experimentally. They also proposed a model which has been used extensively. Recognizing the increase in strength of confined concrete, *Scott, Park and Priestley* [21] modified the Kent and Park model in 1982 on the basis of test data. A comparative study of some of the confinement models was done in 1982 by *Sheikh* [24]. Strong and weak points of the previous models were discussed in this paper.

More recently, *Fafitis and Shah* [5] in 1985 and *Mander, Priestley and Park* in 1988 conducted experimental research on concentrically loaded specimens and proposed analytical models. The model proposed by Fafitis and Shah was derived for circular columns and the application was extended into square concrete sections. The specimens tested by the researchers consisted of small scale circular columns confined by spirals, without any longitudinal reinforcement. The model developed by Mander et al. utilized the concept of effectively confined concrete put forward by Sheikh and Uzumeri and theoretically derived pressure charts derived by previous researchers. However the model is general in nature and is intended for prediction of confined concrete behavior under slow and fast rates of loading, covering circular, square and rectangular column geometry.

As part of the same overall research program as the current investigation , *Razvi and Saatcioglu* [15] recently tested 36 small scale columns reinforced with welded wire fabric (WWF) and/or re-bars. They reported the improvements obtained in concrete confinement by using combinations of WWF and conventional reinforcement as confinement steel. *Saatcioglu and Razvi* [19] later developed an analytical model on the basis of concentrically tested columns.

Although much information was generated for confined concrete under concentric loading, little work was done on concrete confinement under eccentric loading. The study of eccentric application of load dates back to 1955 when *Hognestad, Hanson and McHenry* [6] tested plain concrete specimens under eccentric loading. It was their finding that the stress-strain relationship for a section fully under compression, caused by flexure, had a striking similarity with that obtained under concentric compression.

It was not before 1960's that the controversy over the extent and nature of the effect of applied load eccentricity on the confinement characteristics of reinforced concrete started. There have been researchers who suggested that the existing variation between concentric and eccentric application of load is due only to the strain rate rather than the strain gradient [3,18]. On the other hand, there were other researchers who reported that eccentric application of load would increase the strain corresponding to the peak stress of confined concrete stress-strain relationship [3,20]. Many researchers showed that there was no strength enhancement, but a definite improvement in ductility characteristics of confined concrete due to the eccentric application of load [7,21,25,27].

Among the researchers who reported improvement in ductility were *Soliman and Yu* [27] in 1967. They tested 16 specimens under eccentric loading. In order to keep the neutral axis near the tension side, one major load was applied to the specimen and a minor load was applied through two steel brackets fixed at the enlarged ends of the specimens. The spacing, size and type of transverse reinforcement and the shape of concrete cross-section were the main variables studied. The cross-section dimension of the specimens varied between 75 by 150 mm and 125 by 150 mm. The eccentricity of major load was 25 mm($\frac{e}{h} = 0.33$ to $\frac{e}{h} = 0.2$). The test procedure allowed them to obtain data up to strain values ranging from 0.012 for poorly confined specimens to 0.02 for well confined ones. The curves obtained during

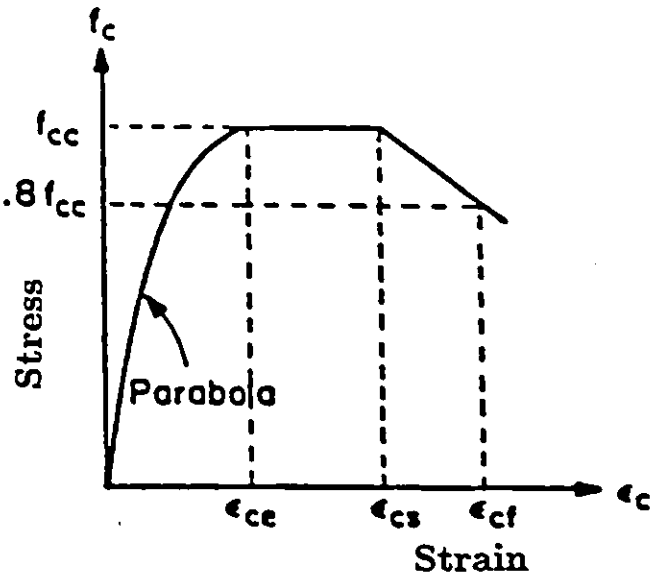

Figure 1.1: Analytical Model Proposed by Soliman and Yu [27]

this test program were examined and a model, shown in Figure 1.1, for stress-strain relationship of confined concrete was proposed. The model consisted of an ascending part, followed by a flat portion and a descending branch up to 20% of maximum stress. The equations which describe the relationship are given below:

$$f'_c = 0.9u_{cyl}(1 + 0.05)q'' \tag{1.1}$$

$$e_{cc} = 0.55f'_c 10^{-6} \tag{1.2}$$

$$e_{cs} = 0.0025(1 + q'') \tag{1.3}$$

$$e_{cf} = 0.0045(1 + 0.85q'') \tag{1.4}$$

In which:

$$q'' = (1.4\frac{A_b}{A_c} - 0.45)\frac{A''_s(s_o - s)}{A''_s S + 0.0028BS^2} \tag{1.5}$$

It is to be noted that Soliman and Yu did not consider any improvement in the strength of confined concrete relative to plain concrete. However the ductility effect was recognized.

In 1982, *Scott, Park and Priestley* [21] tested twenty five reinforced concrete columns with 450 mm square cross-section and different arrangements of longitudinal steel. The specimens were tested under concentric and eccentric loading at different strain rates. Higher strain rate was used to simulate the seismic conditions. The tests were conducted at controlled longitudinal strain rate of either 0.0000033/sec , 0.00167/sec, or 0.0167/sec up to a maximum strain of 0.04. The eccentricities considered were 33 and 49 mm. While the eccentricity was kept constant during the test, the strain was zero at one end of the core concrete when the compressive strain at the opposite face was about 0.01. The examination of test results for concentric loading showed strength enhancement of 20% at low strain rate and 70% at high strain rate. For eccentric loading it was concluded that there was no evidence of further strength enhancement due to eccentricity. However, a very high compresive strain was measured at first hoop fracture and a reduction in strength decay was observed. Higher flexural capacity and ductility was also observed under eccentric loading, as compared to columns with unconfined concrete. The researchers did not propose an analytical stress-strain relationship for core concrete under eccentric loading.

Sheikh and Yeh [25] in 1986 proposed a model for eccentric loading. They used data reported by Sargin [32] and extended the flat portion of the model previously proposed by Sheikh and Uzumeri [23] to introduce the additional ductility observed under eccentric loading. The shape of the model, shown in Fig. 1.2 is the same as that proposed by Soliman and Yu [27] with the exception of strength enhancement which was not considered by Soliman and Yu. The model consisted of an ascending part, up to the minimum strain corresponding to the peak stress and a flat portion up to the maximum strain corresponding to the peak stress. It is the latter strain quantity that reflect the effect of eccentricity. The details of the model are given in Chapter 4 where it is used for analytical predictions of column response.

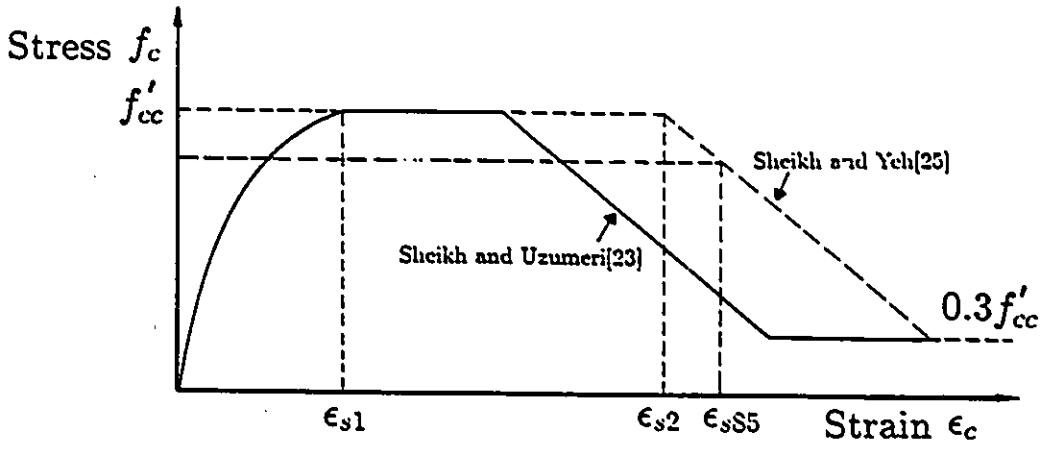

Figure 1.2: Analytical Model Proposed by Sheikh and Yeh [25]

Ozcebe and Saatcioglu [10] in 1987 reported test results of an experimental investigation on column confinement. They tested four full-size columns under constant axial load and reversed cyclic horizontal loading. Hysteretic force-deformation relationships for the specimens were produced and compared. The variables studied were configuration and spacing of lateral steel. The results show that the response of columns to cyclic loading improves very significantly with the use of proper confinement configuration. Columns with well distributed longitudinal reinforcement and small tie spacing showed little strength and stiffness degradation when subjected to lateral load reversals. They concluded that the confined concrete model proposed by Sheikh and Uzumeri produces reasonably good predictions of column ductility when columns are well confined.

In 1987 *Sheikh, Yeh and Menzies* [26] reported an experimental program that involved columns tested under eccentric loading. The tests consisted of fifteen and sixteen specimens tested under concentric and eccentric compression, respectively. Specimens in set one which were tested under concentric compression had cross-sectional dimensions of 203 mm square and

178 by 254 mm.The specimens were 813 mm long. The specimens in set two were 305 mm square and 2740 mm long. They were tested under a constant axial load and a variable lateral load to achieve strain gradient. The amount of lateral steel, tie spacing, precracking and cyclic loading were the main variables for columns tested under concentric loading. The distribution of laterally supported and unsupported longitudinal bars, overlapping hoops and cross ties, amount of lateral steel, tie spacing and level of axial load were investigated in columns tested under eccentric loading. The emphasis was mostly on the level of axial load. The results which were presented in the form of load-deflection and moment-curvature relationships show the effects of different variables. In the case of eccentric application of load, they concluded that decrease in axial load and tie spacing, and increase in the amount of lateral ties resulted in improvement of ductility.

Chapter 2

Experimental Program

2.1 General

Twelve large scale column specimens were designed, constructed and tested in the experimental program. This chapter provides details of the preparation and testing of the column specimens.

The main parameter in the experimental program was the eccentricity of loading. Two levels of end eccentricity were selected. The effect of eccentricity was investigated on poorly confined and well confined columns. Therefore, two additional confinement parameters; tie spacing and reinforcement arrangement were also considered as test variables. The following sections present the properties of each specimen and the test variables considered.

2.2 Test Specimens

The geometry of a typical test specimen is illustrated in Figure 2.1. The specimens have square cross-sections with either 8 or 12 bar arrangements. Deformed reinforcing bars of 11.3 mm diameter were used as longitudinal reinforcement. Plain bars of 6.35 mm diameter were used as hoop reinforcement. Three different reinforcing arrangements were used as illustrated in Figure 2.2. The first arrangement consisted of perimeter hoops. The second and third arrangements included inside hoops in addition to the perimeter ties. Approximately the same volumetric ratio of lateral steel was used to eliminate this parameter as a variable. This necessitated the use of double perimeter hoops in the first arrangement. Figure 2.3 illustrates typical reinforcing cages.

The columns were cast horizontally in the Structural Laboratory of the University of Ottawa. The bottom side of columns during casting was subjected to compression during loading. Two batches of concrete were used to cast all the columns. One batch was used to cast a set of six columns. The specimens were cured by wet burlap and plastic sheet covers. The curing continued until the standard cylinder tests indicated that the required strength was attained.

The specimens were labeled based on the sequence of testing and the eccentricity of applied loading. As an example, column label C2-1 indicated second column tested under the first level of eccentricity. Three different arrangements of reinforcement, two different tie spacings and two eccentricities were considered in preparing twelve columns. Table 2.1 provides a summary of specimen properties and test variables.

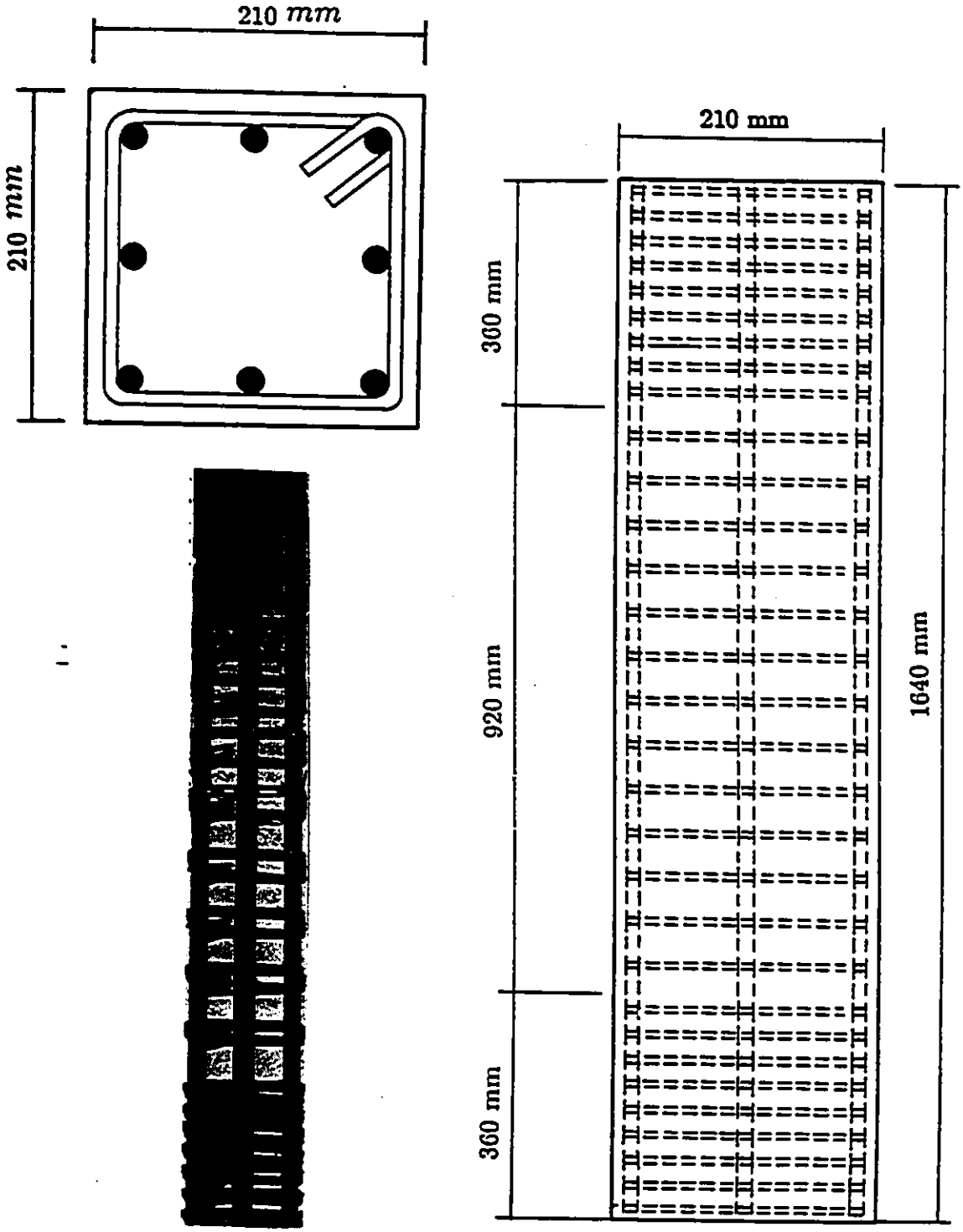

Figure 2.1: Overal Geometry of a Typical Column

Table 2.1: Properties of Test Specimens

Column designation	f'_c (Mpa)	Longitudinal Reinforcement		Lateral Reinforcement			$e(mm)$	Configuration
		$\rho_{gross}(\%)$	f_y(Mpa)	$\rho_s(\%)$	f_{yh}(Mpa)	$s(mm)$		
C1-1	34.26	1.814	517	2.977	410	$d/4$	60	1
C2-1	34.56	1.814	517	2.541	410	$d/4$	60	2
C3-1	33.98	2.721	517	2.687	410	$d/4$	60	3
C4-2	34.96	1.814	517	2.977	410	$d/4$	75	1
C5-2	34.96	1.814	517	2.541	410	$d/4$	75	2
C6-2	34.39	2.721	517	2.687	410	$d/4$	75	3
C7-1	25.20	1.814	517	1.489	410	$d/2$	60	1
C8-1	25.26	1.814	517	1.271	410	$d/2$	60	2
C9-1	26.09	2.721	517	1.344	410	$d/2$	60	3
C10-2	27.44	1.814	517	1.489	410	$d/2$	75	1
C11-2	26.36	1.814	517	1.271	410	$d/2$	75	2
C12-2	25.98	2.721	517	1.344	410	$d/2$	75	3

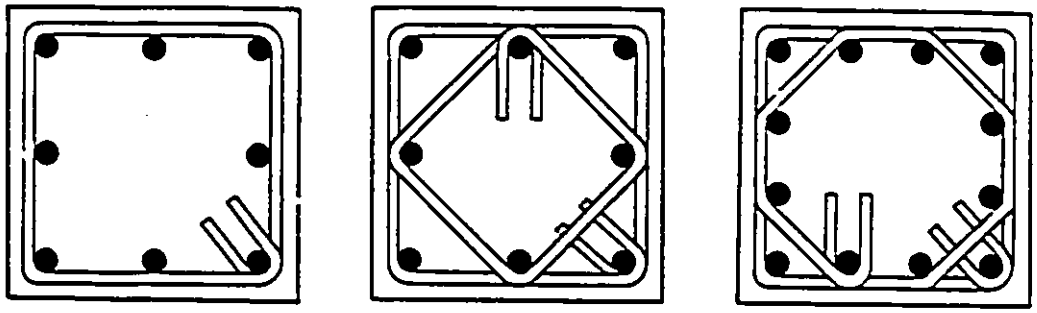

Figure 2.2: Arrangement of Logitudinal Steel and Resulting Configurations

2.3 Material Properties

2.3.1 Concrete

Ready mix concrete was used in two batches to cast the specimens. The maximum size of aggregate used was 10 mm. The slump was 100 mm and 120 mm for Batch 1 and Batch 2 respectively.

Standard cylinders were cast to determine the plain concrete properties. A total of 70 cylinders were cast from the first batch and 60 from the second. They were covered with wet burlap and plastic sheets and cured under identical environmental conditions as the specimens themselves for two days. Afterwards the concrete strength was monitored by testing the cylinders. Concrete strength measured on the day of testing was about 34 MPa and 25.5 MPa for Set 1 and 2 columns, cast from Batch 1 and Batch 2 respectively.

The stress-strain relationship of concrete was determined experimentally by testing standard cylinders. A gauge length of 300 mm was used for strain

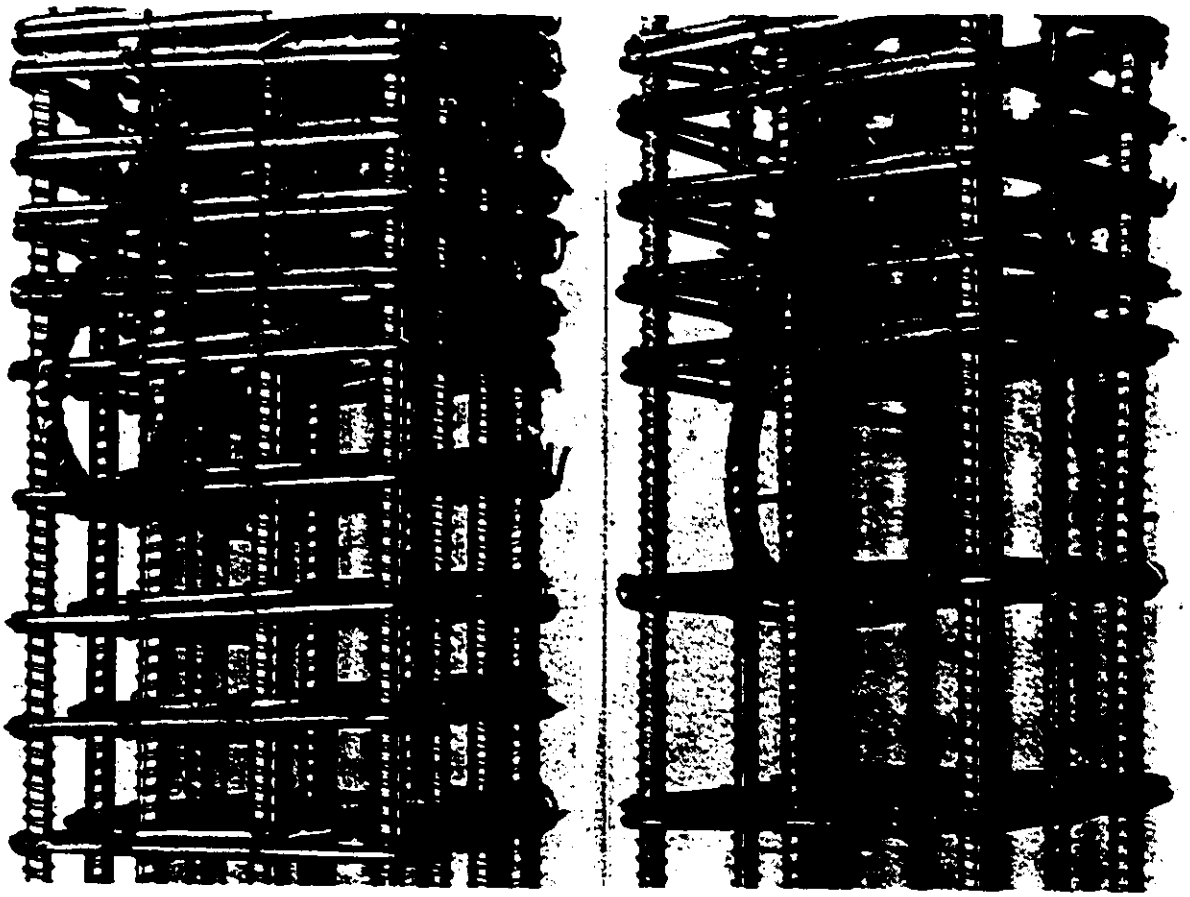

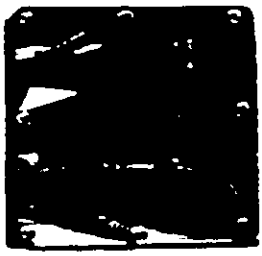

Configuration 1

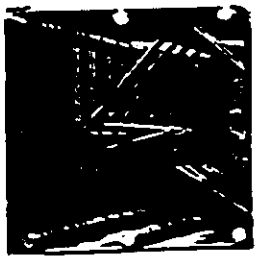

Configuration 2

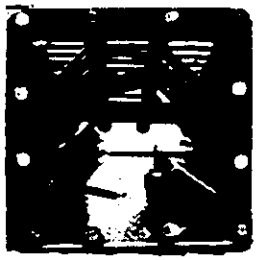

Configuration 3

Figure 2.3: Typical Reinforcement Cages

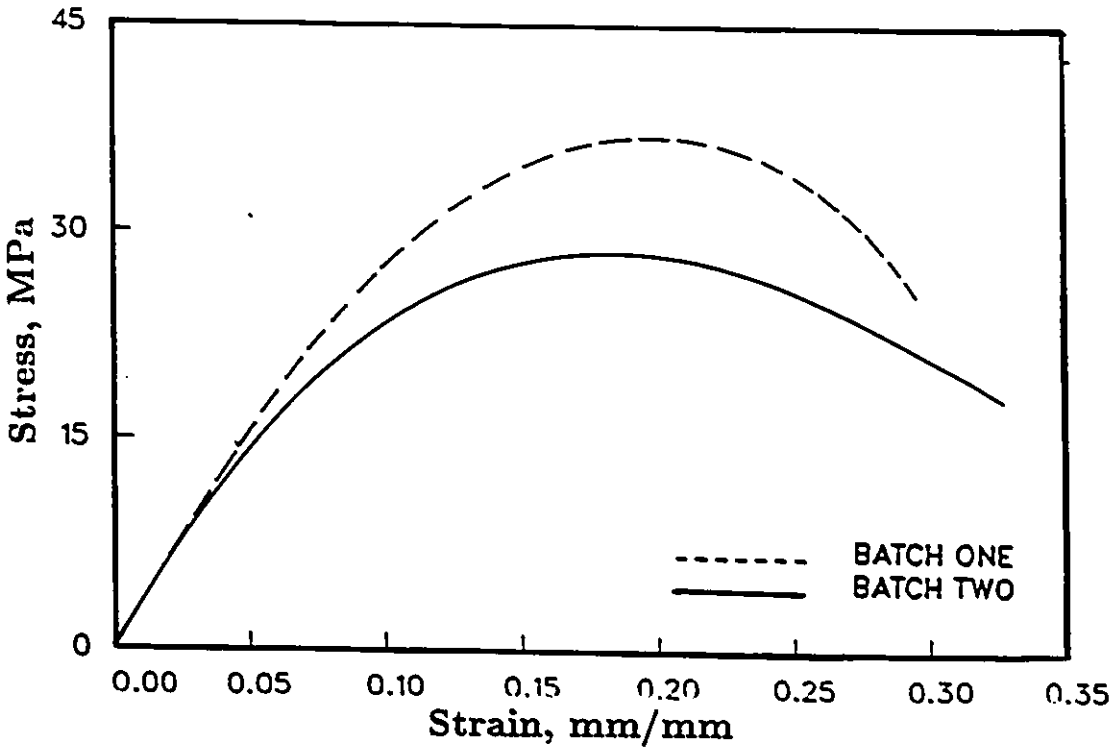

Figure 2.4: Strain-stress Relationship of Plain Concrete

measurement. Figure 2.4 shows the stress-strain relationship of concrete from each batch.

2.3.2 Steel

The longitudinal reinforcement consisted of No.10 deformed bars. They were from the same batch of shipment, and were ordered to be Grade 400 steel. Sample coupons, selected randomly were tested, and the average stress-strain relationship was determined.

Plain bars of 6.35 diameter were used for lateral reinforcement. These bars were from a different batch of shipment. The same procedure was followed, and the stress-strain relationship was determined by means of coupon tests. Figure 2.5 illustrates the stress-strain relationships for both the longitudinal

and hoop steel.

2.4 Test Set Up

A Tinus Olson Universal Testing Machine with 1500 kN load capacity was used for testing the columns. Figure 2.6 illustrates the overall test set-up. The specimens were first externally confined at the ends by means of steel brackets, specially manufactured for this purpose. This would prevent premature failure of the column at the end regions. The brackets were made of steel angles and were bolted together as shown in Figure 2.7.

Steel end plates were used to provide the required level of eccentricity. The eccentricity was changed by means of adjustable V-blocks. The end plates were bolted to the specimen ends by casting threaded rods in the concrete. A load cell was used to record the applied load. This would give a back-up reading of the load, in addition to that obtained from the test machine manually. The load cell was hooked up to the data acquisition system and hence facilitated fast data recording, especially necessary in the descending branch of the curve.

2.5 Instrumentation

Instrumentation of column specimens formed an important and crucial aspect of the experimental program. Although the mid-span deflection of columns could easily be obtained, this would not give the necessary information to have an insight on the behavior of the critical section. Therefore, Linear Variable Differential Transducers (LVDTs) were used to mea-

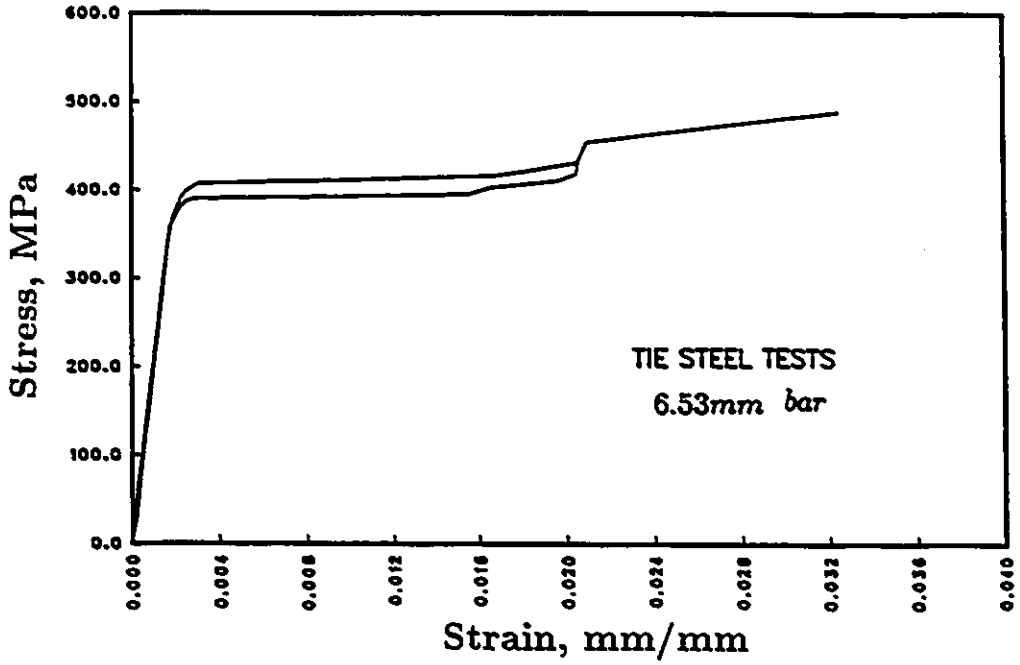

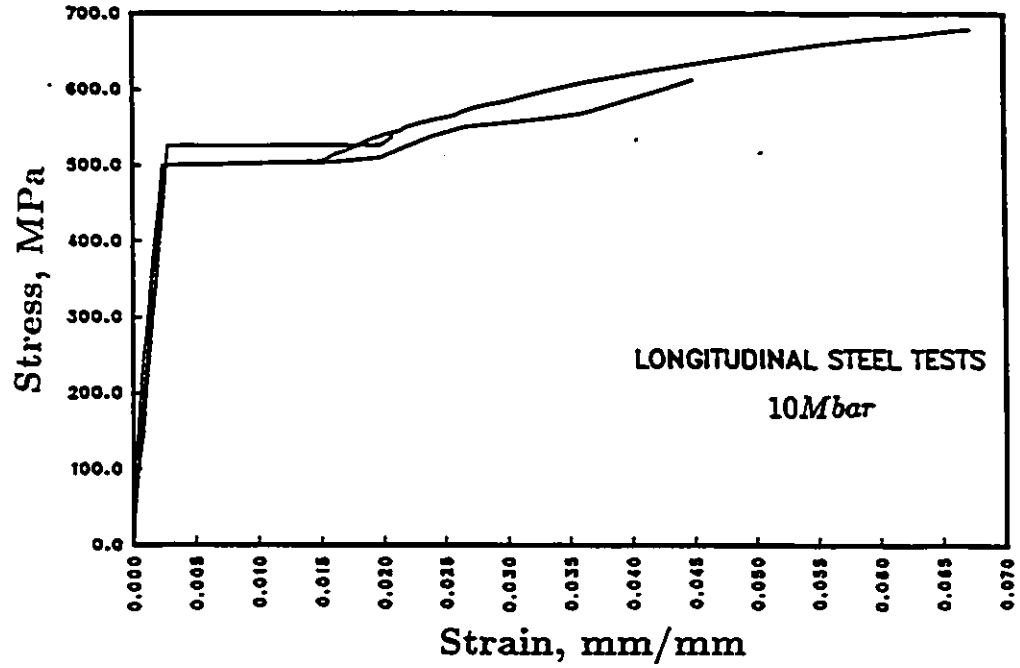

Figure 2.5: Stress-Strain Relationships of Steel Bars

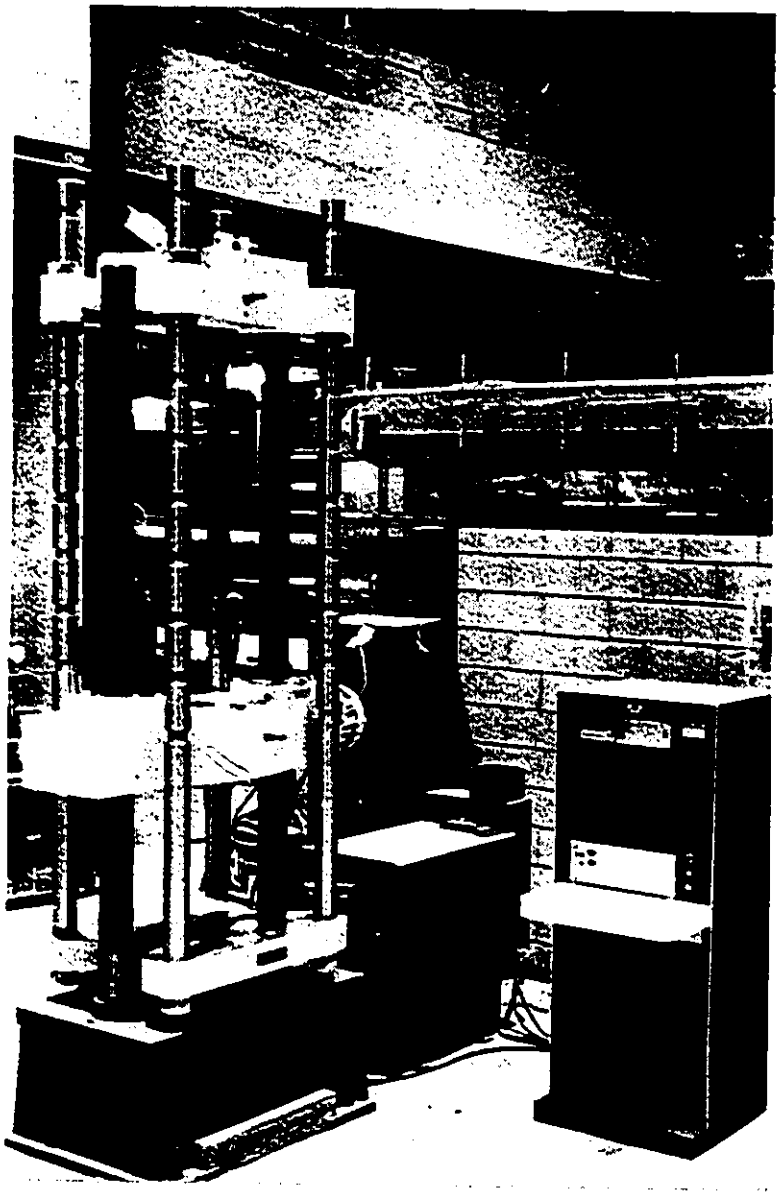

Figure 2.6: Test Setup

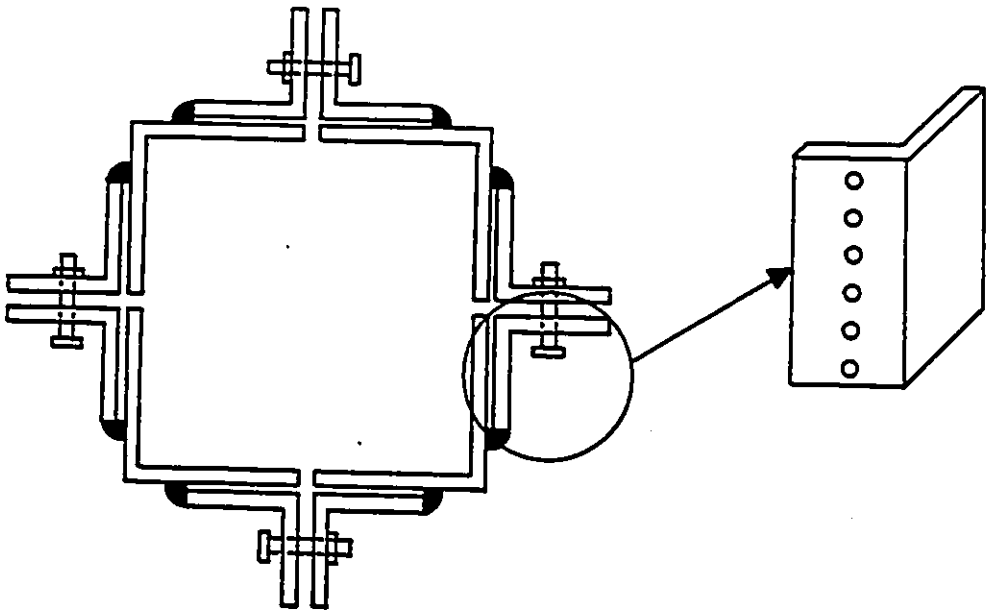

Figure 2.7: External End Confinement for the Specimens

sure axial deformations in tension and compression, in the critical region. The LVDTs were mounted on two threaded rods 300 mm apart , cast in the column core. This was done to eliminate the possibility of losing the LVDTs upon spalling of concrete under compression. The readings from these LVDTs would give strain profiles of the critical section at each load stage. In addition, the lateral mid-span deflection was recorded by means of another LVDT, supported by a light steel frame, bolted to the strong floor. Figure 2.8 depicts the locations of the LVDTs used.

Strain in the ties and longitudinal reinforcement were measured using electrical strain gauges. The strain gauge on lateral ties would indicate hoop tension under lateral confinement pressure, and the gauges on longitudinal reinforcement would provide additional data to establish the strain profiles more accurately. A total of eight strain gauges were used in each column. Four of the strain gauges were mounted on the longitudinal bars and the remaining four on the mid-height ties. The strain gauge locations can be

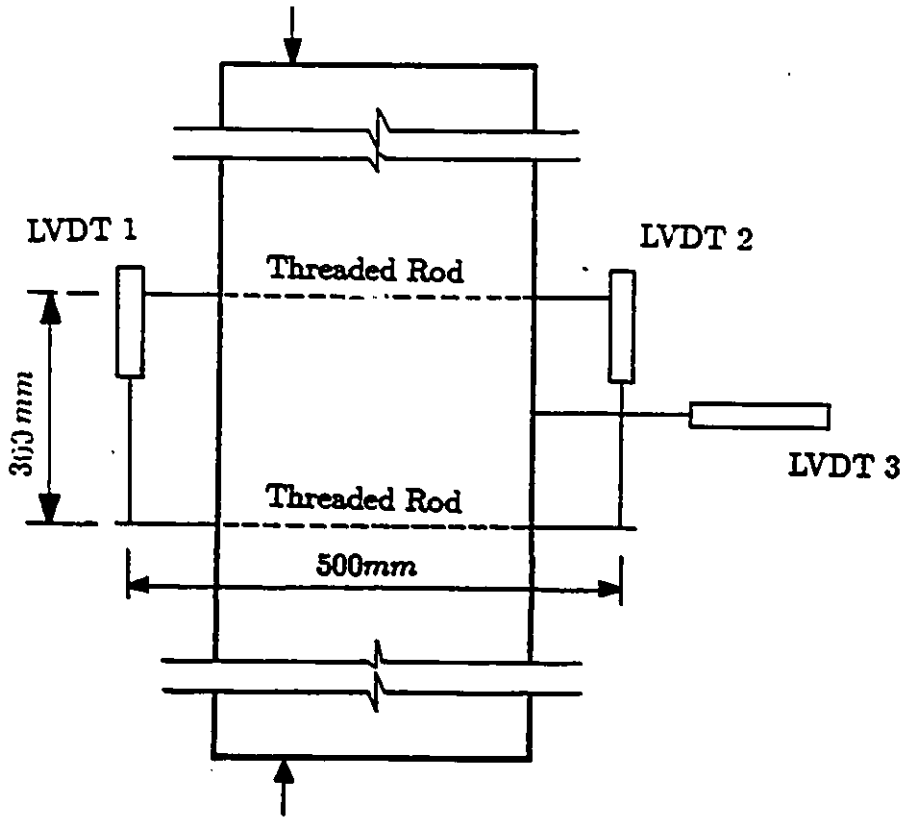

Figure 2.8: LVDT Positioning on the Specimens

seen in Figure 2.9.

All the test data were recorded by an HP Data Acquisition System. The Data Acquisition system consisted of an HP 9845B Desktop Computer, HP 3497A Control Unit, a power supply and a voltmeter. All the data was recorded on a magnetic tape, and was later processed through the Mainframe computer system.

2.6 Test Procedure

The specimens were first prepared for testing by placing the end brackets and the end plates. They were carefully positioned in the machine for proper level of eccentricity. The load was applied through the universal

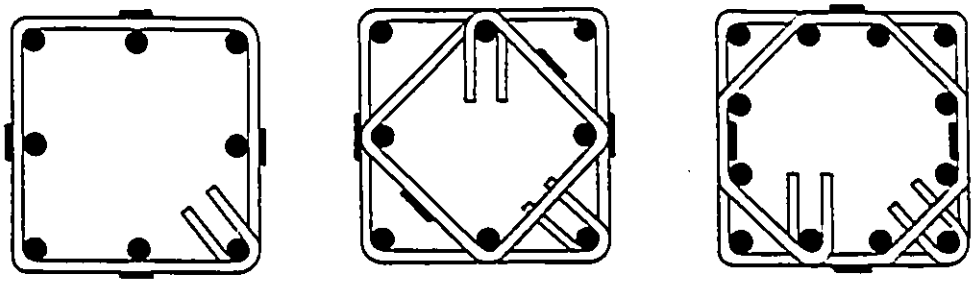

Configuration 1 Configuration 2 Configuration 3

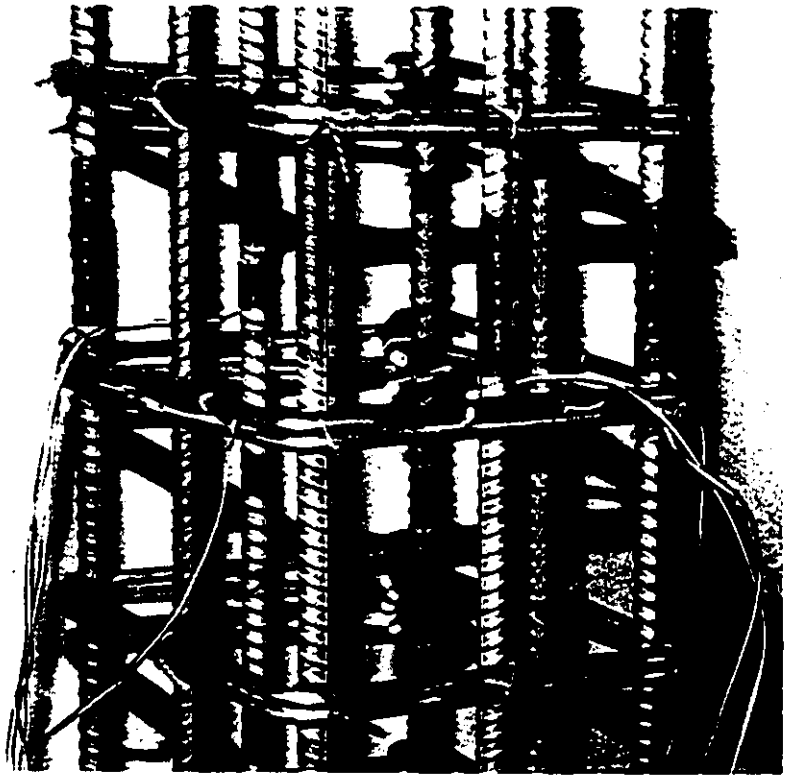

Figure 2.9: Strain Gauges Positions on Ties and Longitudinal Bars

Figure 2.10: A Typical Column Before and After Testing

testing machine. Load and deformation measurements were taken in small increments as the applied load was increased. The strain gauge readings were monitored during the testing. The overall behavior of specimens were manually recorded and the crack patterns were observed. As the peak load was approached, the application of load was slowed down. The readings were taken at a faster rate as deformations were increasing faster under approximately constant or reducing load. An attempt was made to record as many points as possible beyond the peak load. Testing continued until a significant drop in load resistance was recorded. Figure 2.10 illustrates a typical test specimen before and after testing.

Chapter 3

Observed Behavior and Test Results

3.1 General

The behavior of column specimens during testing , and the results of experimental program are discussed in this chapter. Test data is presented in the form of moment-midheight deflection relationship. Additional data is presented in the form of critical section strain profiles. The strain gauge data is used , where available, to confirm the strain profiles obtained from the LVDT readings. Core force-core strain relationships as recorded by the data acquisition system are presented in Appendix A.

The chapter also includes comparisons of column behavior as affected by test variables. A summary of test variables is given in Table 3.1.

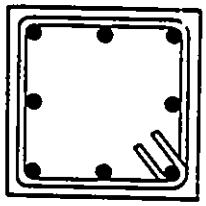

Configuration 1

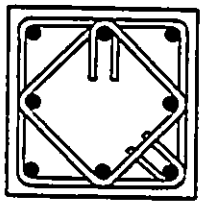

Configuration 2

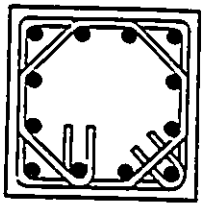

Configuration 3

Column designation	Test Variables		
	$s(mm)$	$e(mm)$	Configuration
C1-1	$d/4$	60	1
C2-1	$d/4$	60	2
C3-1	$d/4$	60	3
C4-2	$d/4$	75	1
C5-2	$d/4$	75	2
C6-2	$d/4$	75	3
C7-1	$d/2$	60	1
CS-1	$d/2$	60	2
C9-1	$d/2$	60	3
C10-2	$d/2$	75	1
C11-2	$d/2$	75	2
C12-2	$d/2$	75	3

Table 3.1: Test Variables

3.2 Behavior of Columns in Set 1

Set 1 consisted of six columns with a lateral tie spacing of 50 mm ($d/4$). They represented confined columns used in practice, in terms of tie spacing. The tie spacing was equivalent to that required in the building codes for seismic resistant columns. The specimens had three different arrangements and were subjected to two different levels of end eccentricity.

Figures 3.1 through 3.6 show experimentally obtained moment-midheight deflection relationships. These relationships include the secondary moments due to $P - \Delta$ effect. The same figures include critical section strain profiles at selected load stages.

All specimens behaved in much the same manner initially. No cracking was observed until the peak load was approached. Buckling of longitudinal reinforcement was observed at or shortly after the peak load. The load resistance started dropping immediately after the attainment of the load capacity. Crushing of concrete was observed on the compression face, as the load started dropping. The strain gauge readings indicated yielding of longitudinal reinforcement at or near the peak. Yielding of hoop steel was recorded at different load stages, mostly after the peak load. Strength decay beyond the peak load took place at different rates depending on the test parameters. Columns with inside hoops showed slower rate of strength decay. Columns with perimeter ties only, showed buckling of middle bars at or near the peak load. The strength decay observed in these specimens was relatively more rapid than those with inside hoops providing proper support to the middle bars. This can be seen when Figures 3.4, 3.5 and 3.6 are compared. Specimen C4-2 without the inside hoop support to the middle bars show higher rate of strength degradation beyond the peak than C5-2 and C6-2. Furthermore, specimen C6-2 clearly shows the superior response

of a column with well distributed longitudinal reinforcement, where each bar is supported by a corner of a hoop. This column maintained its peak strength up to 3 times the deflection corresponding to the initial development of the peak load. The strength decay thereafter was very slow, and the column had a very high deformability. However, all columns showed a somewhat ductile behavior, developing 3 times or more the deflection corresponding to peak load after a 15% loss in strength, within the inelastic range.

3.3 Behavior of Columns in Set 2

Set 2 consisted of six columns with a lateral tie spacing of 100 mm ($d/2$). They represented poorly confined columns used in practice, in terms of tie spacing. The spacing level was equivalent to that recommended for nonseismic construction. The same reinforcement arrangements and load eccentricities used in Set 1 were also used in Set 2.

Figures 3.7 to 3.12 illustrate moment deflection relationships of specimens in Set 2. Strain profiles of the critical section are also illustrated in the same figures.

The behavior of Set 2 columns was similar to that of Set 1 columns up to the peak load. First cracking was observed shortly before the peak load. Buckling of compression reinforcement took place beyond the peak load. Middle bars of column C7-1 and C10-2 buckled at or near the peak, as these bars were not laterally supported by inside hoops. This lead to a higher rate of strength decay in these columns. The ductility of columns in Set 2 was generally less than that observed in Set 1. This was expected since the tie spacing in this set was larger.

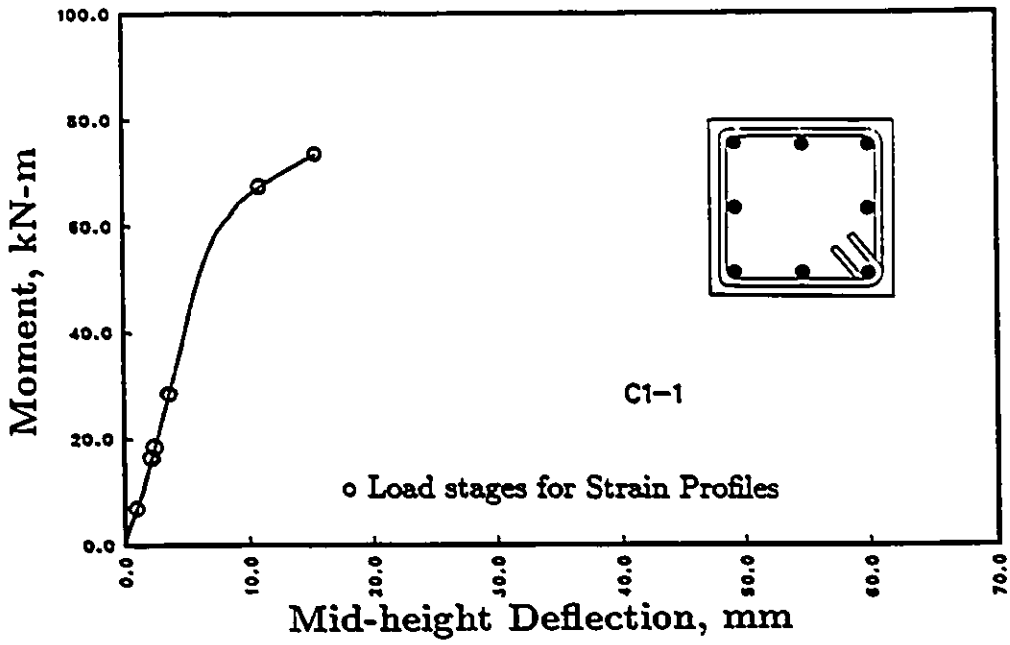

a)Moment-Midheight Deflection Relationship

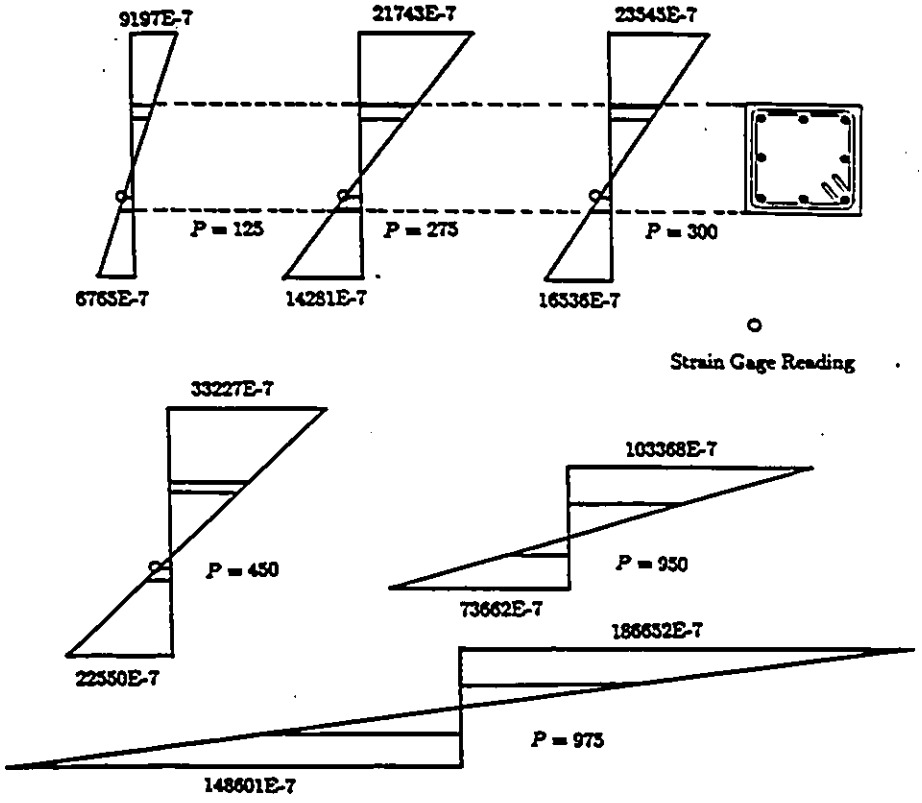

b)Strain Profiles at Selected Load Stages

Figure 3.1: Test Results for Column C1-1

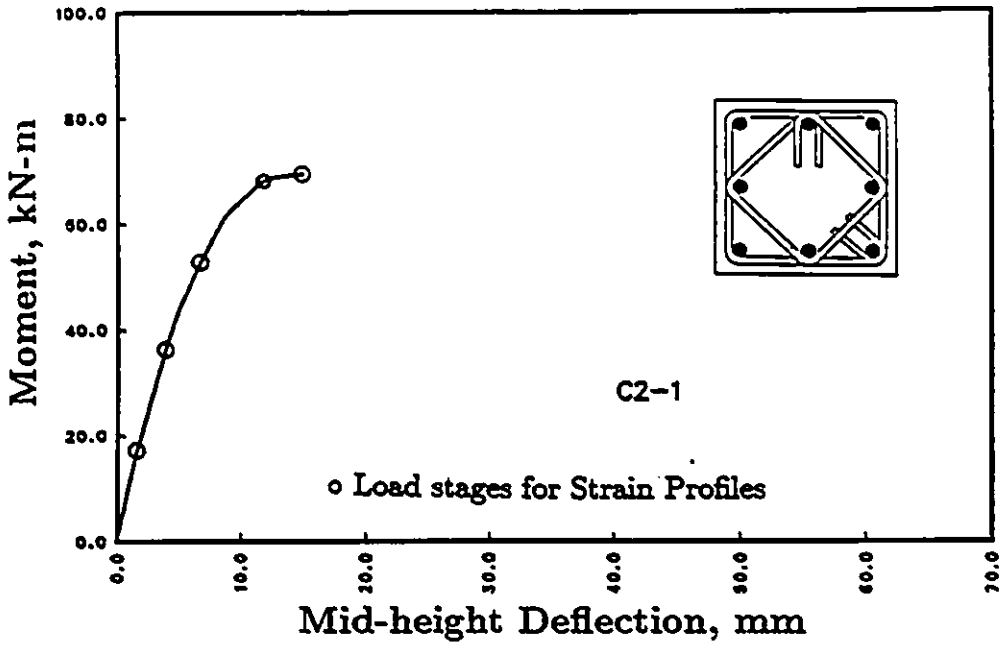

a)Moment-Midheight Deflection Relationship

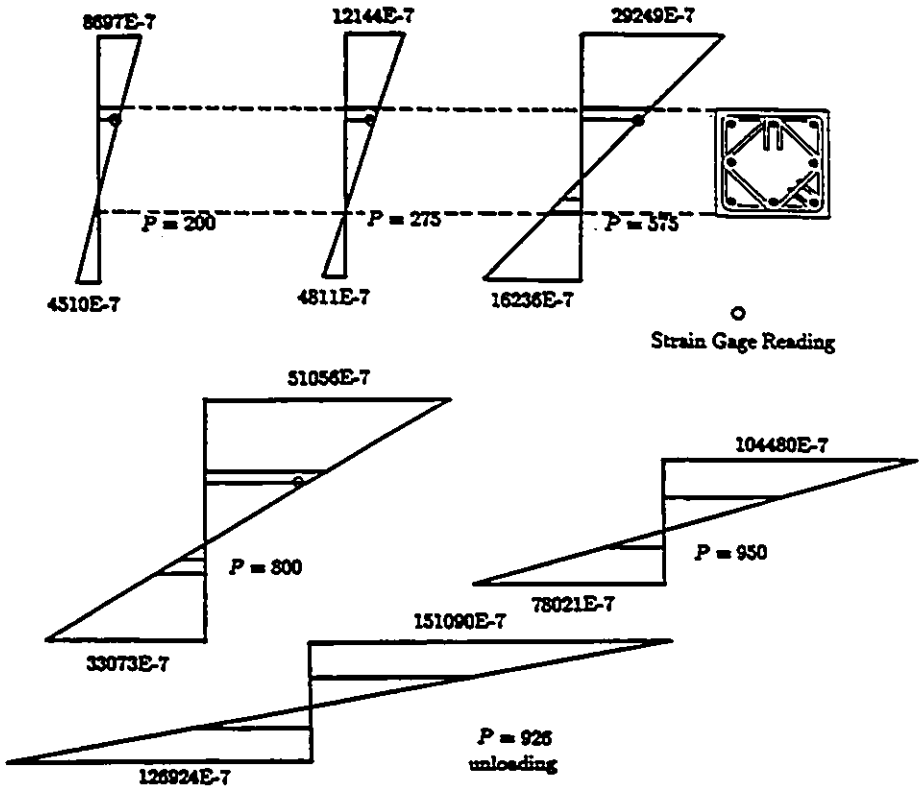

b)Strain Profiles at Selected Load Stages

Figure 3.2: Test Results for Column C2-1

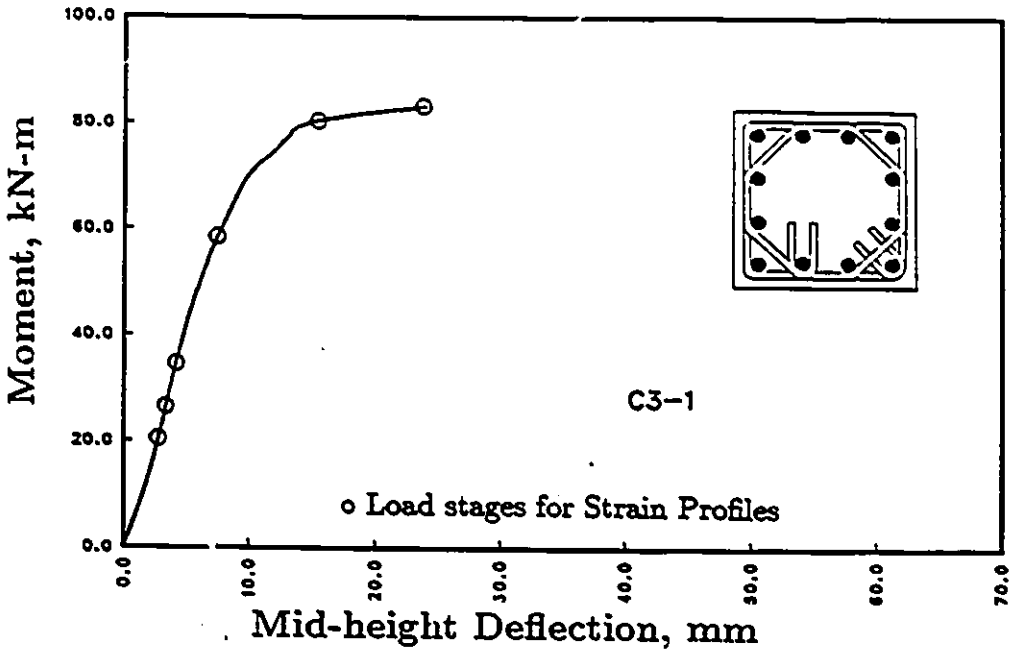

a)Moment-Midheight Deflection Relationship

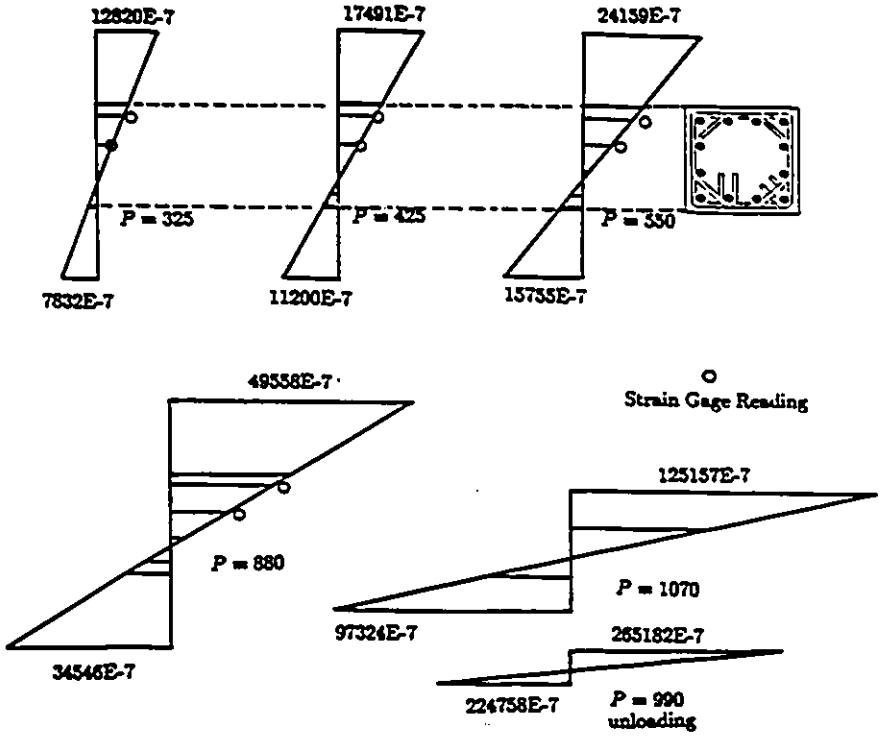

b)Strain Profiles at Selected Load Stages

Figure 3.3: Test Results for Column C3-1

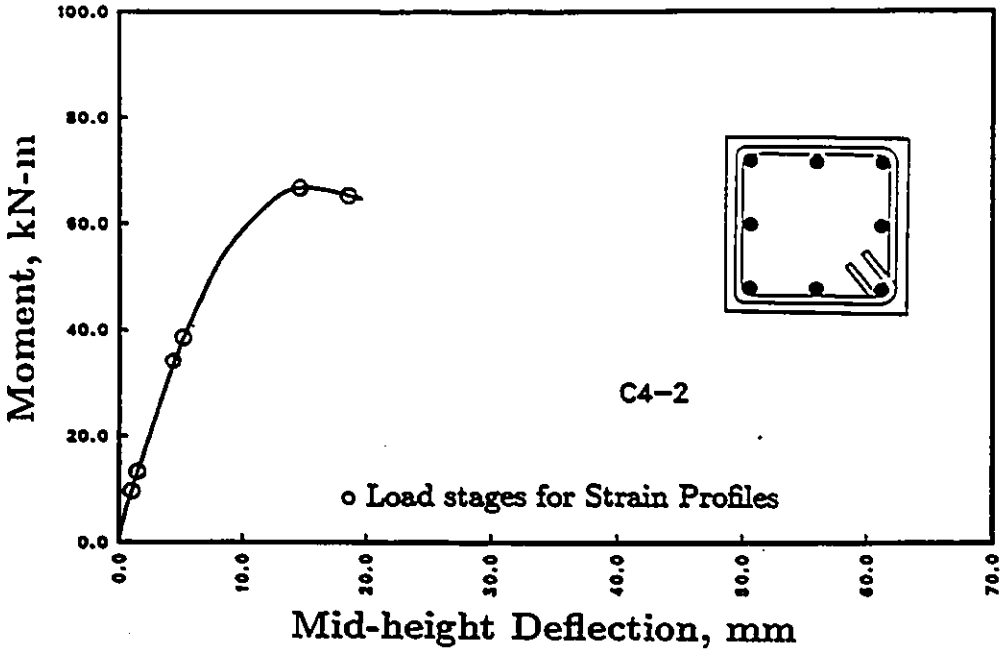

a)Moment-Midheight Deflection Relationship

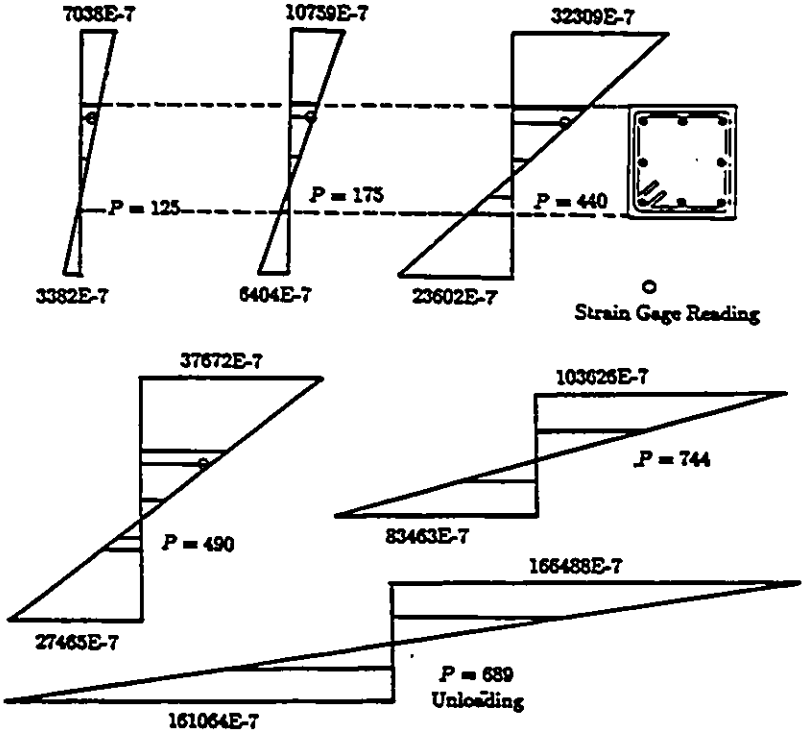

b)Strain Profiles at Selected Load Stages

Figure 3.4: Test Results for Column C4-2

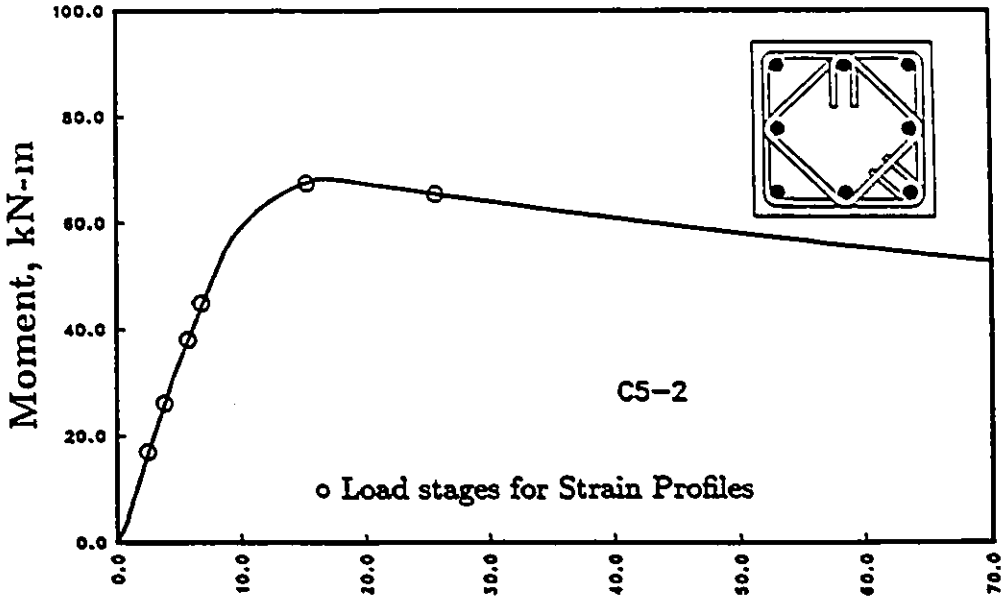

a)Moment-Midheight Deflection Relationship

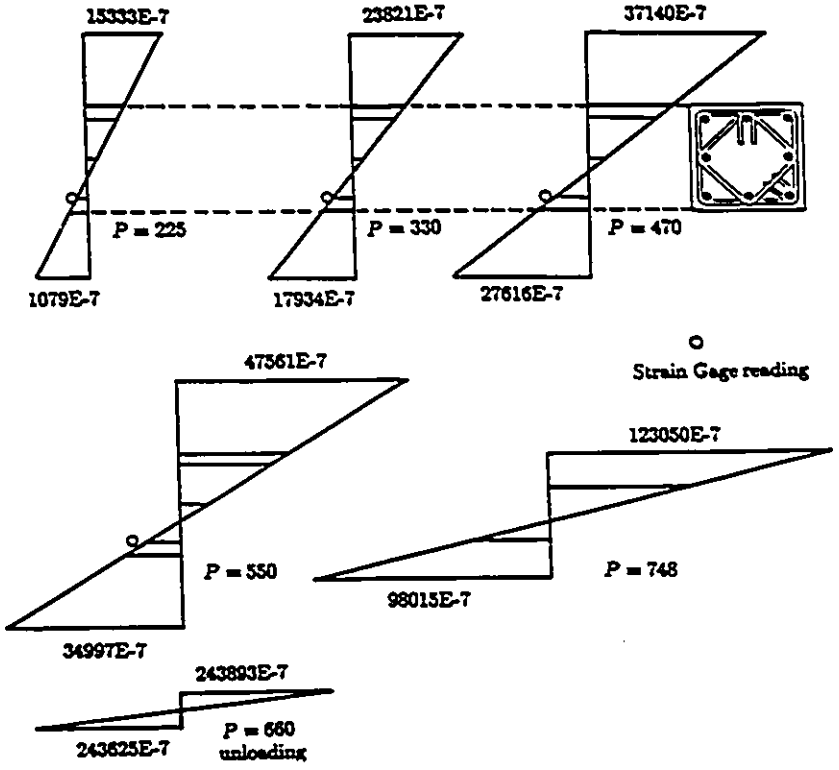

b)Strain Profiles at Selcted Load Stages

Figure 3.5: Test Results for Column C5-2

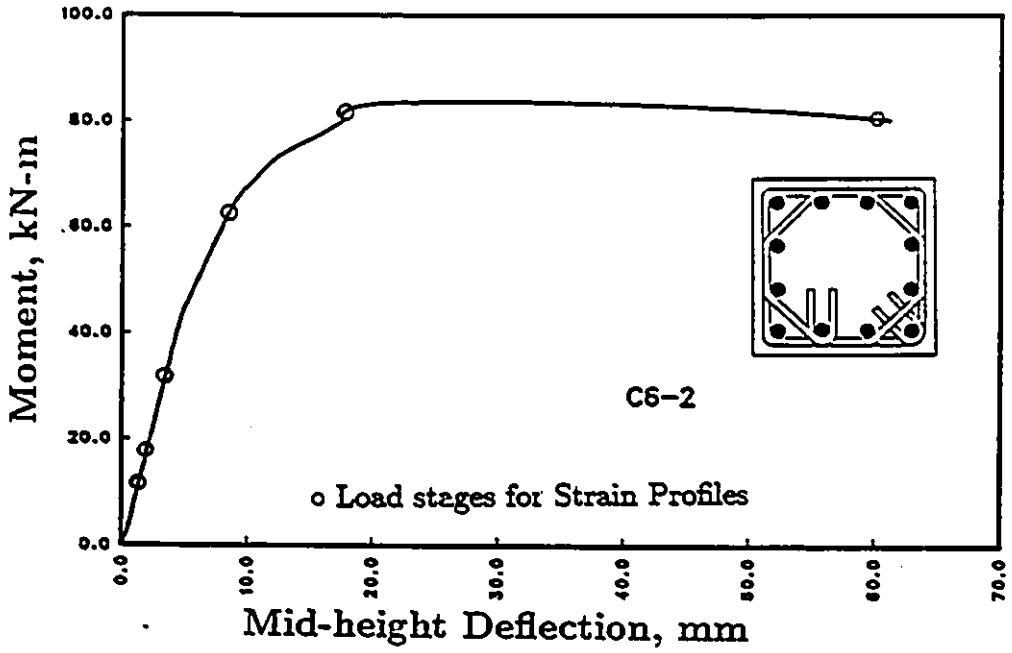

a)Moment-Midheight Deflection Relationship

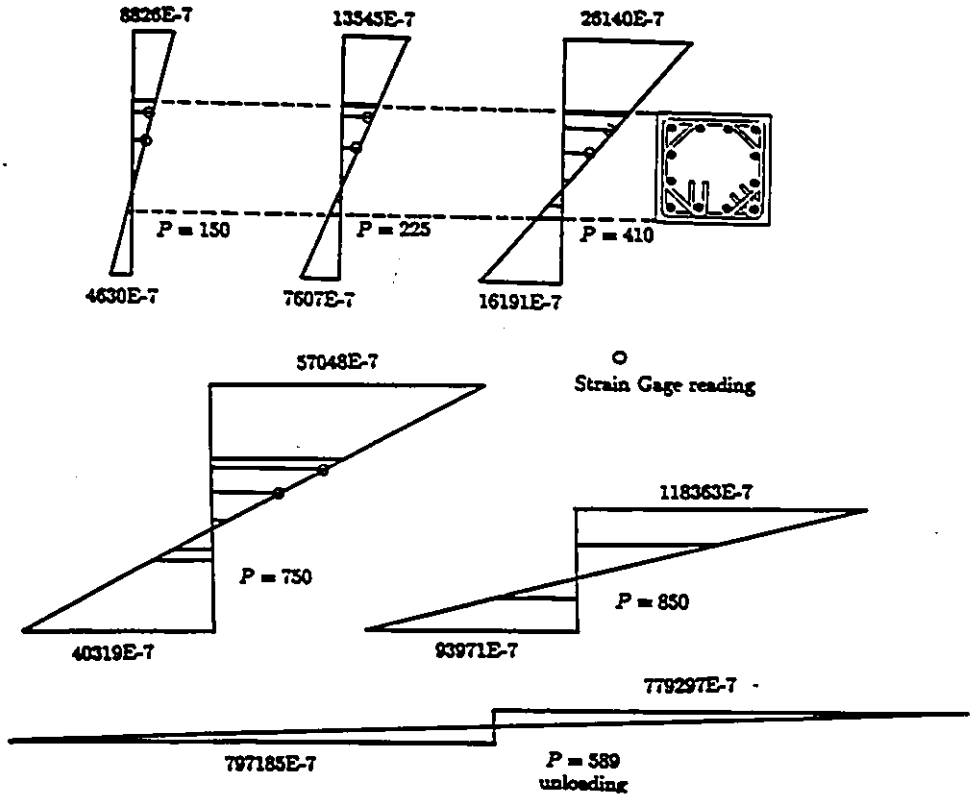

b)Strain Profiles at Selected Load Stages

Figure 3.6: Test Results for Column C6-2

More data was recorded during the unloading range of specimens in Set 2. However, two problems were encountered. Column 9-1 did not fail in the mid-height region, which was instrumented as the critical region. Also, during the initial loading of column C10-2, the end anchorage bolts sheared off, and the test was stopped. The test continued up to failure upon repairing the end region.

3.4 Effects of Test Variables

Effects of test variables were studied by comparing moment-deflection relationships obtained experimentally. The moments were normalized with respect to the peak moment to eliminate differences resulting from the differences in material strength. Therefore, the comparisons show the effects of test variables on column deformability, rather than strength.

Effect of Eccentricity

The effect of eccentricity on confinement characteristics of columns is investigated by comparing the results of column tests conducted under different levels of eccentricity. Three pairs of columns are compared for this purpose. Each column in a pair was tested either with 60 mm or 75 mm end eccentricity. Each pair had a different reinforcement arrangement and tie spacing. Figure 3.13 shows the comparison of moment deflection relationships for two columns with 8-bar arrangement. The comparison indicates no appreciable difference in behavior. A similar comparison is made in Fig. 3.14 for columns with 12-bar arrangement. Once again, no effect of eccentricity was observed on column deformability. Another comparison of columns with 12-bar arrangement is presented in Figure 3.15. This time

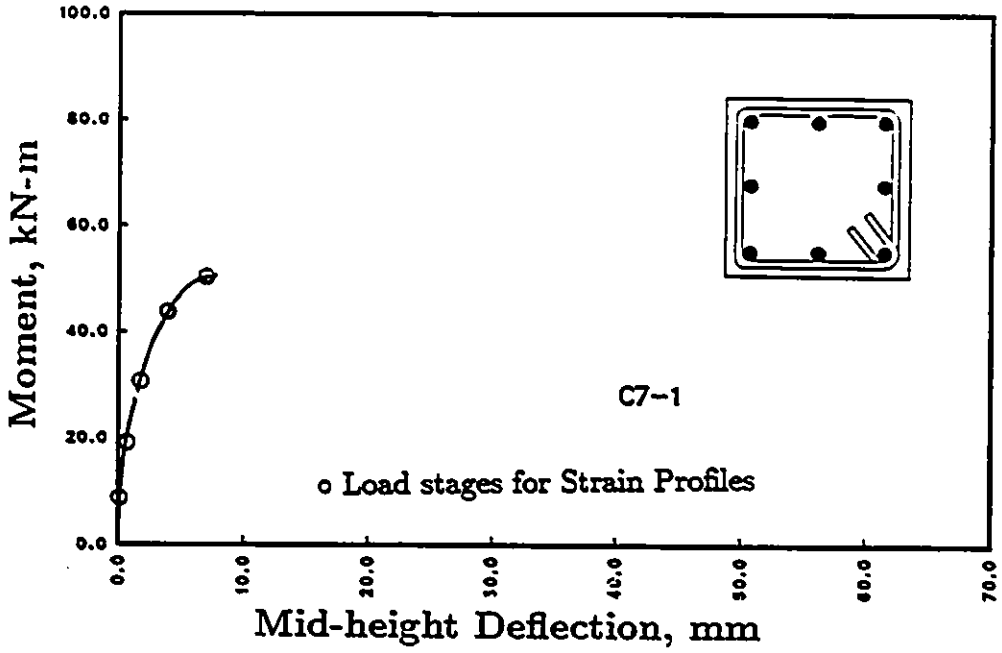

a)Moment-Midheight Deflection Relationship

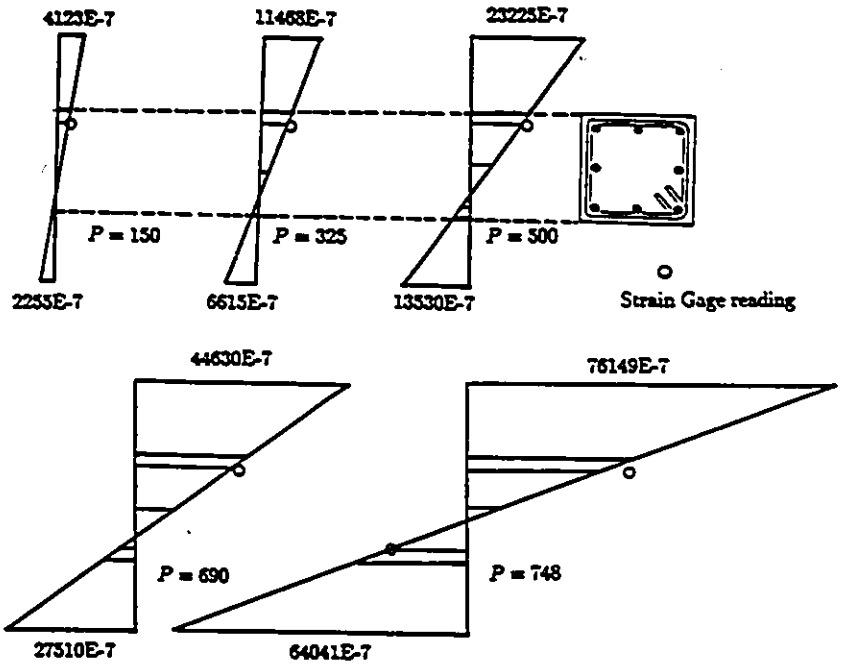

b)Strain Profiles at Selected Load Stages

Figure 3.7: Test Results for Column C7-1

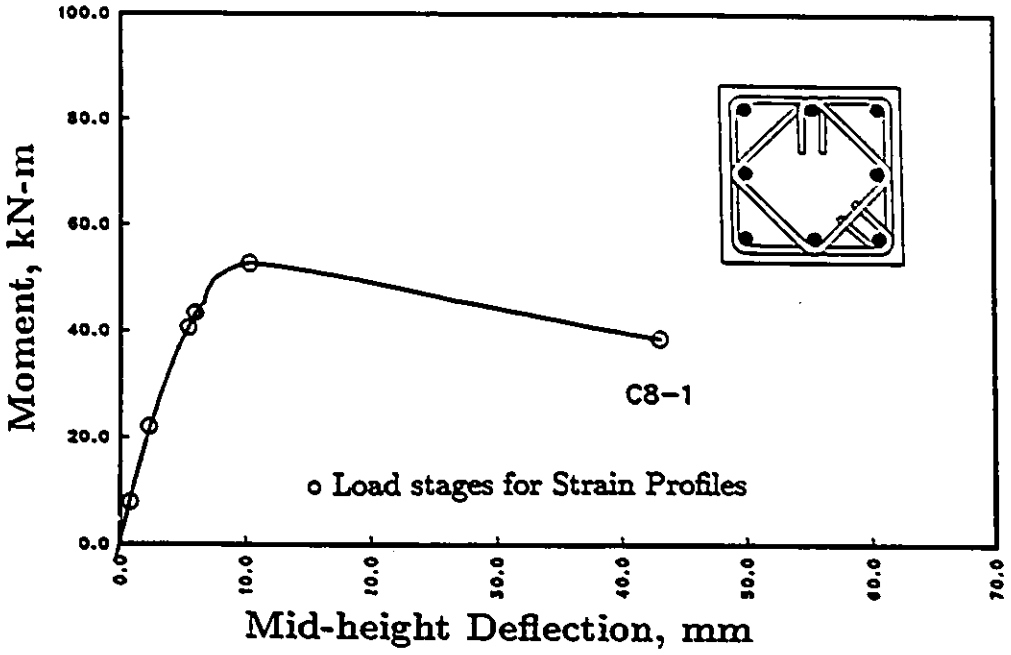

a)Moment-Midheight Deflection Relationship

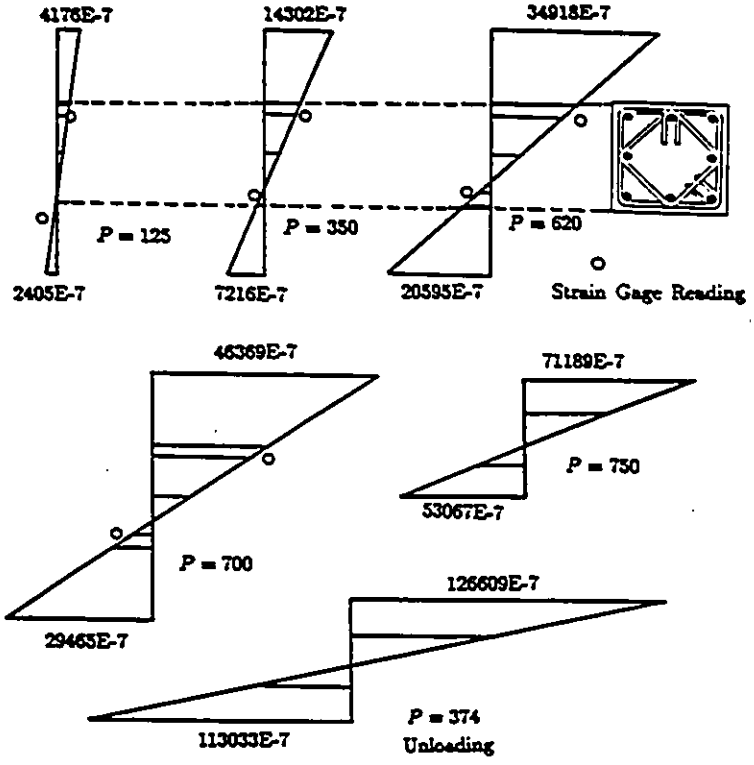

b)Strain Profiles at Selected Load Stages

Figure 3.8: Test Results for Column C8-1

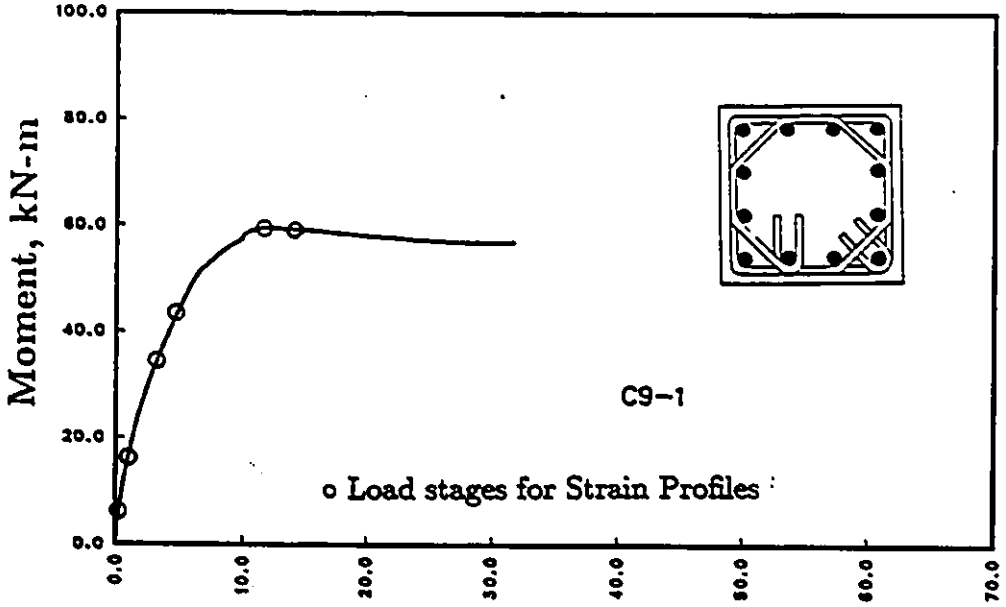

a)Moment-Midheight Deflection Relationship

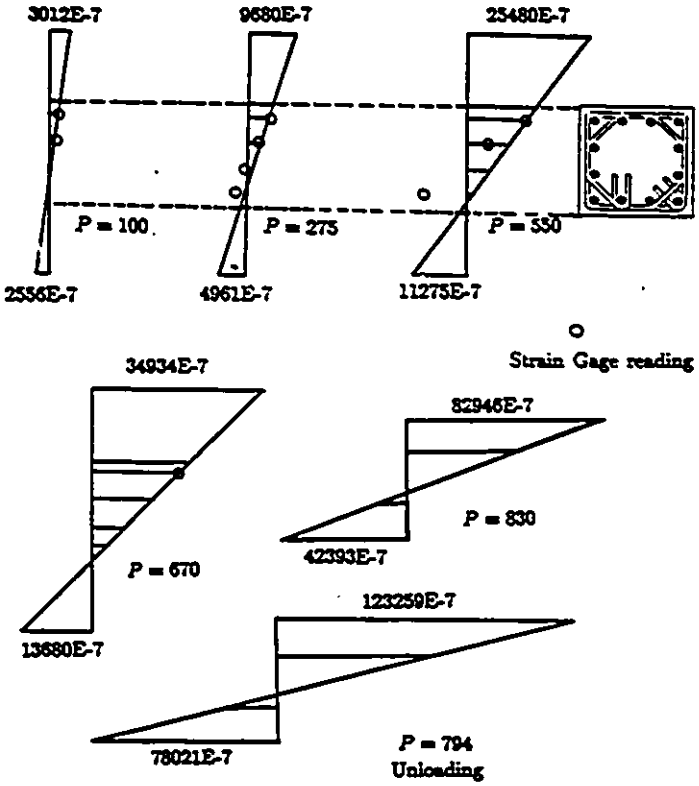

b)Strain Profiles at Selected Load Stages

Figure 3.9: Test Results for Column C9-1

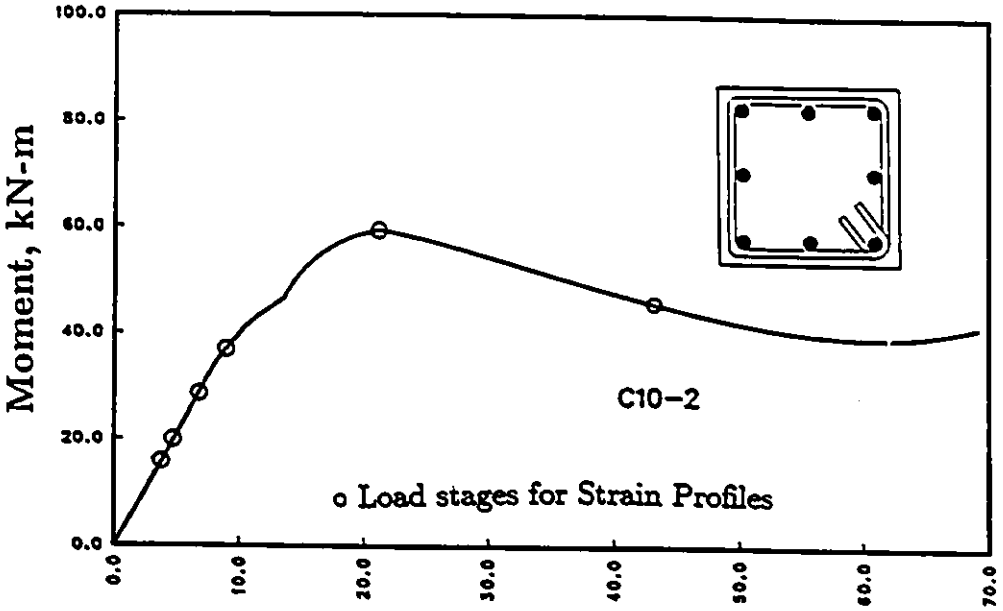

a)Moment-Midheight Deflection Relationship

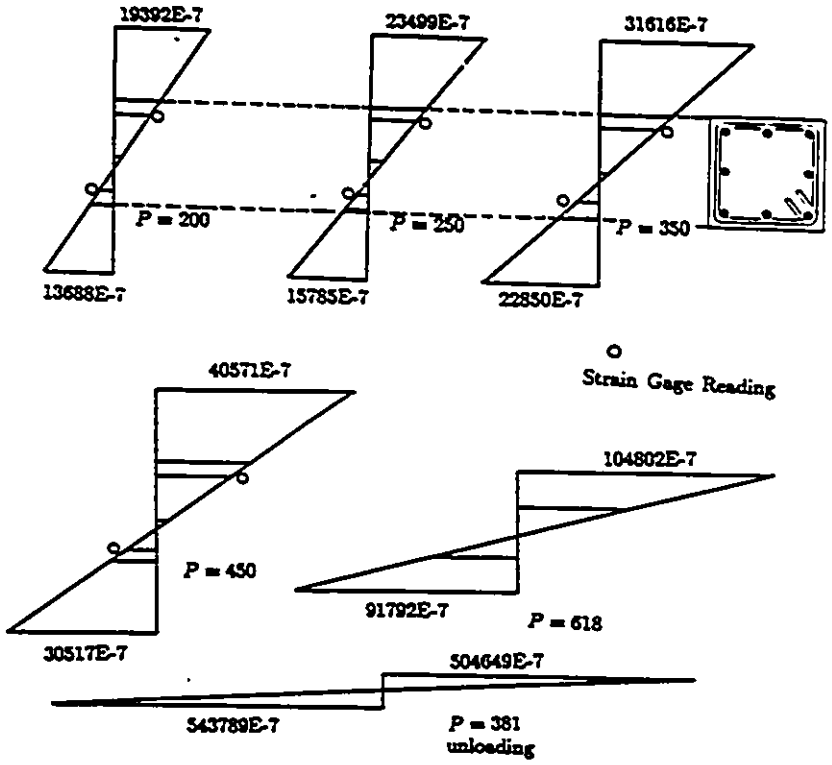

b)Strain Profiles at Selected Load Stages

Figure 3.10: Test Results for Column C10-2

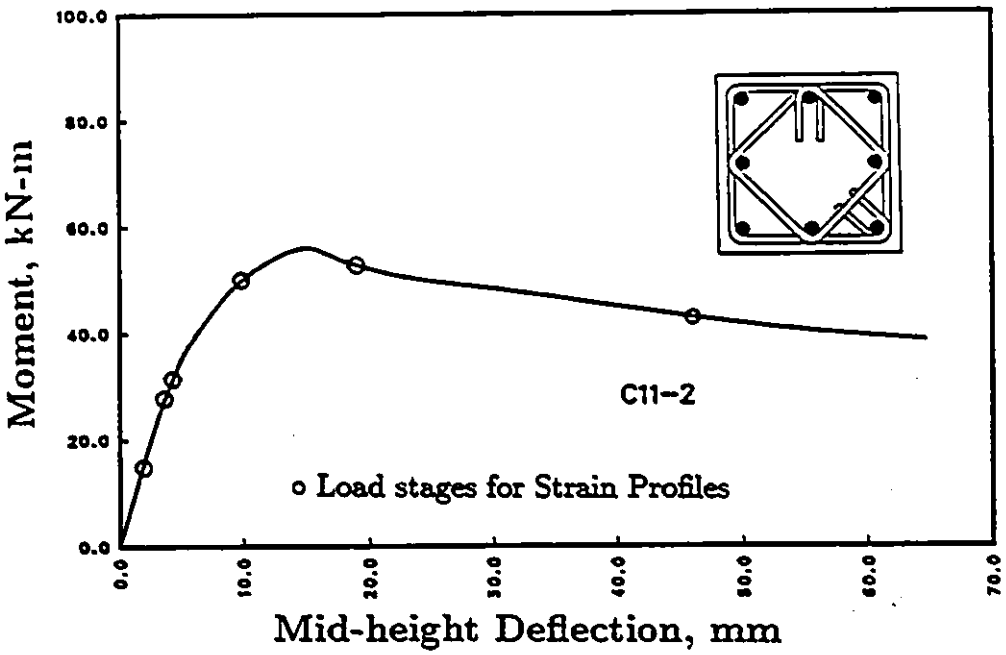

a)Moment-Midheight Deflection Relationship

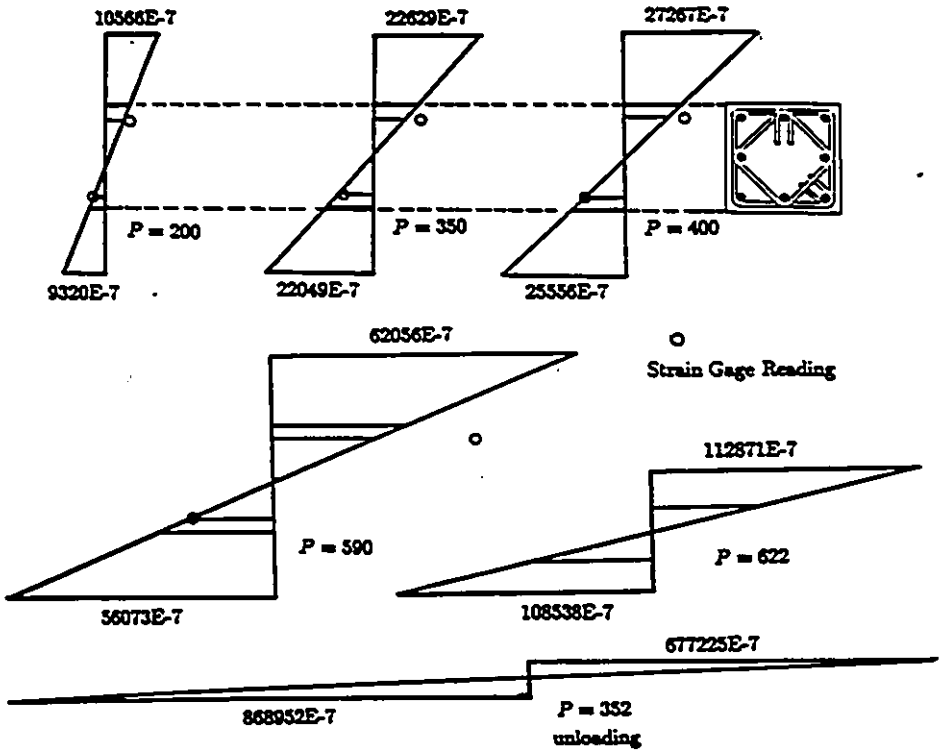

b)Strain Profiles at Selected Load Stages

Figure 3.11: Test Results for Column C11-2

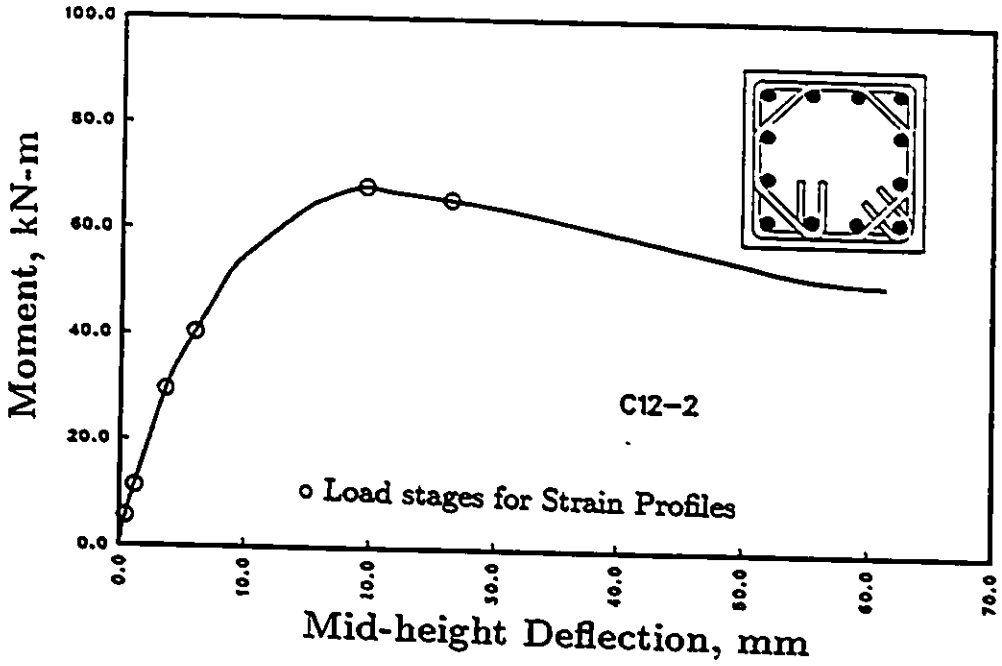

a)Moment-Midheight Deflection Relationship

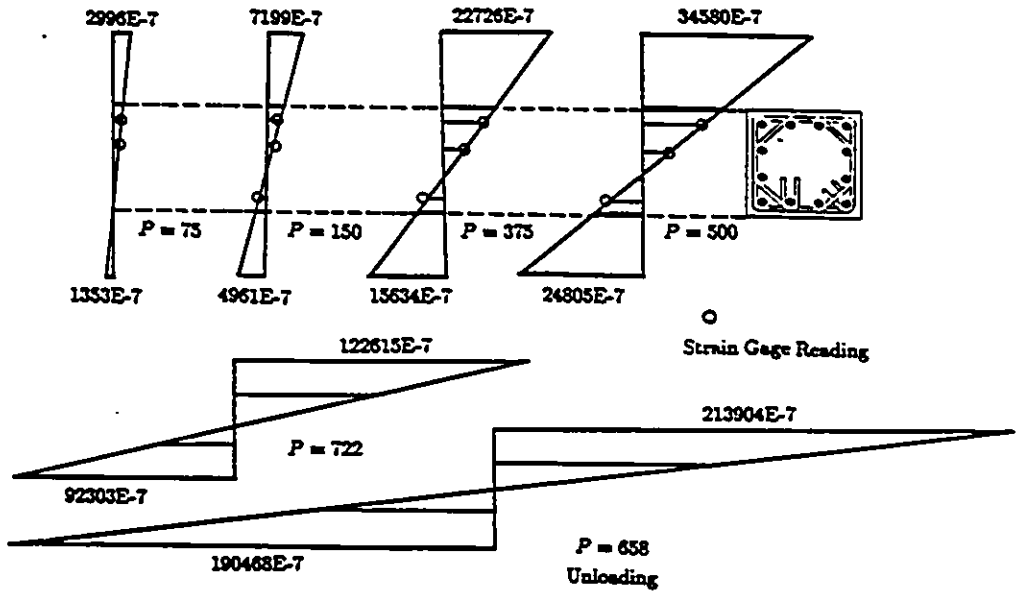

b)Strain Profiles at Selected Load Stages

Figure 3.12: Test Results for Column C12-2

the tie spacing was reduced by 1/2 as compared to the former case. The comparison indicates no effect of end eccentricity on column deformability. Ductility comparisons of columns with 4 laterally suppoted longitudinal reinforcement can not be made due to lack of test data within the descending branch. However, the results of these columns as well as others are used to establish the effect of eccentricity on strength of confined concrete in Chapter 4 in conjunction with analytical investigation.

Effect of Tie Spacing

The spacing of lateral ties in Set 2 was twice as that of Set 1. Comparison of the companion specimens in the two sets illustrates spacing effects on column behavior.

Columns C5-2 and C11-2 are compared in Figure 3.16. Column C11-2 with larger tie spacing shows higher rate of strength decay and reduced deformability. This is because of reduced confinement of core concrete and increased unsupported length of longitudinal bars. The same effect can be observed in Figure 3.17 where two other columns of different tie spacing are compared. The effect of spacing is more pronounced in columns with favorable reinforcement arrangement. For example, columns with 12-bar arrangement, shown in Fig. 3.17 are more sensitive to changes in tie spacing than those with 8-bar arrangement shown in Fig. 3.16. This may be explained by the difference in confinement pressures between columns with small and large spacings of laterally supported longitudinal reinforcement. When the lateral confinement pressure is high due to the close spacing of longitudinal reinforcement, the rate of change in confinement pressure due to the increase in tie spacing is higher than that of already low confinement pressure resulting from unfavorable reinforcement arrangement. Therefore ductility appears to be more sensitive to any variation in tie spacing when

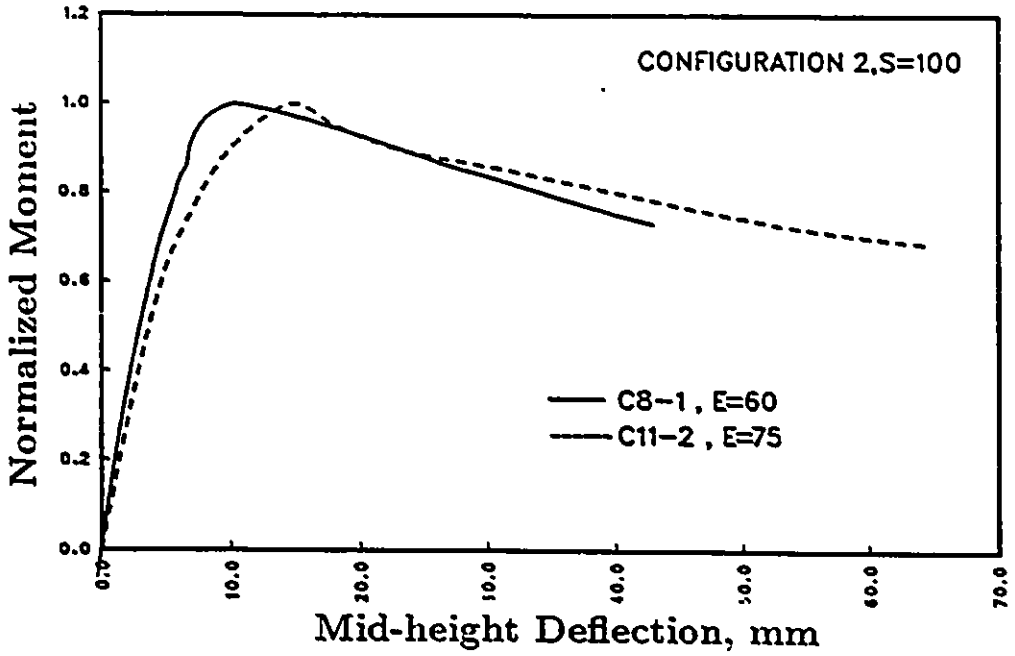

Figure 3.13: Normalized Moment-Displacement for Configuration 2, s=100mm

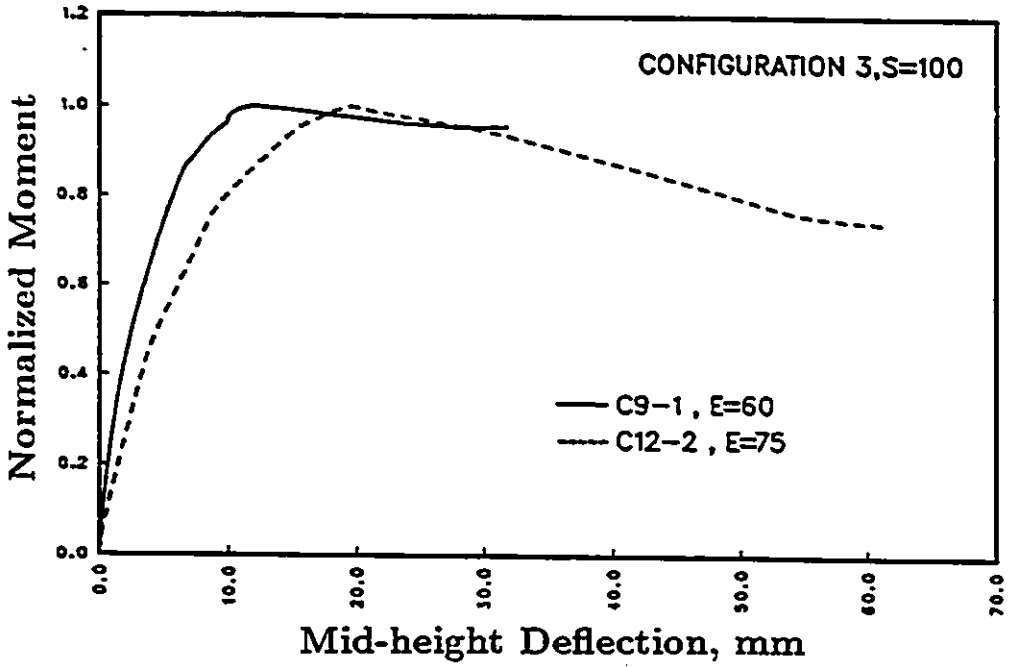

Figure 3.14: Normalized Moment-Displacement for Configuration 3, s=100mm

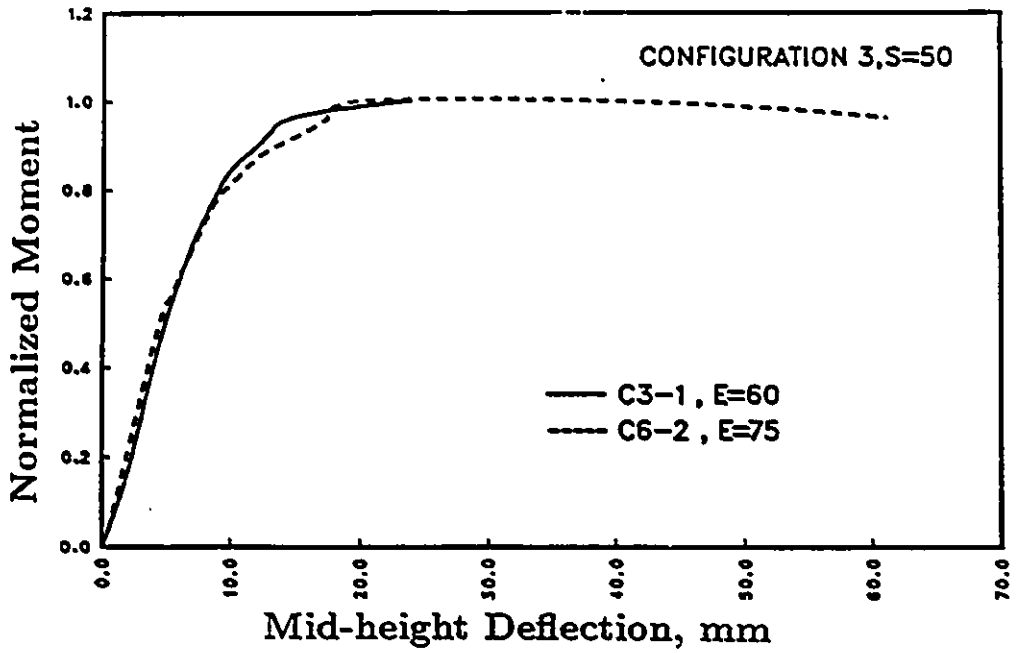

Figure 3.15: Normalized Moment-Displacement for Configuration 3, s=50mm

the column concrete is well confined. Similar observations were made in the past by other researchers for columns subjected to concentric loading. The results of test program reported here confirms the same effects on columns under eccentric loading.

Effect of Reinforcement Arrangement

The effect of reinforcement arrangement on column deformability is investigated by comparing the test results of columns with three different tie arrangements. Columns C4-2, C5-2 and C6-2 had the same spacing and eccentricity of loading but different arrangements. The moment deflection relationships of these columns are compared in Figure 3.18. The results indicate that columns with well distributed and laterally supported longitu-

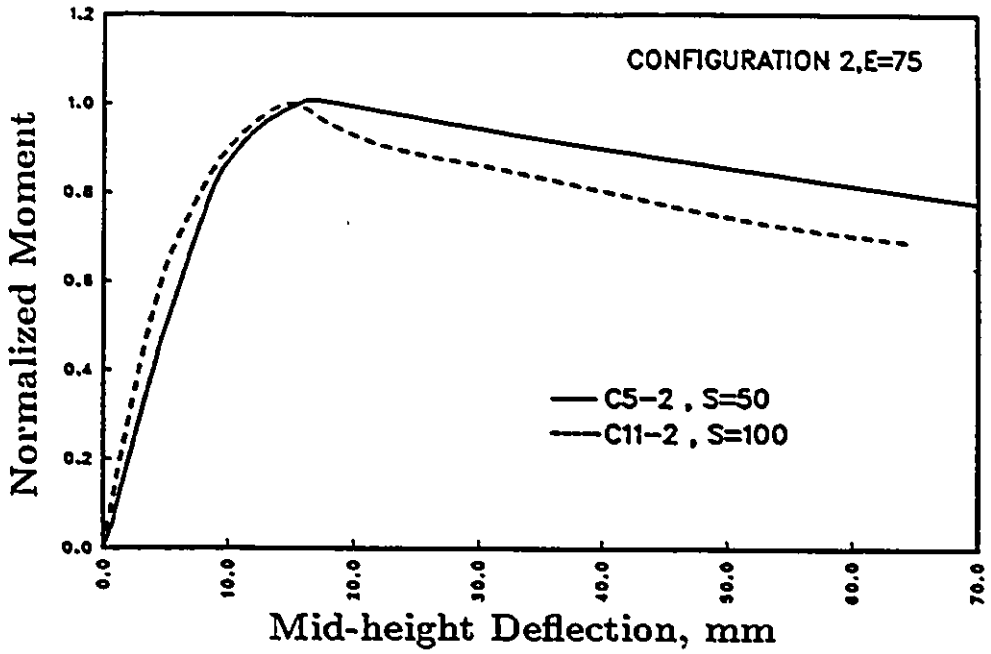

Figure 3.16: Normalized Moment-Displacement for Configuration 2, e=75mm

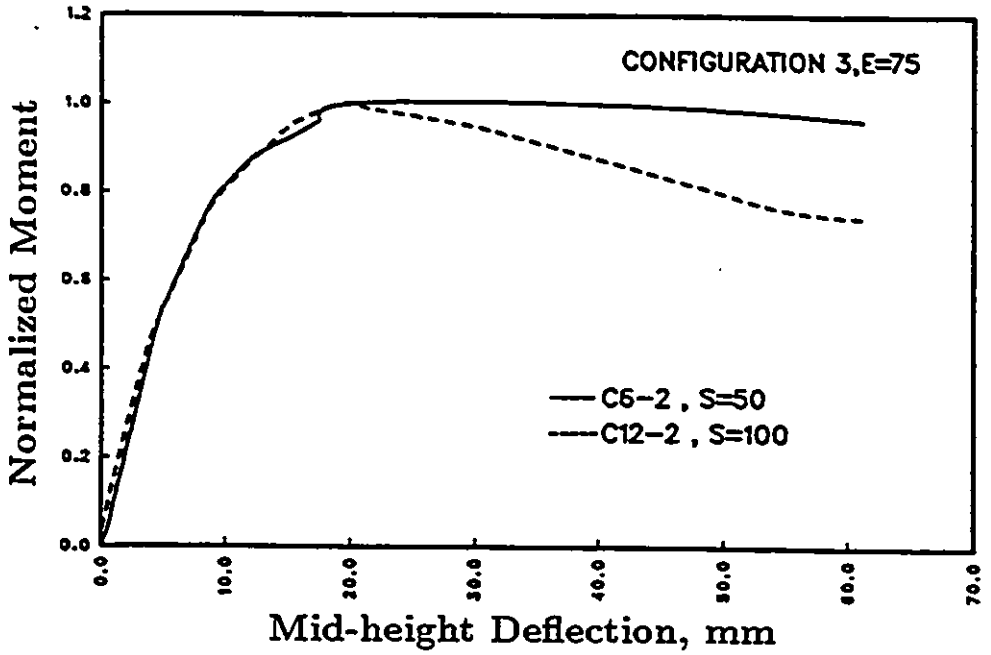

Figure 3.17: Normalized Moment-Displacement for Configuration 3, e=75mm

dinal bars show higher ductility. This can be explained by the improvement obtained in concrete confinement by the use of closely spaced bars. The tie arrangement appears to have higher effect when the tie spacing is small, in which case the confinement action is more pronounced. When the tie spacing is large, any improvement in reinforcement arrangement does not lead to a noticeable improvement in deformability. This is illustrated in Figure 3.19 where the results of three other columns with different reinforcement arrangement but larger tie spacing are compared. In all the columns compared in Figures 3.18 and 3.19 the eccentricity of load was 75 mm. When the eccentricity is low, the response is dominated by concrete compression, and the effect of reinforcement arrangement may become more pronounced even under a large tie spacing. This is shown in Fig. 3.20, where another set of three columns, tested under a lower eccentricity, are compared.

The above comparisons indicate that the arrangement of reinforcement plays a very important role on column confinement and hence column ductility when the other confinement parameters are favorable and the eccentricity is low so that the response is dominated more by concrete compression.

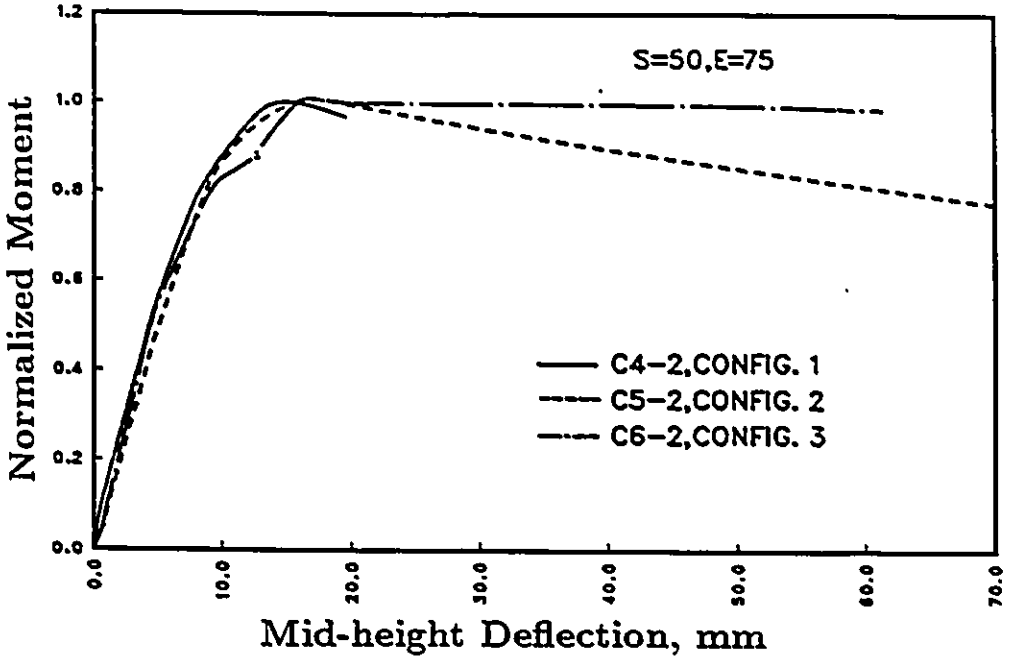

Figure 3.18: Normalized Moment-Displacement for Different Configurations

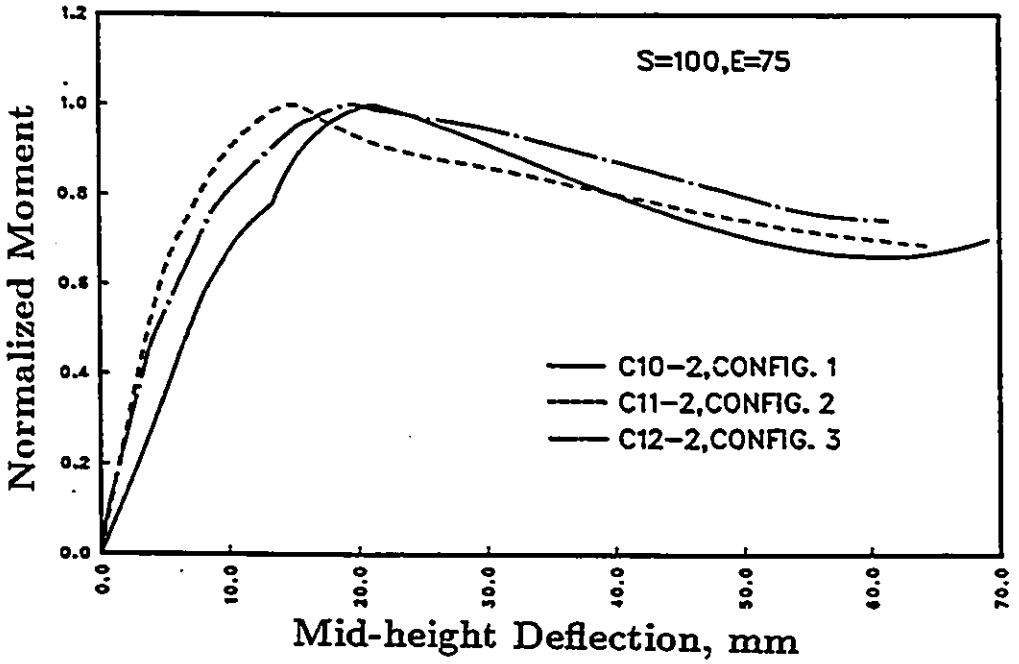

Figure 3.19: Normalized Moment-Displacement for Different Configurations

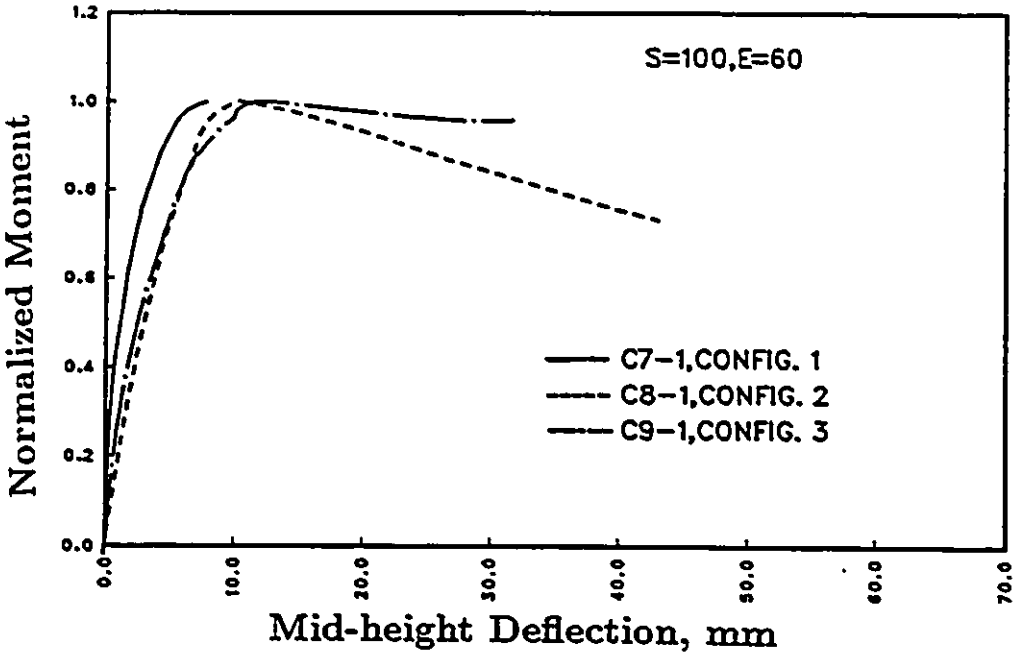

Figure 3.20: Normalized Moment-Displacement for Different Configurations

Chapter 4

Analytical Predictions of Confined Concrete Behavior

4.1 General

Stress-strain characteristics of confined concrete under strain gradient was investigated analytically. Analytical models were used to reproduce experimentally obtained results. Three of the recently proposed models were selected for this purpose. The first one was proposed by Saatcioglu and Razvi [19] in 1990 as part of a research work that formed the initial phase of this investigation. This model was developed on the basis of concentrically tested columns. The applicability of the model to eccentrically loaded columns was investigated in detail. The second model considered was proposed by Sheikh and Uzumeri [23]. This model was shown to be superior to all other models proposed prior to 1980 [24]. It was also developed on the basis of column tests conducted under concentric loading. The model was applicable to well confined columns, producing inconsistent results for

poorly confined concrete columns. Therefore, only the results of six of the twelve columns tested in the experimental program were used for comparison with this model. The third model was proposed by Sheikh and Yeh [25] for eccentrically loaded columns. This model was obtained by modifying the Sheikh and Uzumeri model for the effects of eccentricity. A computer program was prepared to evaluate the test data. The program was used to separate concrete core response from the experimentally measured column response. The analytical predictions include stress-strain relationships for core concrete and moment-curvature relationships for the critical section. The details of the analytical work and comparison between analytical and experimental results are presented in this chapter.

4.2 Analytical Models for Stress-Strain Relationship of Confined Concrete

4.2.1 Saatcioglu and Razvi Model

This model was developed for concrete subjected to concentric compression. It was based on the concept of estimating lateral confinement pressure induced by reinforcement, and its effect on concrete strength and ductility [19]. Accordingly, concrete strength under triaxial stress conditions can be written as:

$$f_{cc} = f'_{co} + k_1 f_{le} \tag{4.1}$$

where f_{cc} and f'_{co} are concrete strengths under confined and unconfined conditions respectively. The pressure term f_{le} represents the equivalent lateral pressure caused by transverse reinforcement. Coefficient k_1 reflects the relationship between the lateral pressure and increase in concrete strength

due to confinement.

$$k_1 = 6.7 f_{le}^{-0.17} \tag{4.2}$$

The term f_{le} is uniform pressure and can be directly computed from hoop tension, if the pressure distribution is uniform, as in the case of circular spirals and hoops. In this case the equivalent lateral pressure is equal to average lateral pressure f_l:

$$f_{le} = f_l = \frac{\sum_{i=1}^{n} A_{si} f_{yi}}{s b_c} \tag{4.3}$$

Where n is the number of legs of transverse reinforcement in one direction. The above equation gives the average lateral pressure acting on one side of a column cross-section. If the lateral pressure is not uniform, as in the case of rectilinear ties, pressure concentrations occur at the corners and at cross tie locations. In this case the equivalent pressure can be found by modifying the average pressure by coefficient k_2 as shown below:

$$f_{le} = k_2 f_l \tag{4.4}$$

where:

$$k_2 = 0.26\sqrt{(\frac{b_c}{s})(\frac{b_c}{s_l})(\frac{1}{f_l})} \leq 1.0 \tag{4.5}$$

The expression for k_2 was found through regression analysis of a large volume of test data.

The analytical model is illustrated in Figure 4.1. The ascending branch of the model consists of a parabola. The descending branch shows a linear variation down to 25% of confined concrete strength. Beyond this point a constant value of crushed concrete strength is assumed.

The expressions which were proposed to establish this model are as follows:

$$f_{cc} = f'_{cc}[2(\frac{\epsilon}{\epsilon_1}) - (\frac{\epsilon}{\epsilon_1})^2]^{(\frac{1}{1+2K})} \tag{4.6}$$

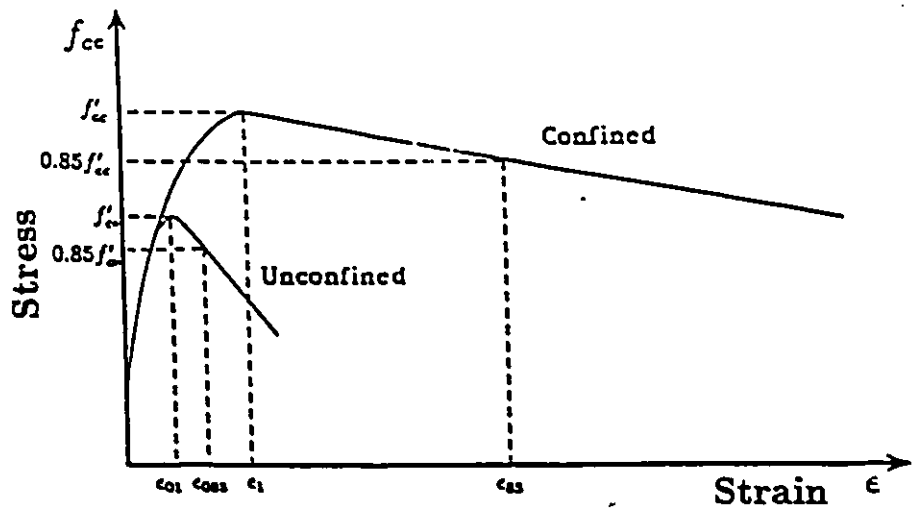

Figure 4.1: Analytical Model proposed by Saatcioglu and Razvi [19]

$$\epsilon_1 = \epsilon_{01}(1 + 5K) \tag{4.7}$$

$$\epsilon_{85} = 260\rho\epsilon_1 + \epsilon_{085} \tag{4.8}$$

Where:

$$K = \frac{k_1 f_{le}}{f'_{co}} \tag{4.9}$$

Rectangular stress block parameters for the model were generated in this thesis and are included in Appendix B. These parameters can be used conveniently for manual calculations of section capacity, eliminating the need for integration of the stress-strain relationship to find concrete contribution to sectional capacity.

4.2.2 Sheikh and Uzumeri Model

Sheikh and Uzumeri proposed an analytical model which incorporated the effect of tie arrangement on concrete confinement [23]. The model was based on effectively confined core area, defined by the tie arrangement. Increase in strength due to confinement was reflected by the ratio of effectively confined core area to total core area. The model is illustrated in Figure 4.2.

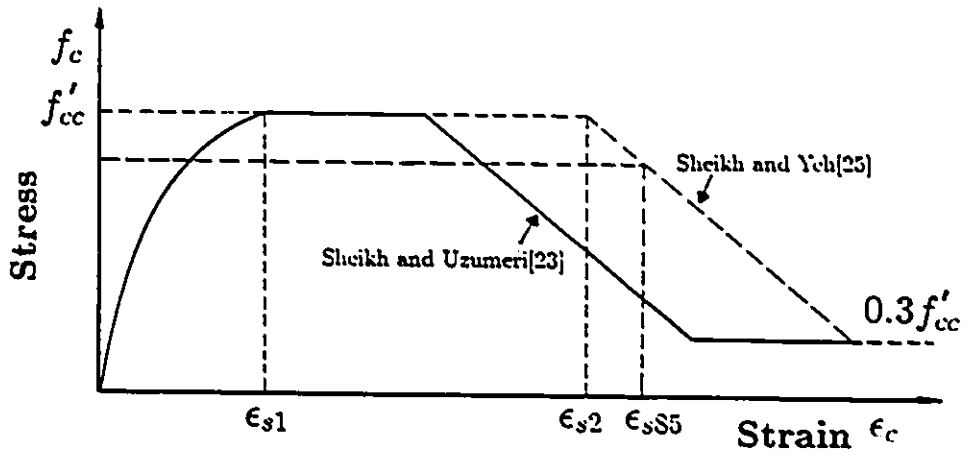

Figure 4.2: Analytical Model proposed by Sheikh and Uzumeri [23]

The ascending branch of the model consists of a second degree parabola. Hognestad's expression [6], shown below, can be used for the ascending branch:

$$f_c = f'_{cc}[2(\frac{\epsilon}{\epsilon_{s1}} - (\frac{\epsilon}{\epsilon_{s1}})^2] \tag{4.10}$$

Where f'_{cc} is confined concrete strength. The confined concrete strength is obtained by applying strength enhancement factor K_s, which is based on effectively confined core area. The following expression is derived for square columns with cross sectional dimension "B":

$$K_s = 1 + \frac{B^2}{140P_{occ}}[(1 - \frac{nC^2}{5.5B^2})(1 - \frac{s}{2B})^2]\sqrt{\rho_s f'_s} \tag{4.11}$$

$$f'_{cc} = K_s f_{cp} \tag{4.12}$$

Coefficient "n" reflects the effect of reinforcement arrangement and resulting effectively confined core area. It is equal to the number of spacings between laterally supported longitudinal reinforcement. The other control points of the model in Figure 4.2 are given by the following expressions:

$$\epsilon_{s1} = 80K_s f'_c 10^{-6} \tag{4.13}$$

$$\frac{\epsilon_{s2}}{\epsilon_{oo}} = 1 + \frac{248}{C}[1 - 5(\frac{s}{B})^2]\frac{\rho_s f'_s}{\sqrt{f'_c}} \tag{4.14}$$

$$\epsilon_{s85} = 0.225\rho_s\sqrt{\frac{B}{s}} + \epsilon_{s2} \tag{4.15}$$

4.2.3 Sheikh and Yeh Model [25]

The model previously proposed by Sheikh and Uzumeri for concentric loading was extended in 1986 by Sheikh and Yeh [25] to cover eccentric loading. The model is based on an effectively confined concrete core area, which is smaller than the concrete core area enclosed by centerlines of the perimeter tie. The model, also shown in Figure 4.2 is the same as the original Sheikh and Uzumeri model except the modification introduced to ϵ_{s2}. All other expressions that define the stress-strain relationship are the same as those proposed in the original Sheikh and Uzumeri model.

In order to include the effect of strain gradient on ductility which was believed to be the only difference between concentric and eccentric loading, Sheikh and Yeh modified the maximum strain corresponding to maximum stress ϵ_{s2} as follows:

$$\frac{\epsilon_{s2}}{\epsilon_{oo}} = 1 + \frac{24S}{C}[1 - 5(\frac{s}{B})^2 + 3\sqrt{\frac{B}{c}}]\frac{\rho_s f'_s}{\sqrt{f'_c}} \tag{4.16}$$

The additional term in the above expression is a function of the ratio of core dimension to the depth of neutral axis. Therefore the value of ϵ_{s2} and the concrete stress-strain relationship are different everytime the neutral axis assumes a new location.

4.3 Comparisons of Experimental and Analytical Stress-Strain Relationships

Experimental and analytical stress-strain relationships for confined concrete are compared in this section. Strength and ductility of confined concrete in columns tested in the experimental program were obtained by evaluating the test data.

The test data consisted of column axial load resistance and corresponding deflection and strain profiles at each load stage. While this test data was used in Chapter 3 to present the results of experimental program, it did not provide any information on the stress-strain characteristics of confined core concrete. Therefore, the test data had to be further evaluated to extract the stress-strain characteristics of the confined core concrete. In order to evaluate the test data the following assumptions were made:

1. The longitudinal strain in the steel is equal to that of the surrounding concrete.

2. Steel stress-strain relationship obtained from tension coupon tests was assumed to represent the actual behavior of reinforcement in compression. Fig. 4.3 illustrates the stress-strain relationship used for the longitudinal reinforcement.

3. Cover concrete was considered to behave the same as plain concrete. The stress-strain relationship for the plain concrete was established by using Hognestad's second degree parabola [6] up to the peak stress at 0.2% strain. The relationship consisted of a straight line between the peak stress (f'_c) and 25% of f'_c at 1% strain, and a horizontal line beyond this point. Fig. 4.4 illustrates the stress-strain relationship used for the cover concrete.

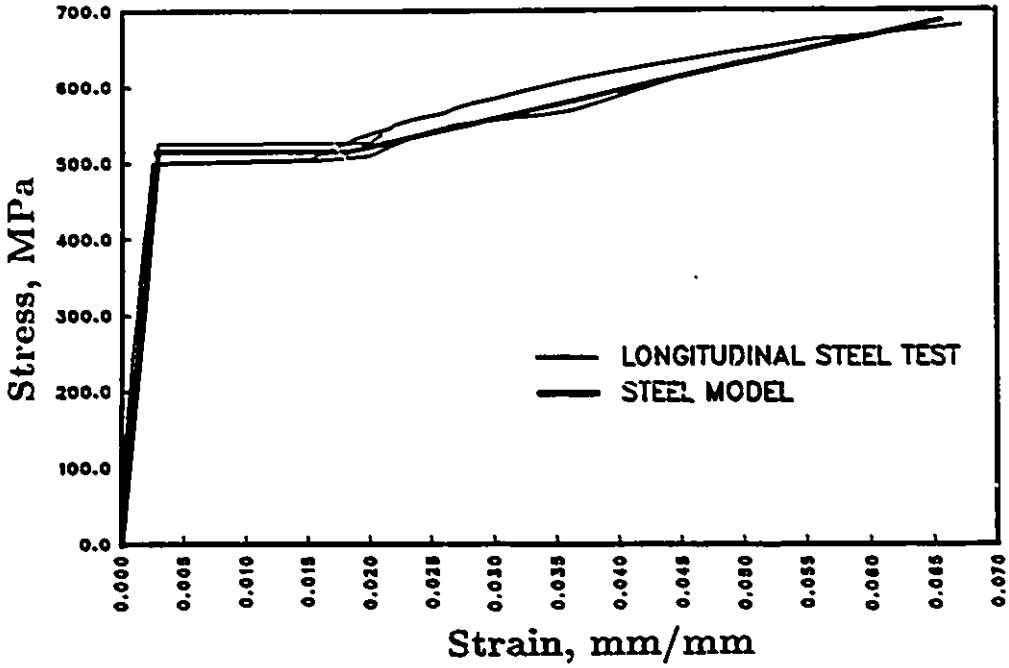

Figure 4.3: Stress-Strain Model for Longitudinal Reinforcement

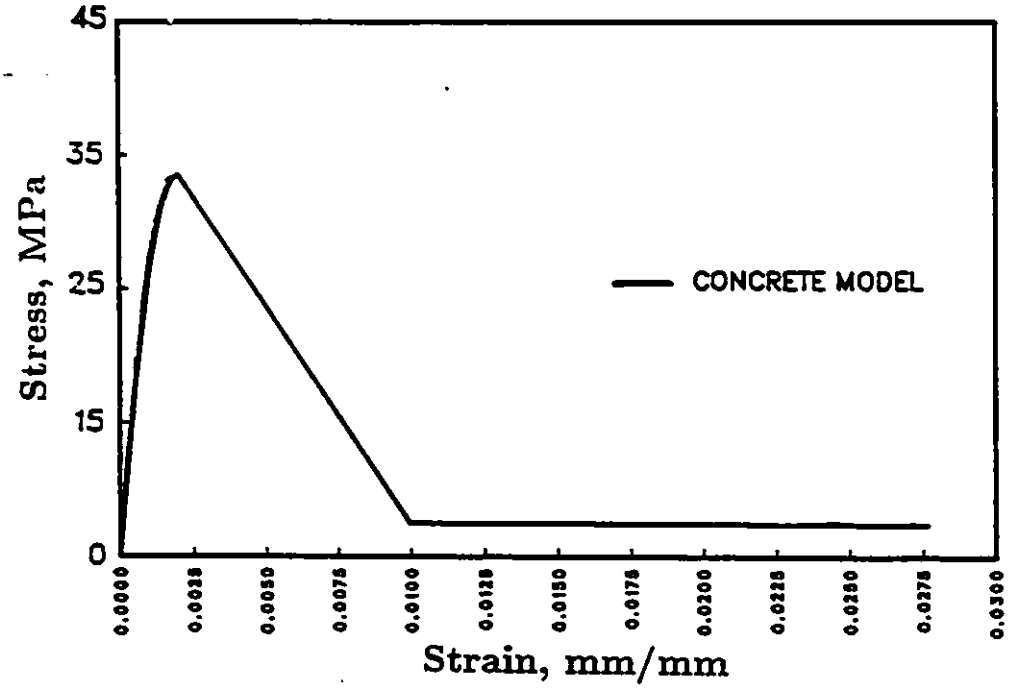

Figure 4.4: Stress-Strain Model for Plain Concrete

A computer program was written to evaluate the test data. Force and LVDT readings were used as input data for the program. In cases where the LVDT readings were not reliable, the values obtained from strain gauges were used to establish the strain profile at each load stage. Then, the extreme fiber strains at the core, and column cross-section as well as the strains in the longitudinal bars were evaluated. Internal forces in concrete and steel were calculated for different load stages.

The column section consisted of four side covers, reinforcing steel bars and confined concrete inside the core. The force carried by the cover concrete was evaluated using the stress-strain relationship for plain concrete shown in Fig.4.4. The force contribution by the longitudinal steel was found using the stress-strain relationship shown in Fig.4.3. Subtraction of all these forces from the applied load yielded the force carried by the core concrete. This force in the core concrete computed from the experimental data was used to establish the experimental stress-strain relationship of core concrete.

Area under the stress-strain relationship of concrete, distributed over the compressed area gives the compression force resisted by concrete. Core compression force was computed from the experimental data. If the actual stress-strain relationship of core concrete was known, integration of this relationship up to the extreme core strain would give the same force as that obtained from the experimental data. In this part of the investigation, the shape of the actual stress-strain relationship of core concrete was assumed to be the same as that given by the model proposed by Saatcioglu and Razvi [19]. However, knowing the shape alone was not sufficient to establish the actual stress-strain relationship. In the analytical model, the shape of the stress-strain relationship was directly related to the concrete strength. Hence, the strength remained as unknown, while the overall shape was assumed to be the same as that of the analytical model. The area under the

curve, up to specific values of maximum strains at different load stages were set equal to the corresponding core forces obtained from the experimental data. The unknown in such equality was the strength. Solving for the strength at each load stage gave as many values for the strength as the number of load stages. Theoretically, strength values should be identical if the experimental measurements were accurate and the assumed shape of the stress-strain relationship were to be exact. Since this was not the case, the strength values showed scatter. Therefore a statistical approach was employed to determine the strength. The peak stress was expressed in terms of strength enhancement coefficient K. A K value was found for each specimen such that the error between the experimental core force and the area under the stress-strain relationship was minimum in a least square sense.

The concrete strength obtained by the procedure described above was used as the experimental strength for core concrete. These strength values were compared with those obtained by the use of the analytical model in Table 4.1. The results indicate good correlations of experimental and analytical strength values.

The experimental strength values were next used to generate the "experimental" stress-strain relationships using the shape of the analytical model. Since not all the columns had experimental data beyond the peak load, the descending branches of stress-strain relationships for some of the columns could not be obtained. The stress-strain relationships obtained by this procedure are shown in Fig.4.5 through 4.16. The analytical curves are also plotted in the same figures. The comparisons include some variations between the experimental and analytical values. However, in general the agreement is good.

Table 4.1: Comparison of test result and Analytical Model
Proposed by Saatcioglu and Razvi [19]

Column designation	Saatcioglu and Razvi [19]				Test Program				$\frac{f'_{ccexp}}{f'_{ccanaly}}$	$\frac{Z_{exp}}{Z_{analy}}$
	K	ϵ_1	f'_{cc}	Z	K	ϵ_1	f'_{cc}	Z		
C1-1	0.257	0.00457	38.97	9.42	0.25	0.0045	38.75		0.994	
C2-1	0.321	0.00521	40.95	10.06	0.19	0.0039	36.89		0.901	
C3-1	0.379	0.00579	42.75	9.31	0.43	0.0063	44.33		1.037	
C4-2	0.257	0.00457	38.97	9.42	0.16	0.0036	35.96		0.923	
C5-2	0.321	0.00521	40.95	10.06	0.13	0.0033	35.03	8.28	0.885	0.823
C6-2	0.379	0.00579	42.75	9.31	0.29	0.0049	40.00	4.81	0.936	0.517
C7-1	0.195	0.00395	27.49	21.28	0.35	0.0055	31.05		1.13	
C8-1	0.243	0.00443	28.59	23.92	0.33	0.0053	30.59		1.07	
C9-1	0.288	0.00488	29.62	23.00	0.27	0.0047	29.21		0.986	
C10-2	0.195	0.00395	27.49	21.28	0.20	0.004	27.60		1.004	
C11-2	0.243	0.00443	28.59	23.92	0.60	0.008	36.80		1.287	
C12-2	0.288	0.00488	29.62	23.00	0.18	0.0038	27.14	17.06	0.916	0.740

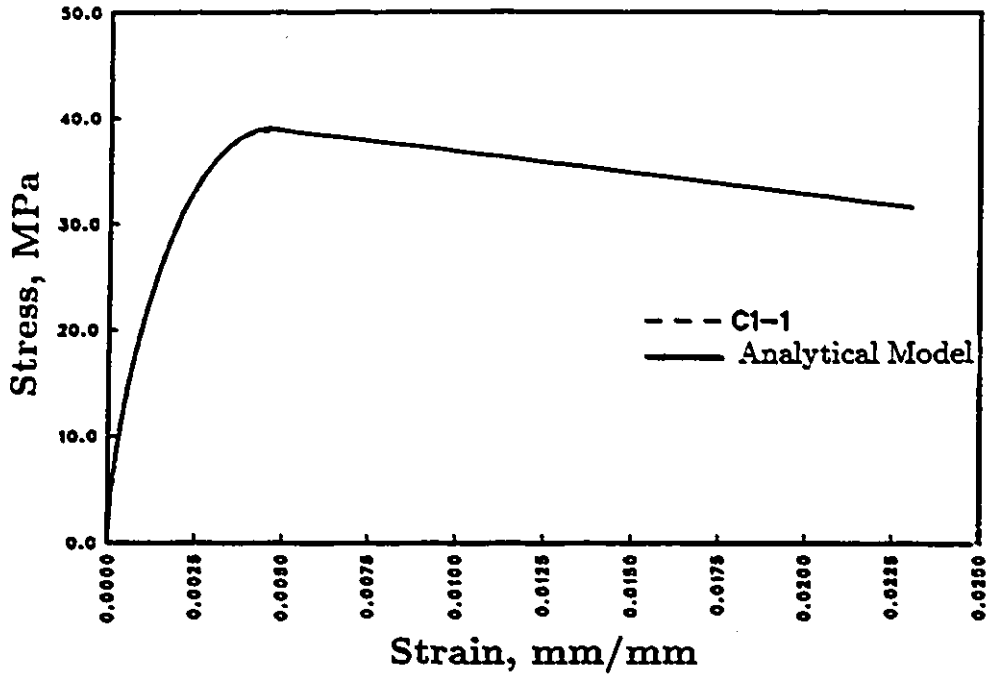

Figure 4.5: Stress-Strain Relationships of Core Concrete for C1-1

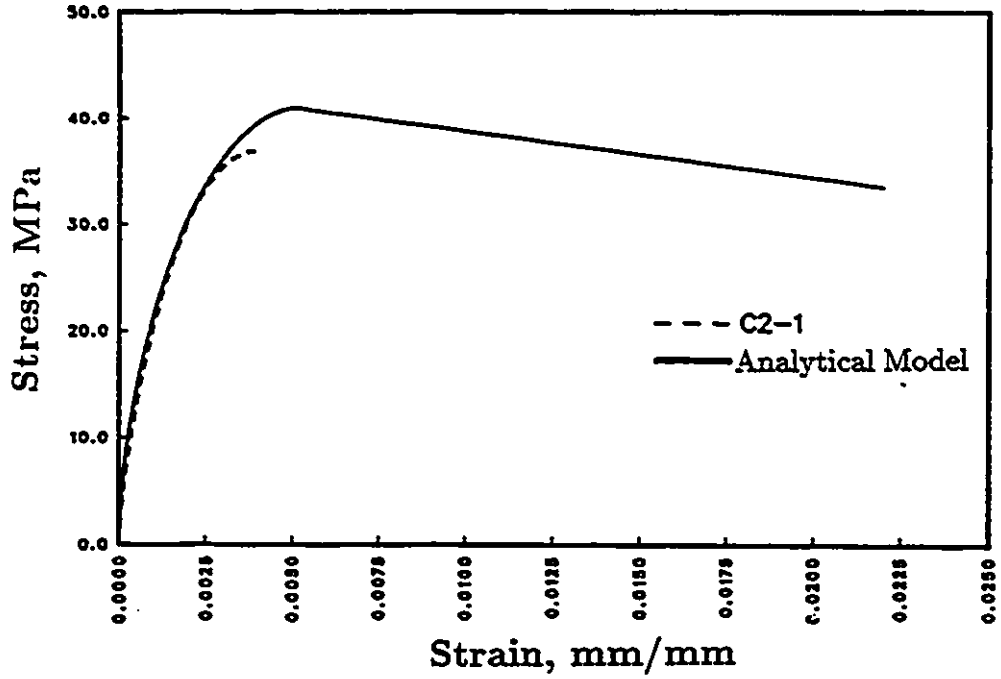

Figure 4.6: Stress-Strain Relationships of Core Concrete for C2-1

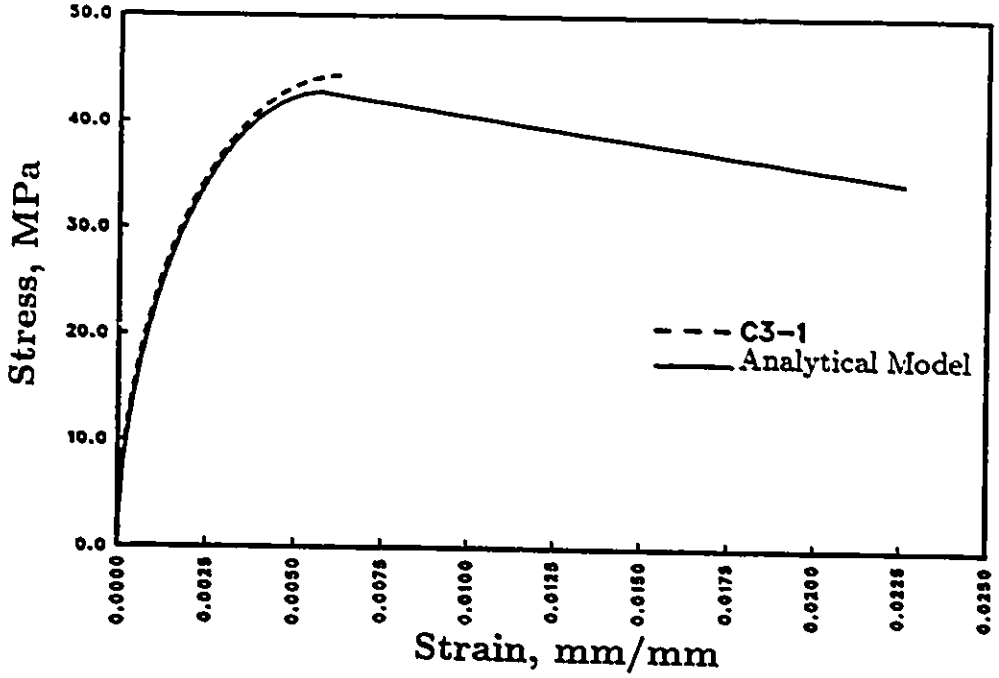

Figure 4.7: Stress-Strain Relationships of Core Concrete for C3-1

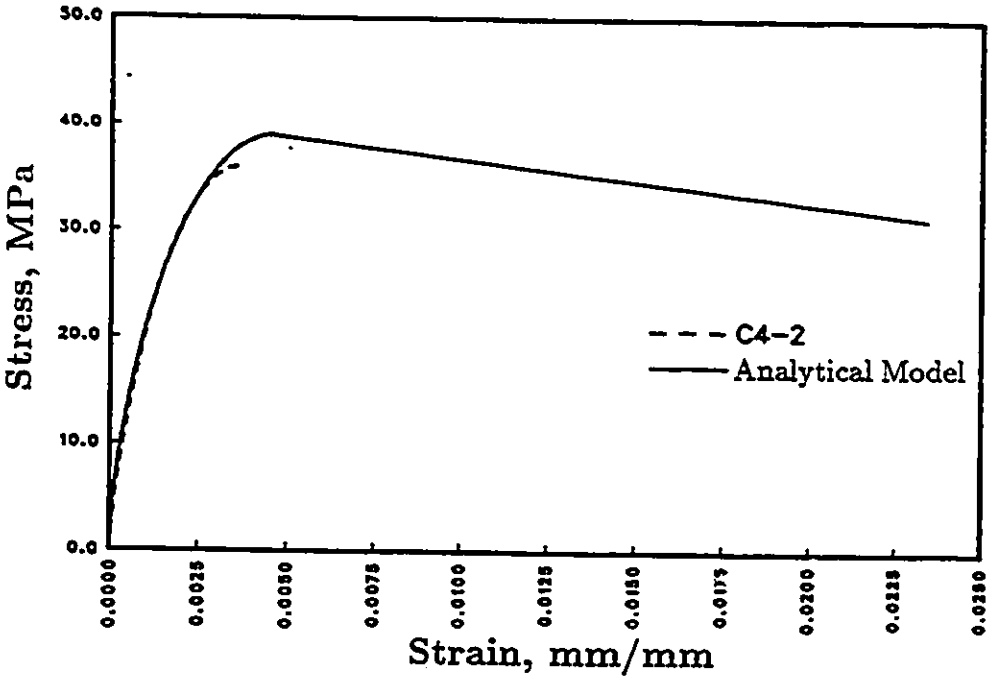

Figure 4.8: Stress-Strain Relationships of Core Concrete for C4-2

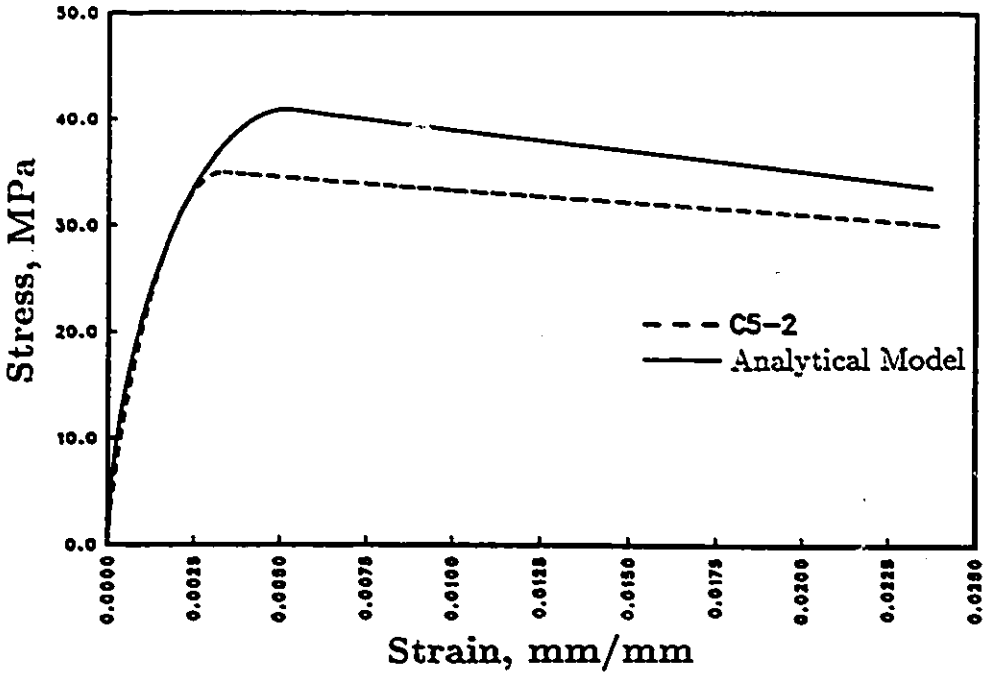

Figure 4.9: Stress-Strain Relationships of Core Concrete for C5-2

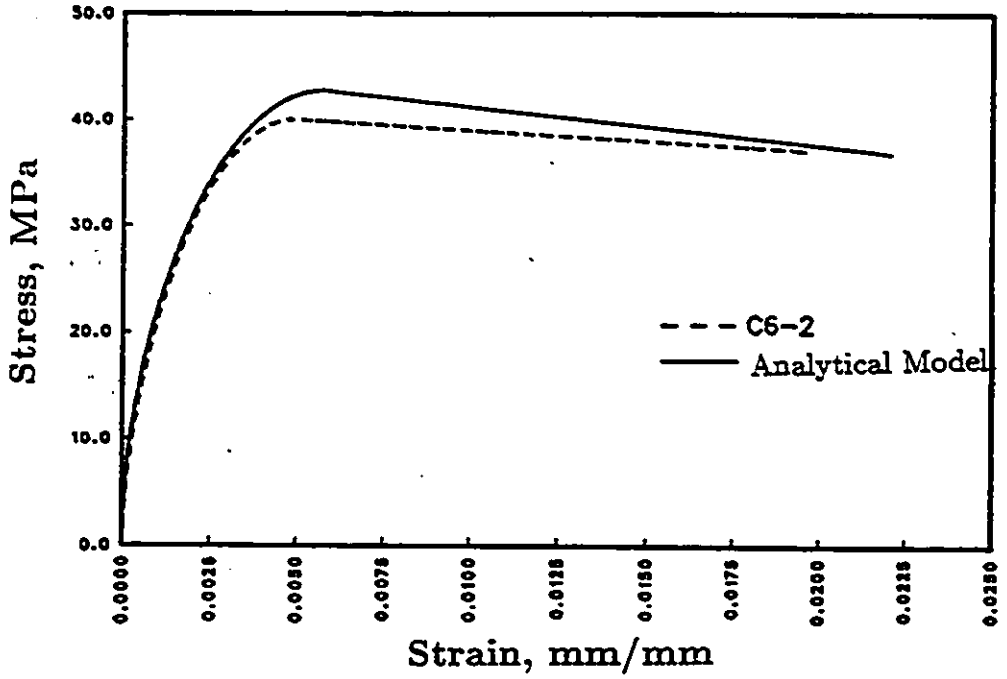

Figure 4.10: Stress-Strain Relationships of Core Concrete for C6-2

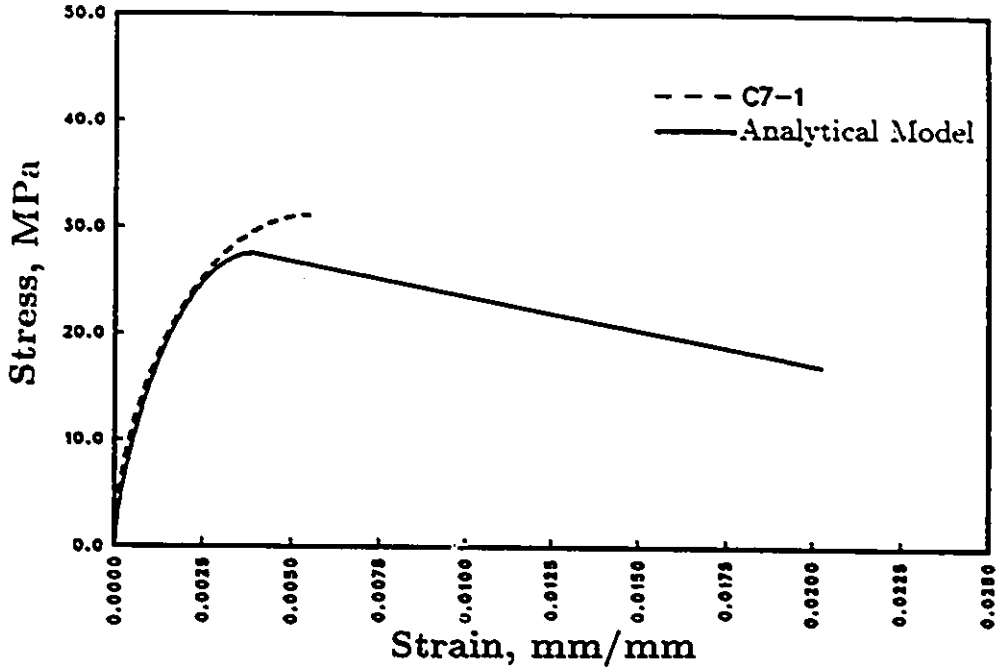

Figure 4.11: Stress-Strain Relationships of Core Concrete for C7-1

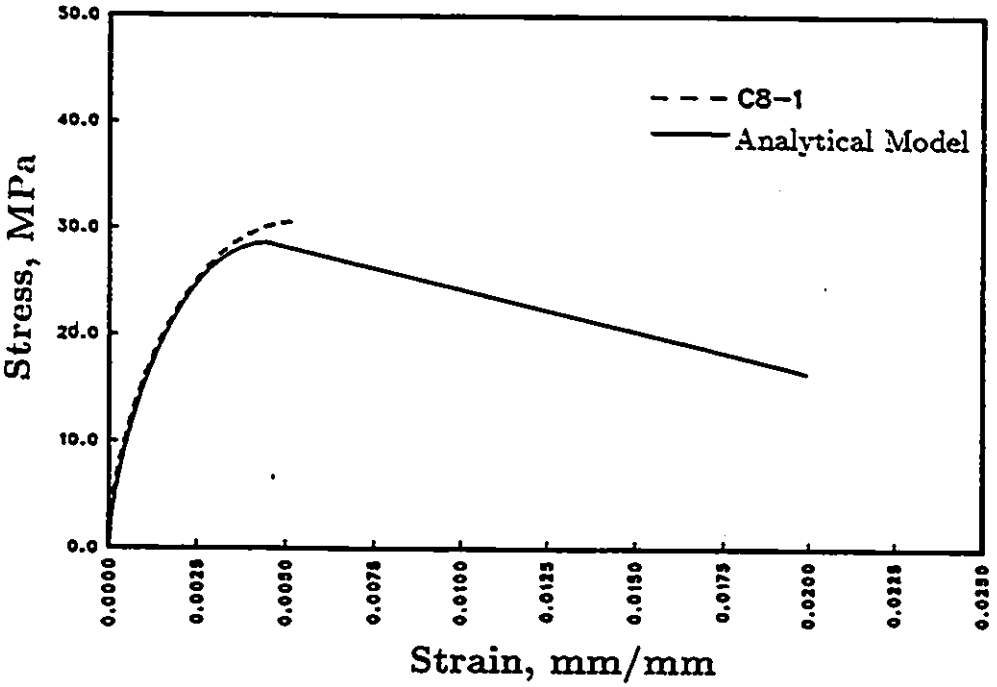

Figure 4.12: Stress-Strain Relationships of Core Concrete for C8-1

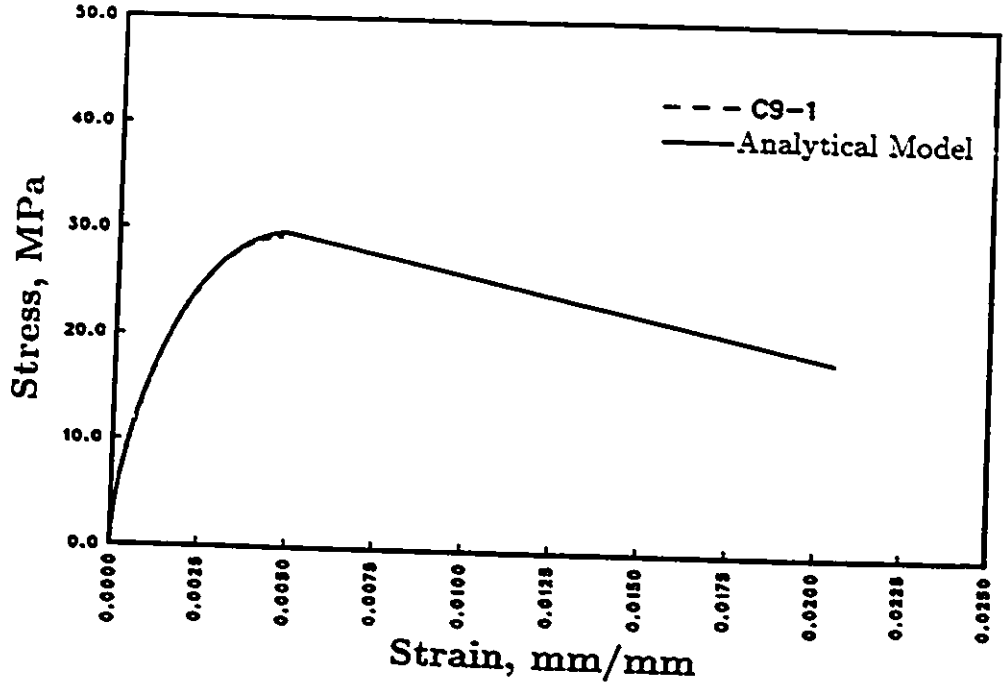

Figure 4.13: Stress-Strain Relationships of Core Concrete for C9-1

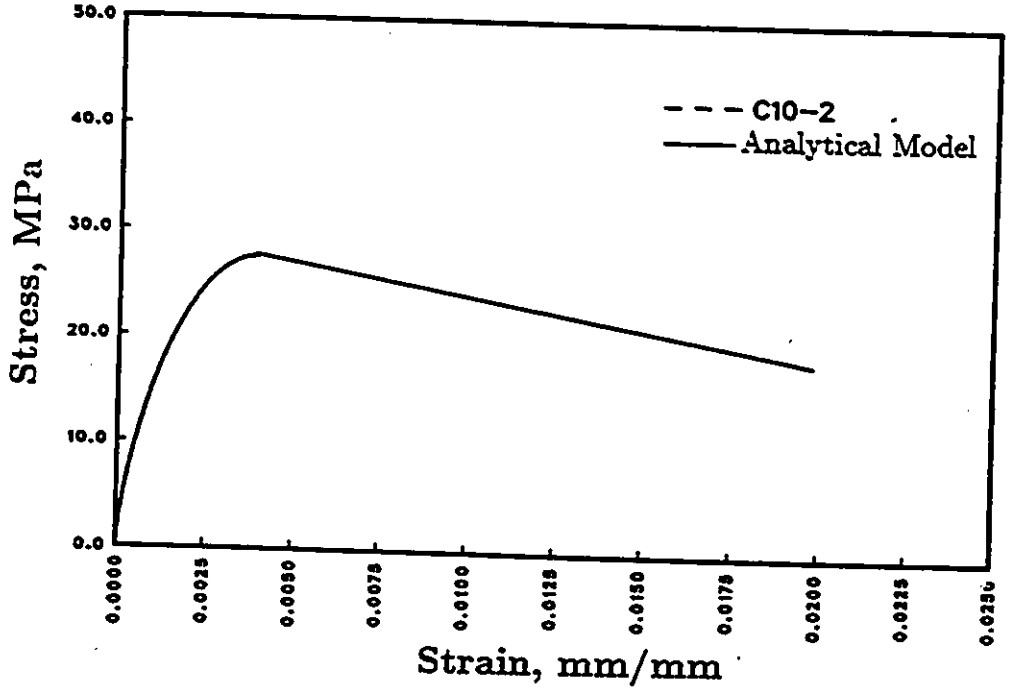

Figure 4.14: Stress-Strain Relationships of Core Concrete for C10-2

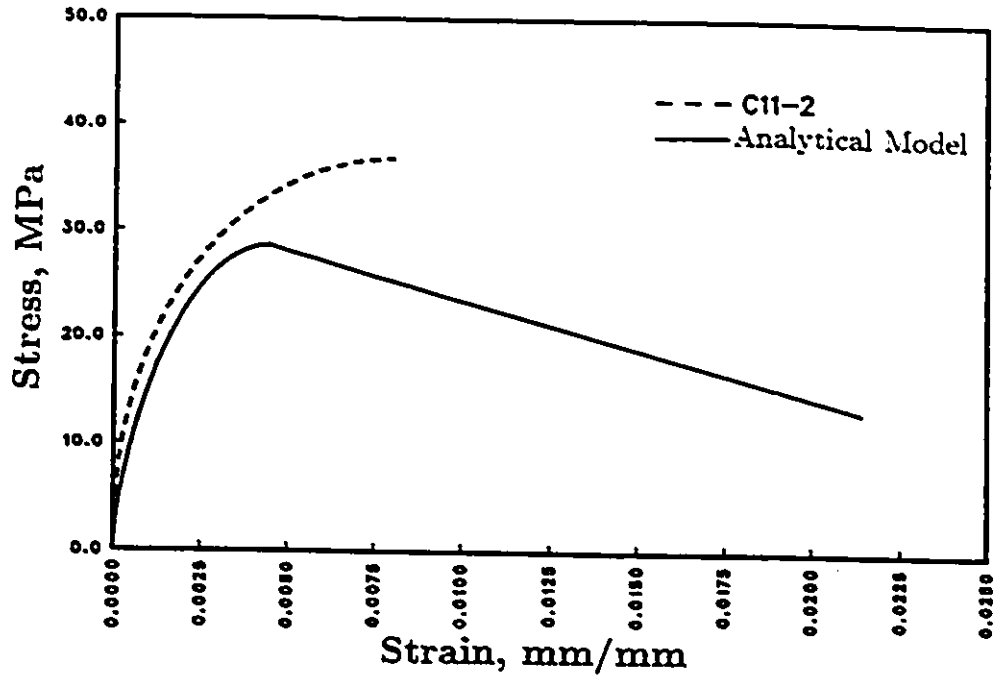

Figure 4.15: Stress-Strain Relationships of Core Concrete for C11-2

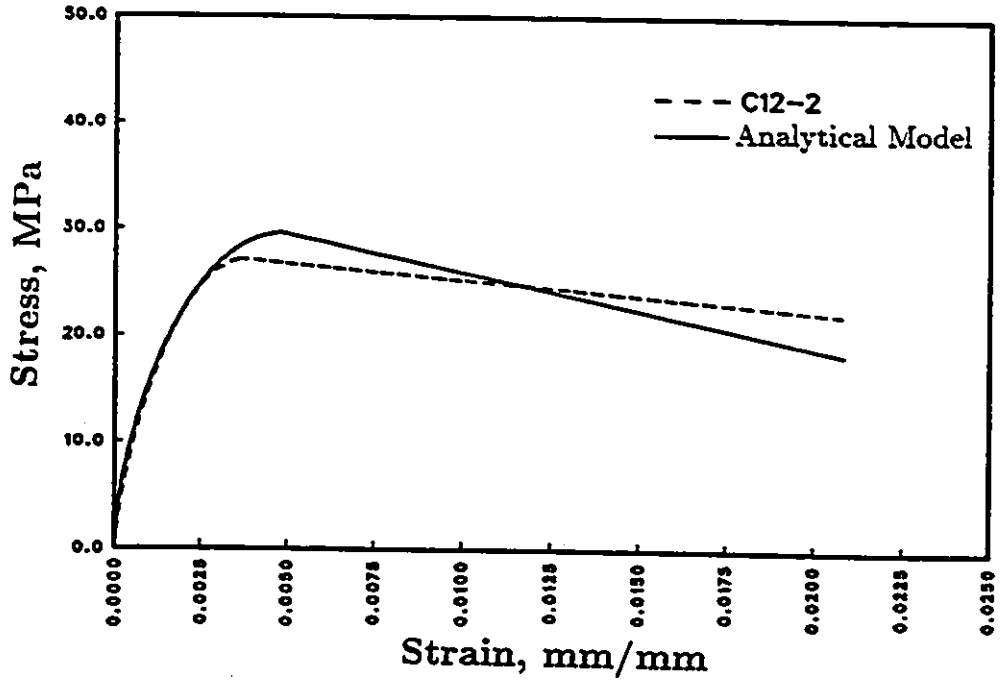

Figure 4.16: Stress-Strain Relationships of Core Concrete for C12-2

4.4 Comparisons of Experimental and Analytical Moment-Curvature Relationships

The analytical models discussed earlier were used to conduct plane section analyses to establish moment-curvature relationships. These relationships are then compared with those obtained experimentally.

The stress-strain relationship for reinforcing steel used in the analyses was that determined from tension coupon tests. The cover concrete was assigned plain concrete properties as defined by Hognestad [6]. The three confinement models discussed previously were used separately for the core concrete. The analyses were conducted using an available computer software for sectional analysis, modified for this project to handle the analytical material models discussed above.

The sectional analyses were conducted for constant levels of axial load. Selected levels of axial compression, ranging between zero and maximum experimental load, were considered. The axial load levels included load stages beyond the peak load, in the strength decay zone. Moments and corresponding curvatures at different axial load levels are then plotted to obtain moment-curvature relationships under variable axial loads. This would facilitate a meaningful comparison of the analytical and experimental results, since the experimental plots were for the case of variable axial loading. The individual moment-curvature plots for each of the selected levels of constant axial force are included in Appendix C.

The analytical and experimental moment-curvature relationships are compared in Figures 4.17 to 4.28. The results generally indicate good agreement between the experimental and analytical relationships. The Sheikh and Uzumeri model could not be used to predict the behavior of Set 2

columns. This model gave negative strain increment in establishing the strain corresponding to the peak stress, for columns with large tie spacings.

All models slightly underestimated the strength. Sheikh and Yeh model produced the closest strength prediction at the peak load region. However, it overestimated curvatures in the high deformation range, when the confinement was poor. Saatcioglu and Razvi model either underestimated or produced better predictions of response in the high inelasticity zone.

The correlation of experimental and analytical values are not affected by the eccentricity of the load. This can be seen by comparing moment-curvature relationships for columns C3-1 and C6-2, CS-1 and C11-2, and C9-1 and C12-2. It is worth noting that although Saatcioglu and Razvi model was developed for concentric loading, the predictions under different levels of eccentricity are reasonably good, implying that the level of eccentricity on column confinement is not significant. This is one the conclusions of the experimental research reported in Chapter 3.

The tie arrangement was one parameter which was not accounted for in all other models, except the model proposed by Mander, Priestley and Park [9] and the ones considered in this investigation. The comparisons of analytical and experimental moment-curvature relationships for C10-2, C11-2, and C12-2 as well as C7-1, CS-1, C8-1, and C4-2, C5-2, C6-2 illustrate that this effect was properly accounted for even under different levels of eccentricity.

In conclusion, the comparisons confirm the experimental observation that the level of eccentricity considered in this investigation, does not have a significant effect on concrete confinement. The analytical model proposed by Saatcioglu and Razvi, on the basis of concentrically loaded tests also produce good predictions of column behavior under eccentric loading. The

analytical predictions obtained by this model are very close to those obtained by Sheikh and Yeh model, which is intended for eccentric loading. Considering the complications involved in using Sheikh and Yeh model, which requires construction of concrete stress-strain relationship for every value of neutral axis location, it appears more feasible to use Saatcioglu and Razvi model for columns subjected to concentric as well as eccentric loading.

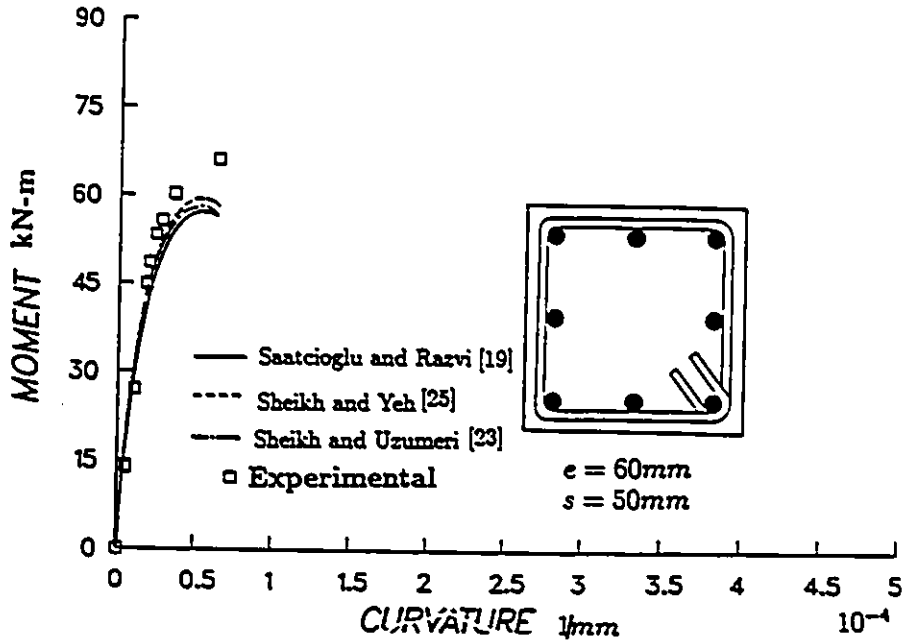

Figure 4.17: Comparison of Moment-Curvature Relationships for C1-1

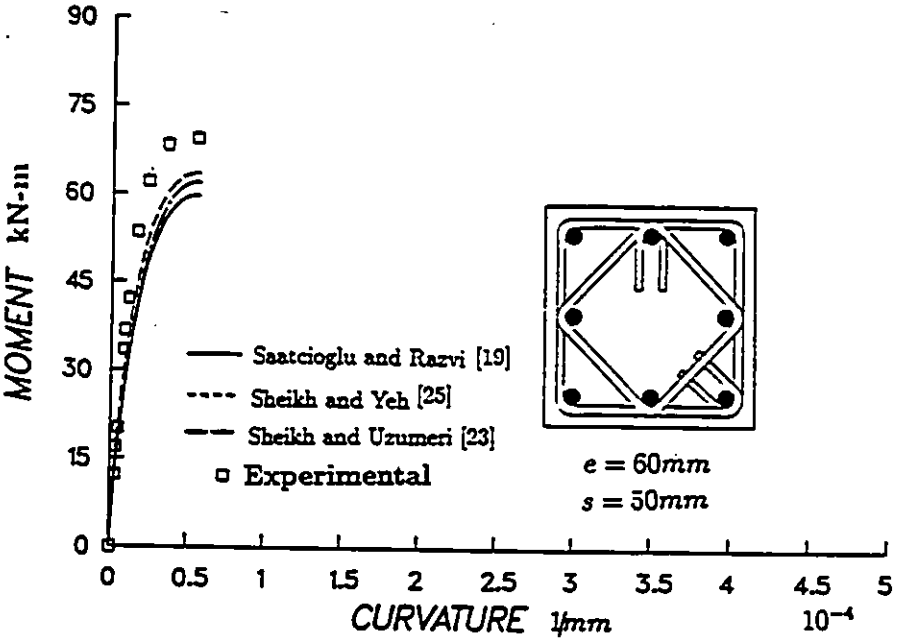

Figure 4.18: Comparison of Moment-Curvature Relationships for C2-1

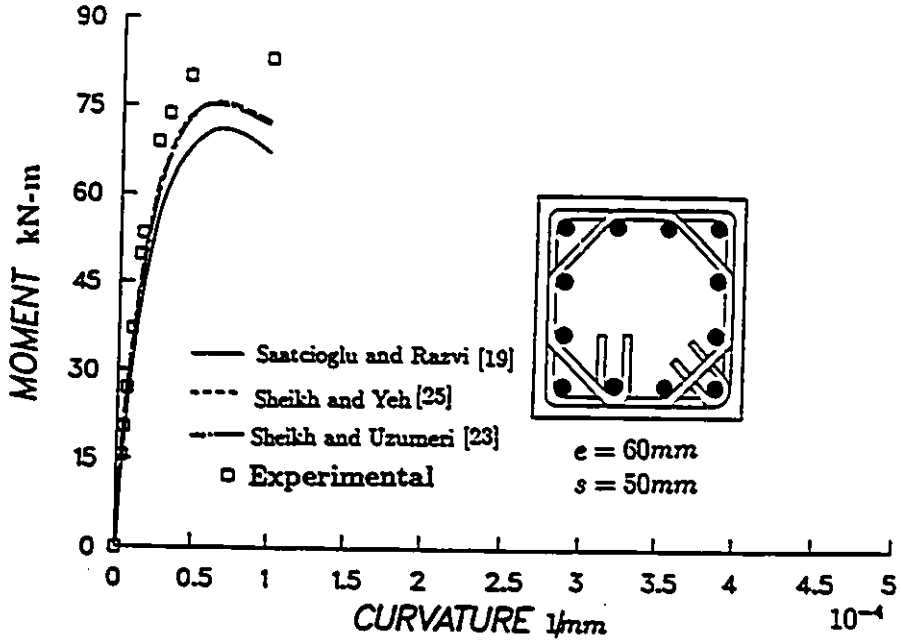

Figure 4.19: Comparison of Moment-Curvature Relationships for C3-1

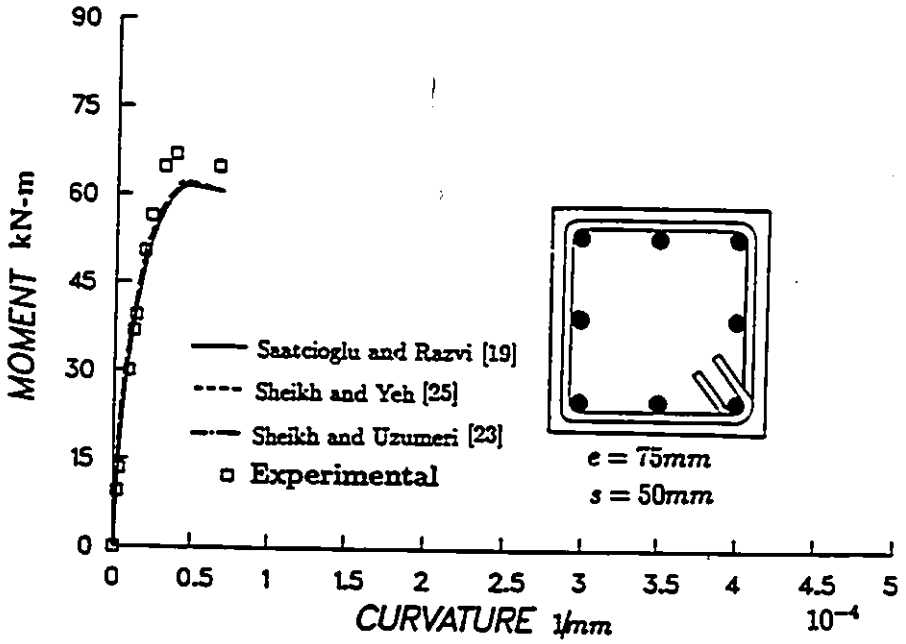

Figure 4.20: Comparison of Moment-Curvature Relationships for C4-2

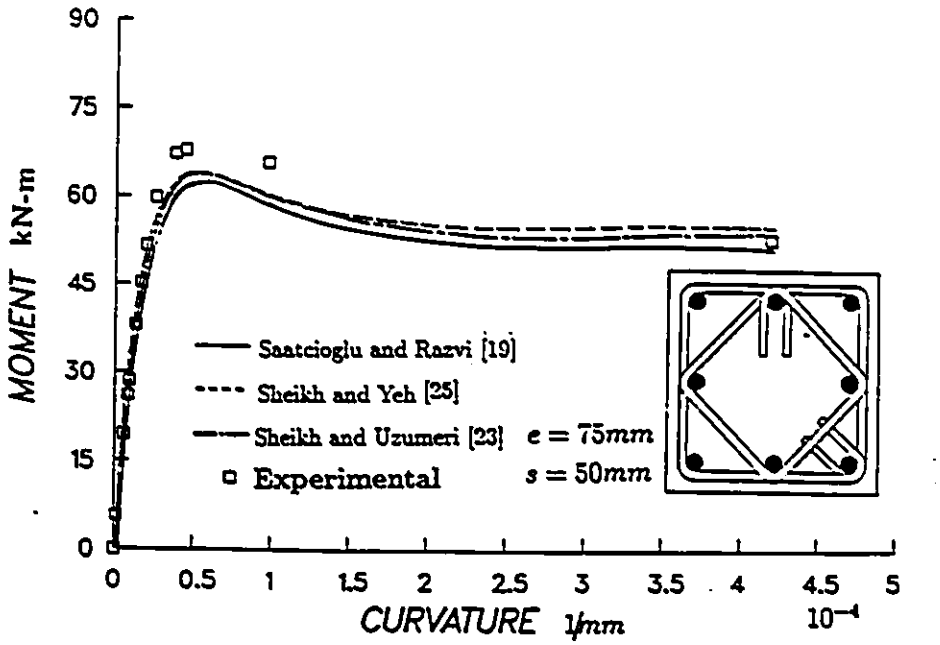

Figure 4.21: Comparison of Moment-Curvature Relationships for C5-2

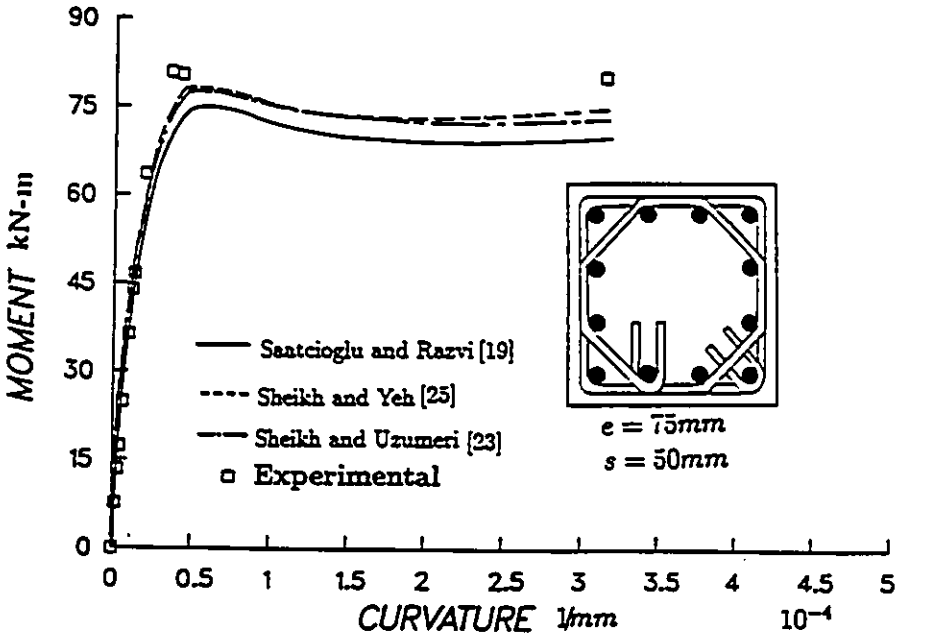

Figure 4.22: Comparison of Moment-Curvature Relationships for C6-2

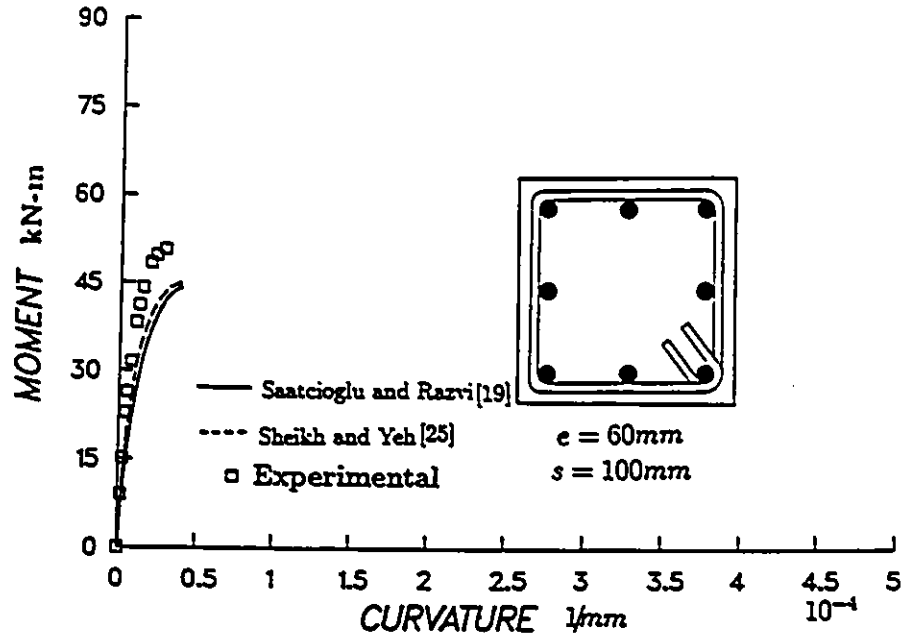

Figure 4.23: Comparison of Moment-Curvature Relationships for C7-1

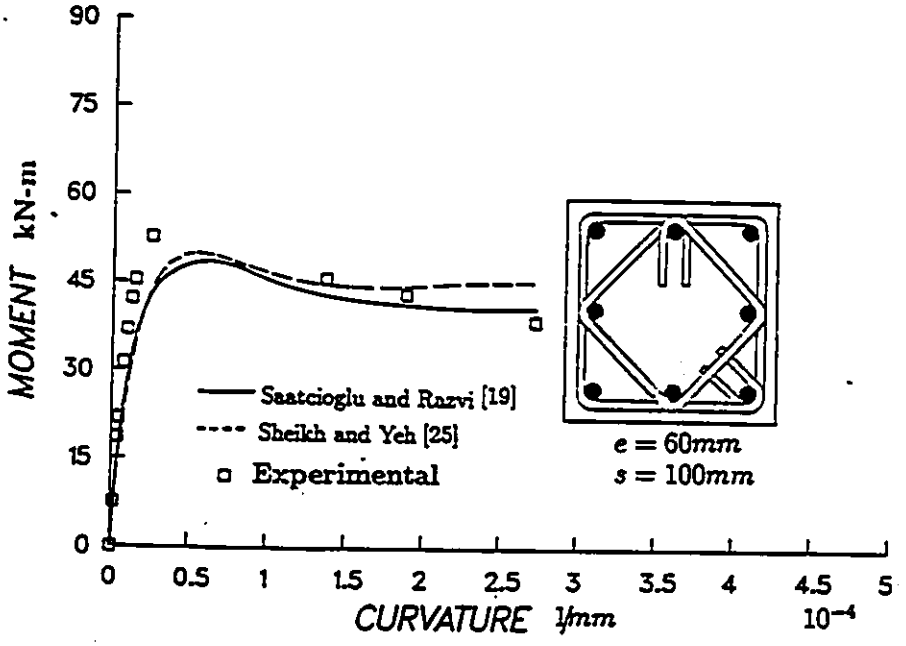

Figure 4.24: Comparison of Moment-Curvature Relationships for C8-1

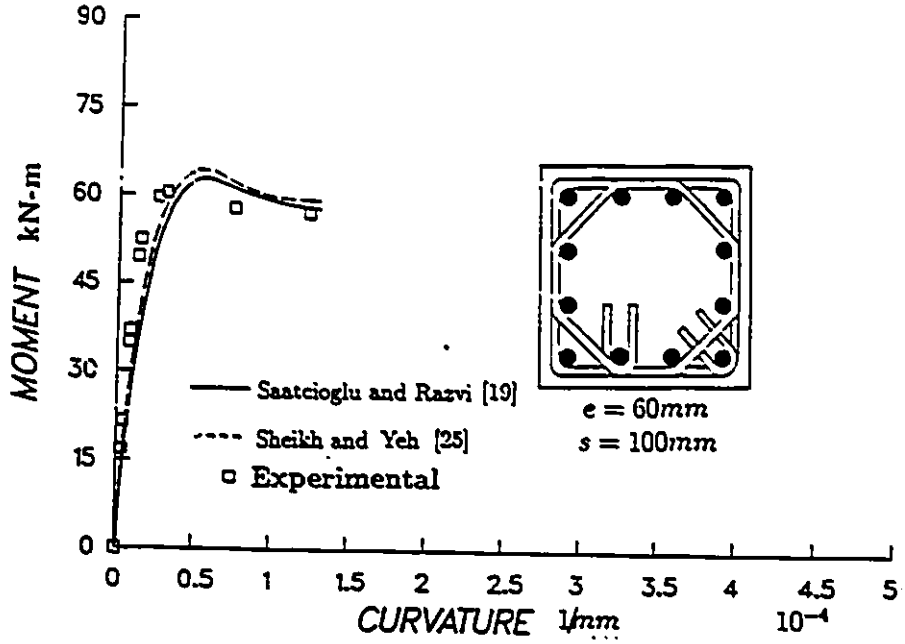

Figure 4.25: Comparison of Moment-Curvature Relationships for C9-1

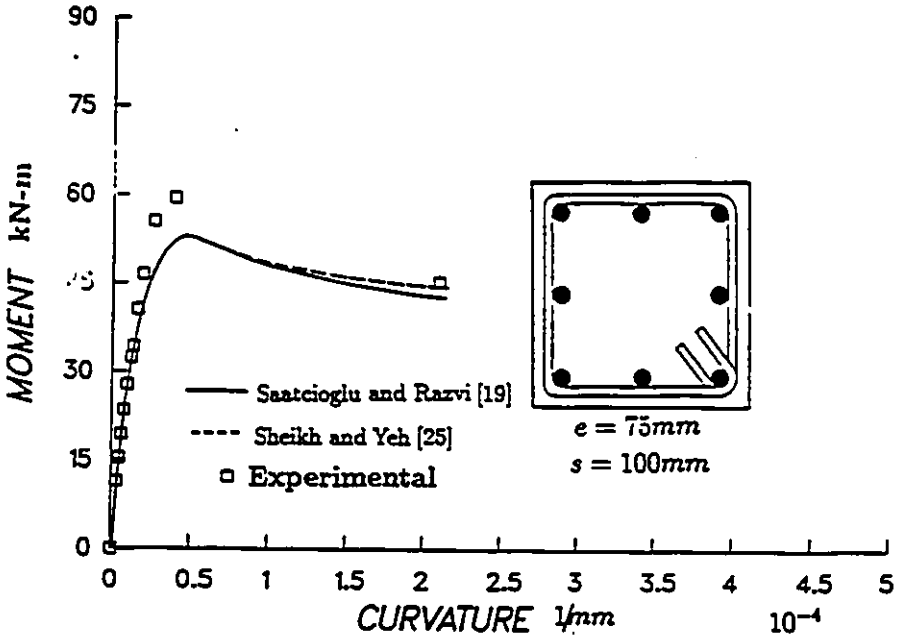

Figure 4.26: Comparison of Moment-Curvature Relationships for C10-2

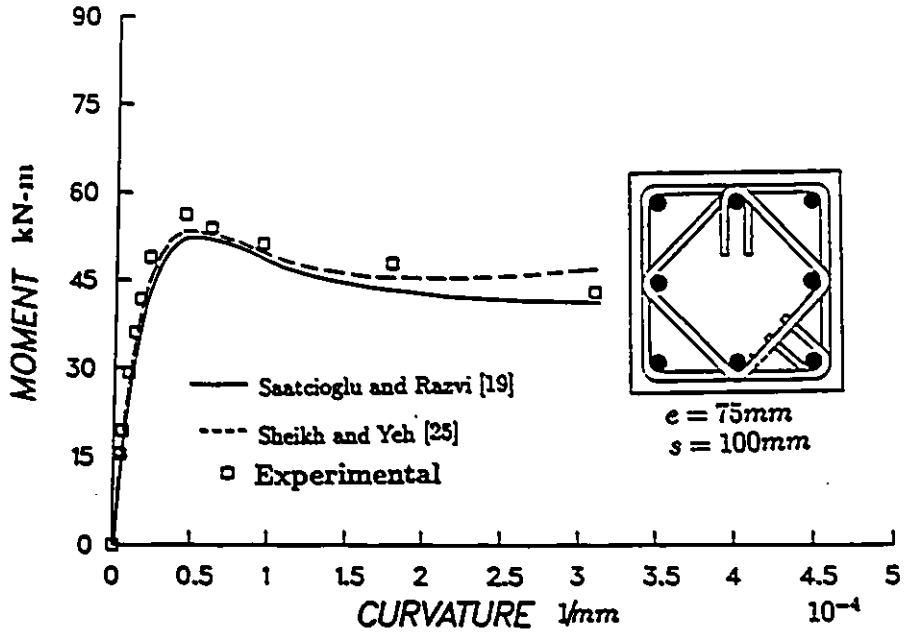

Figure 4.27: Comparison of Moment-Curvature Relationships for C11-2

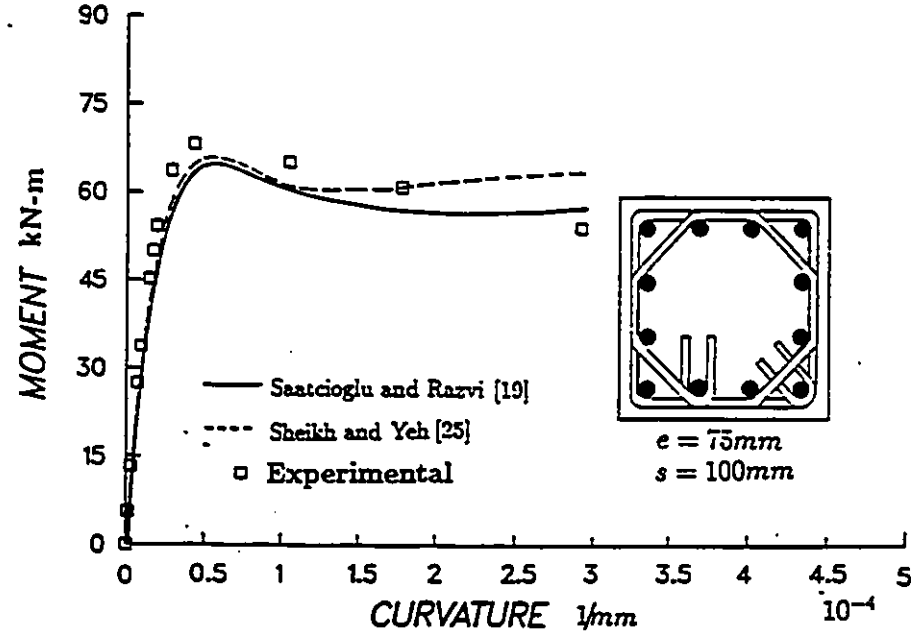

Figure 4.28: Comparison of Moment-Curvature Relationships for C12-2

Chapter 5

Recommendations and Conclusions

5.1 Conclusions

The following conclusions can be made based on the experimental and analytical investigations carried out in this research program:

1. Reduction in tie spacing and better distribution of laterally supported longitudinal reinforcement around the core perimeter enhance both strength and ductility of core concrete in reinforced concrete columns.

2. The behavior of columns under strain gradient with tie spacing of $d/2$ or larger is not affected by the arrangement of longitudinal reinforcement. However this effect has been shown to be very significant for columns with closely spaced ties. This may be explained by the effectiveness of lateral reinforcement in providing confinement pressure.

If the confinement pressure is low due to large tie spacing, any improvement in reinforcement arrangement is not sufficient to improve the confinement action.

3. The comparison of columns with two different levels of end eccentricity indicates that variation in eccentricity,within the range considered in this investigation, does not have a significant effect on stress-strain characteristics of confined concrete. This may be explained by the contribution of concrete to overall column response under eccentric loading. If the eccentricity and the resulting strain gradient is high, compressed area of column section is small. Therefore concrete plays a relatively small role on overall column response. In this case any effect of eccentricity on stress-strain characteristics of concrete is not likely to produce significant effect on column behavior. This was confirmed by comparing moment-curvature relationships of columns with different end eccentricities.

4. The confined concrete model proposed by Sheikh and Yeh [23] for eccentric loading produces column response which is in good agreement with experimental observations. The model slightly underestimates the column resistance near the peak load, and may overestimate the load in the high deformation range.

5. The confined concrete model proposed by Saatcioglu and Razvi [19] for concentric loading produces good estimates of column response under eccentric loading, within the range of eccentricity considered in this investigation. The model slightly underestimates the column resistance near the peak load and may underestimate the load resistance in high inelastic deformation range.

6. Although both Sheikh and Yeh, and Saatcioglu and Razvi Models produce good analytical predictions of experimental column response, Sheikh and Yeh model requires construction of concrete stress-strain

model for each load stage under changing neutral axis location and hence can be impractical especially for manual calcultions.

7. Sheikh and Uzumeri model for confined concrete is not applicable to poorly confined columns with large spacing of ties. Otherwise this model, although derived for concentric loading, produces good estimates of column response under eccentric loading.

5.2 Design Recommendations

Confinement steel requirements of building codes [30,31] are based on early research conducted by Richart et al. [16] in 1928. Accordingly, the amount of confinement steel is determined to make up for the loss in column capacity due to cover spalling by confinement of core concrete. This design criterion was established for spirally reinforced columns, and the empirical expression suggested for the required confinement steel was based on column tests under concentric loading. The same design requirement is also used for columns with rectilinear reinforcement under strain gradient due to lack of a rational concrete model for confined concrete, also applicable to eccentric loading.

The experimental and analytical research reported in this thesis clearly illustrates that the strain gradient effect on concrete stress-strain relationship is small. Confinement models, developed on the basis of concentric testing which include all the relevant parameters of confinement can be used to carry out plane section analysis to establish force-deformation relationships of columns. This provides a sound analytical tool to compute ductility capacities of columns under monotonic eccentric loading. It is therefore recommended that the confinement steel requirements of columns subjected to lateral load reversals be established from analyses of sections using a

proper confined concrete model, rather than using the arbitrary design criterion on which the current building codes are based on. Such analysis can be used to establish the acceptable ranges for confinement parameters, including the volumetric ratio of steel, and spacings of lateral and laterally supported longitudinal reinforcements.

The experimental results of this thesis indicates that the distribution of closely spaced and laterally supported longitudinal reinforcement improves column deformability as much as the improvement expected from the reduction in the spacing. The current design requirements of building codes place an upper limit of 100 mm for tie spacing in seismic resistant columns. This results in sever congestion of steel in the critical plastic zones of columns and sometimes leads to concrete placement problems. It is therefore recommended that the spacing limitations for ties be relaxed and the confinement of concrete is ensured by proper distribution of longitudinal reinforcement. The volumetric steel ratio requirements of building codes appear to provide satisfactory behavior of columns under eccentric loading.

5.3 Recommendations for Future Research

The experimental investigation reported in this thesis forms one of the few research programs conducted to study the effect of strain gradient on concrete confinement. Therefore, there is need for further research in the area. The following are recommended for future research:

- Tests of columns under constant compression and reversed cyclic loading, especially in the high axial load range.
- Tests of columns with circular and rectangular cross-sections.

- Experimental investigation of columns with unequal transverse reinforcement in two orthogonal directions.
- Column tests under compression cycles.
- Comprehensive analytical parametric investigation using a confined concrete model to establish the limits of design parameters.

Bibliography

[1] Bertero, V.V.,Felippa, C.,*Discussion of Ductility of Concrete by H.E.H. Roy and M.A. Sozen* , Proceedings of the International Symposium on Flexural Mechanics of Reinforced Concrete. ASCE-ACI. Miami, November 1964,pp. 227-234

[2] Chan, W.L., *The Ultimate Strength and Deformation of Plastic Hinges in Reinforced Concrete Frameworks* , Magazine of Concrete Research. Vol.7, No.21, November 1955,pp. 121-132

[3] Clark, L.E.,Gerstle, K.H. and Tulin, L.G., *Effect of Strain Gradient on the Stress-Strain Curve of Mortar and Concrete* , ACI Journal, Vol.64. No.9, September 1967,pp. 580-586

[4] Ersoy, U.,Tankut, T. and Uzumari, M.S., *Stress-Strain Relationship for Confined Concrete Under Cyclic Loading and Strain Gradient*

[5] Fafitis, A.,Shah, S.P., *Prediction of Ultimate Behavior of Confined Concrete Columns Subjected to Large Deformation* , ACI Journal. Vol.82, July-August 1985,pp. 423-433

[6] Hognestad, E.,Hanson, N.W. and Mc Henry, D., *Concrete Stress Distribution in Ultimate Strength Design* , ACI Journal, December 1955,pp. 455-479

[7] Karsan, I.D.,Jirsa, J.O., *Behavior of Concrete Under Varing Strain Gradients* , Proceeding of ACI, August 1970,pp. 1675-1696

[8] Kent, D.C.,Park, R., *Flexural Members with Confined Conrete* , ASCE. Vol.97, 1971,pp. 1969-1990

[9] Mander, J.B., Park, R. and Priestley, M.J.N, *Theroretical Stress-Strain Model for Confined Concrete* , Journal of Structural Engineering, Vol.114, No.8, August 1988

[10] Ozcebe, G.,Saatcioglu, M., *Confinement of Concrete Columns for Seismic Loading* , ACI Structural Journal, Vol.84, No.4, July-August 1987,pp. 308-315

[11] Park, R., *A Discussion by R. Park, A. Fafits and S.P. Shah with A.S. Shiekh* , ACI Journal, May-June 1983,pp. 260-265

[12] Park, R.,Paulay, T., *Reinforced Concrete Structures* , John Wiley and Sons, Newyork, Chichester, Brisbane, Toronto, Singapore , 1975

[13] Pillai, S.U.,Kirk, D.W., *Reinforced Concrete Design in Canada* . McGraw-Hill, Ryerson Limited 1983

[14] Park, R.,Nigel, M.J. and Gill, W.D., *Ductility of Square Confined Concrete Columns* , ASCE, Vol.108, No.St4, April 1982,pp. 929-951

[15] Razvi, S., *Behavior of reinforced Concrete Columns Confined with WWF* , A thesis presented to the University of Ottawa in January 1988,in partial fulfillment of the requirements for the degree of M.A.Sc.

[16] Richart, F.E., Brandtzaeg, A. and Brown, R.L., *A Study of the Failure of Concrete under Combined Compressive Stresses*, , Bulletin 185. University of Illinois, Engineering Experimental 1928 , 104 pp.

[17] Roy, H.E.H., Sozen, M.A., *Ductility of Concrete.* , Proceedings of The International Symposium on Flexural mechanics of Reinforced Concrete, ASCE-ACI, Miami, November 1964.pp. 213-224

[18] Rüch, H., *Researches Towards a General Flexural Theory for Structural Concrete* , ACI Journal, Vol. 57, No.1, July 1960.pp. 1-28

[19] Saatcioglu, M., Razvi, S., *Strength and Ductility of Confined Concrete.* Submitted to ASCE Structural Journal for publication, 1990

[20] Sargin, M., Ghosh, S.K., Handa, V.K., *Effects of lateral Reinforcement Upon the Strength and Deformation Properties of Concrete.* Magazine of Concrete Research, Vol.23, 1971, pp. 99-110

[21] Scott, B.D., Park, R. and Priestly, M.J.N., *Stress-Strain Behavior of Concrete Confined by Overlapping Hoops at Low and High Strain Rates,* ACI Journal, Proceedings, Vol.79, No.1, January-Febuary 1982,pp. 13-27

[22] Sheikh, A.S., *Effectiveness of Rectangular Ties as Confinement Steel in Reinforced Concrete Columns.* A thesis presented to the University of Toronto in 1978 in partial fullfillment of the requirement for the degree of PhD.

[23] Shiekh, A.S., Usumari, S.M., *Strength and Ductility of Tied Concrete Columns,* Journal of Structural Division, May 1980, pp. 1079-1103

[24] Sheikh, A.S., *A Comparative Study of Confinement Models,* ACI Journal, July-August 1982, pp. 296-305

[25] Sheikh, A.S., Yeh, C.C., *Flexural Behavior of Confined Concrete,* ACI Journal , May-June 1986, pp.389-404

[26] Sheikh, A.S., Yeh, C.C., and Menzies, D., *Confined Concrete Columns.* Pacific Conference on Earthquake Engineering, Wairakei New Zealand, August 27,1986, Vol.1, pp.177-188

[27] Soliman, M.T.M., Yu, C.W., *The Flexural Stress-Strain Relationship of Concrete Confined by Rectangular transeverse Reinforcement*, Magazine of ConcreteResearch, Vol.19, No.61,December 1967, pp.223-238

[28] Struman, G.M., Shah, S.P. and Winter, G., *Effects of Flexural Strain Gradients on Microcracking and Stress-Strain Behavior of Concrete*. Journal of ACI, July 1965, pp. 805-822

[29] Vallenas, J., Bertero, V.V., Popov, E.P., *Concrete Confined by Rectangular Hoops and Subjected to Axial Loads*, Report No. UCB/EERC 77/13, Earthquake Engineering Research Centre, College of Engineering, University of Berkeley, August 1977, 114 pp.

[30] *Building Code Requirements for Reinforeced Concrete* (ACI 318-89). American Concrete Institute, Box 19150, Redford Station, Detroit. Michigan, U.S.A.

[31] *Design of Concrete Structures for Buildings* (CSA-A23.3 M84), Canadian Standards Association, Rexdale, Dec. 1984, 281 pp.

[32] Sargin, M.,*Stress-strain Relationships for Concrete and the Analysis of Structural Concrete Sections*, study No. 4, Solid Mechanics Division. University of Waterloo, 1971, 167 pp.

APPENDIX A

Experimental Data

The test data consisted of applied axial load and corresponding measured strains at the critical section. A computer program was written to evaluate test data. The force contribution by the longitudinal steel and cover concrete was subtracted from the total column force to quantify the force carried by core concrete. The core concrete strain at the compression side was also calculated using the strain profiles at the critical section. Core force-core strain relationships for all the columns tested here are presented in this appendix.

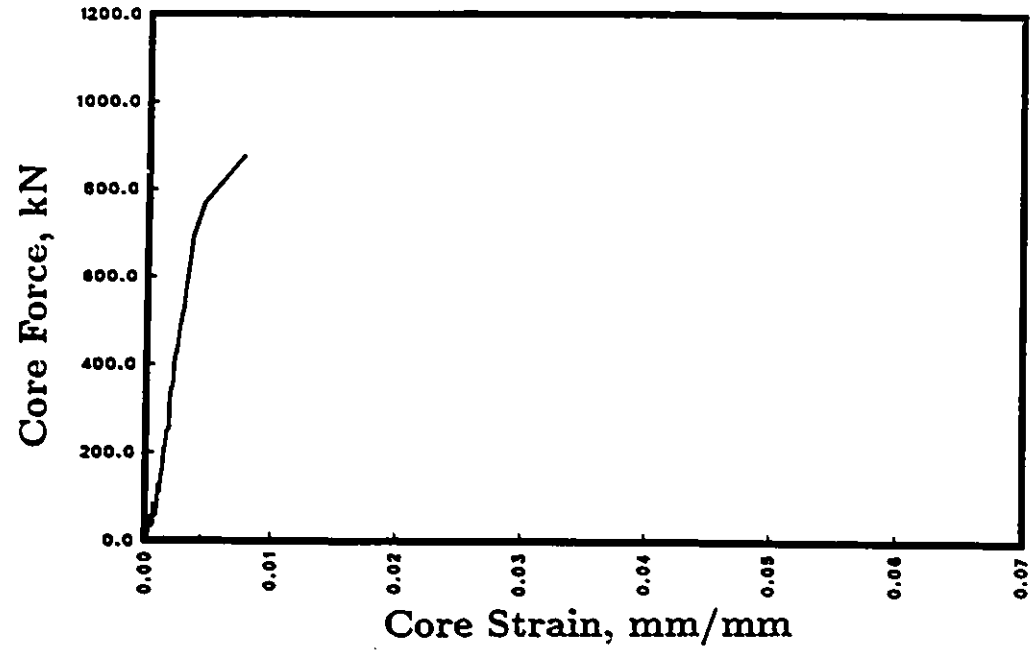

Figure A.1: Core Force-Core Strain Relationship for C1-1

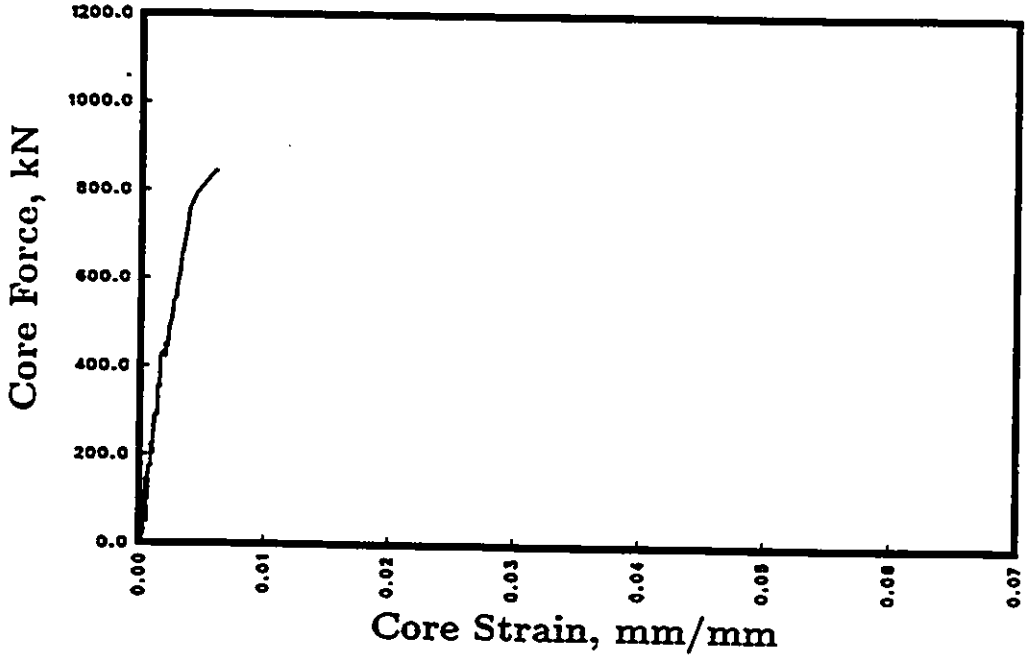

Figure A.2: Core Force-Core Strain Relationship for C2-1

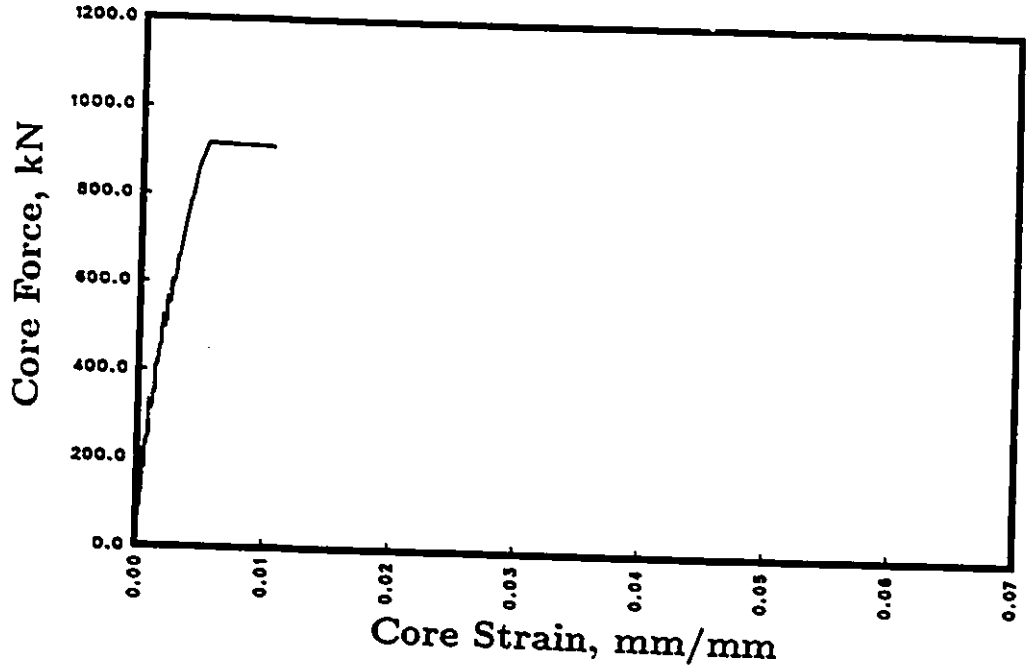

Figure A.3: Core Force-Core Strain Relationship for C3-1

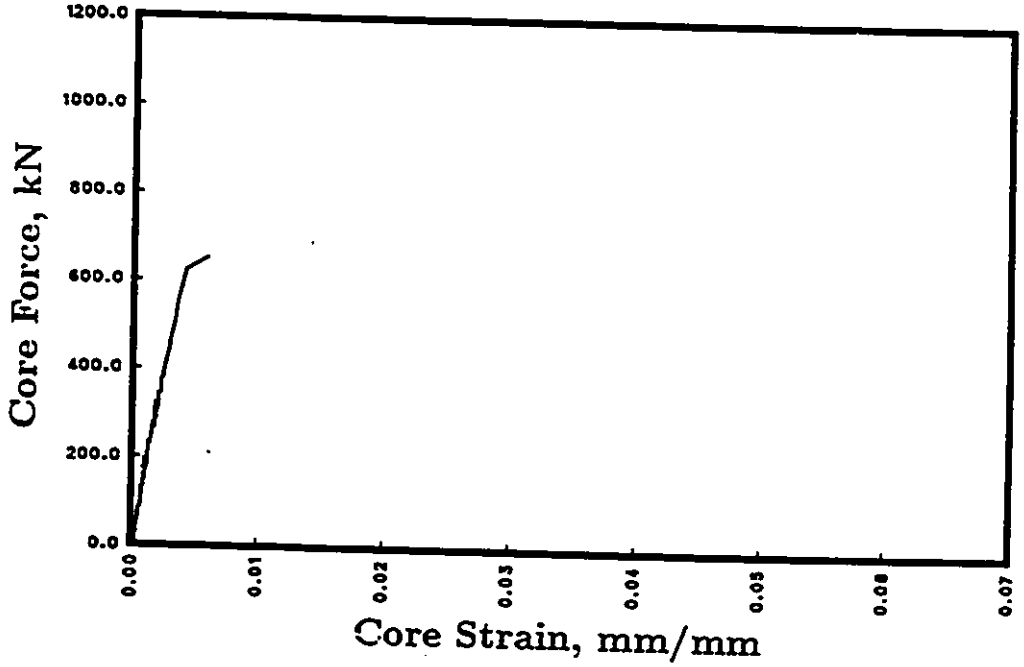

Figure A.4: Core Force-Core Strain Relationship for C4-2

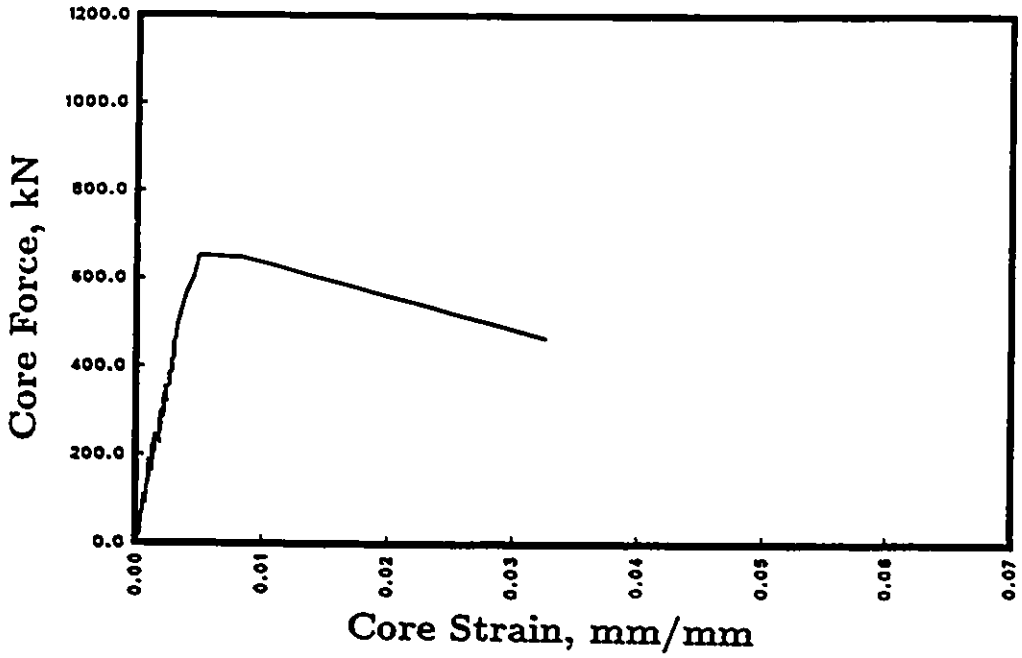

Figure A.5: Core Force-Core Strain Relationship for C5-2

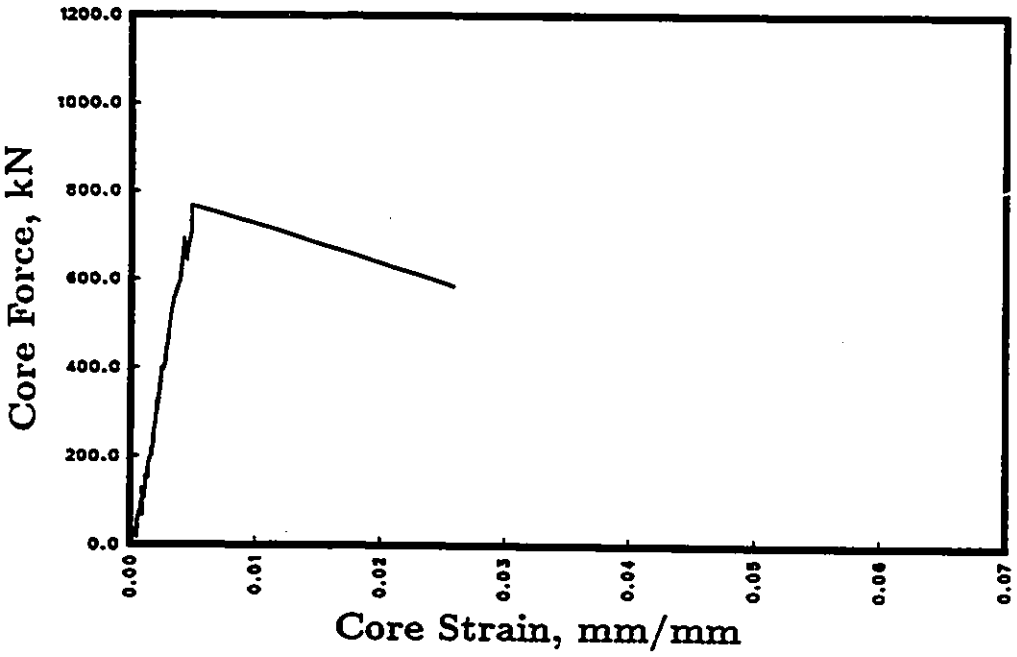

Figure A.6. Core Force-Core Strain Relationship for C6-2

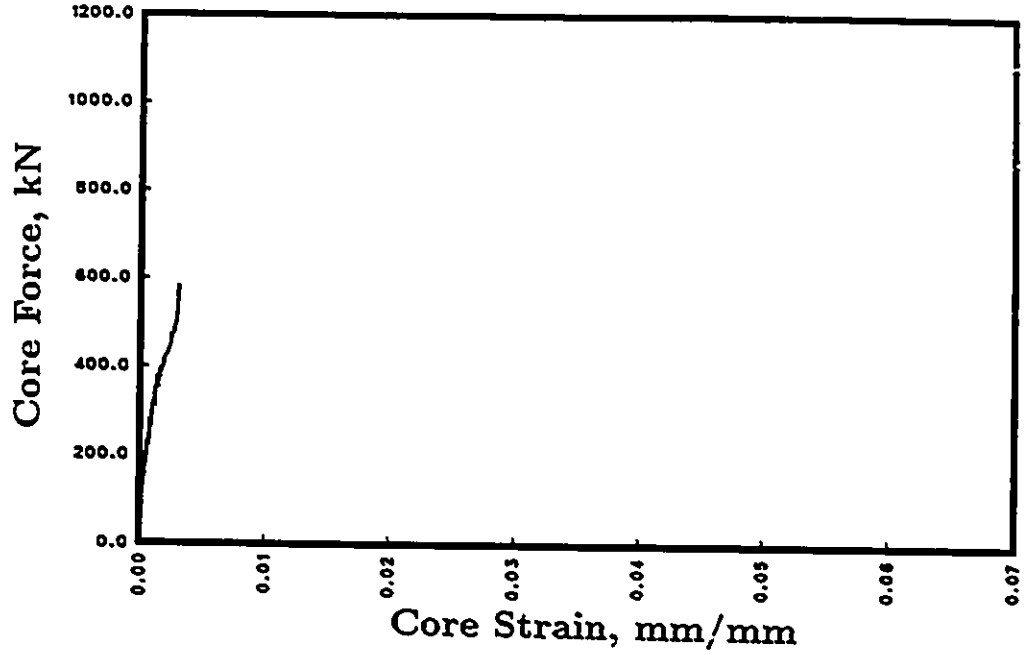

Figure A.7: Core Force-Core Strain Relationship for C7-1

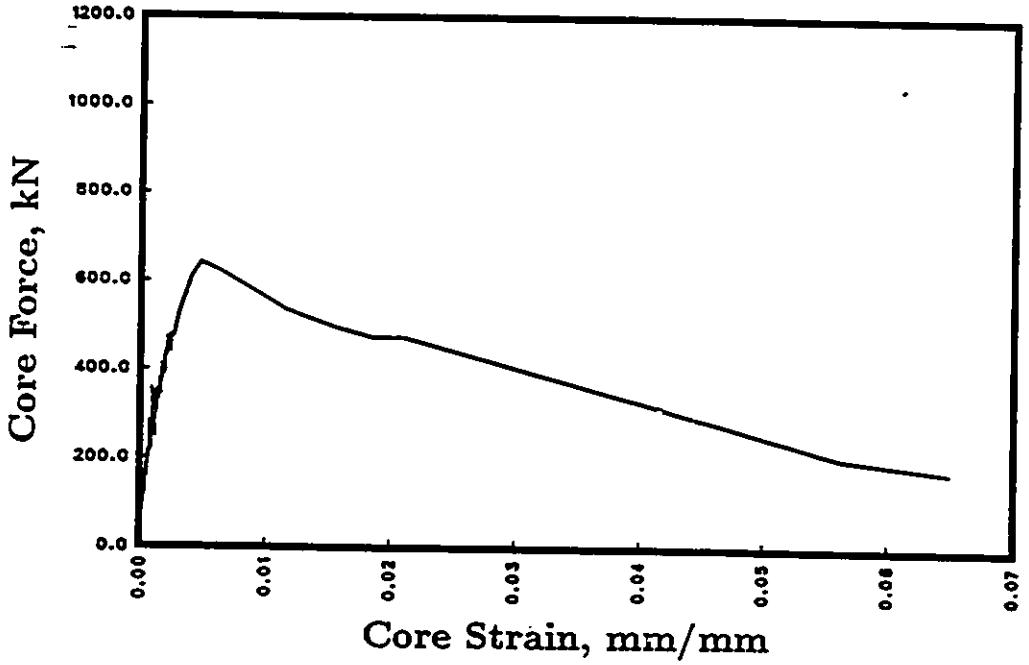

Figure A.8: Core Force-Core Strain Relationship for C8-1

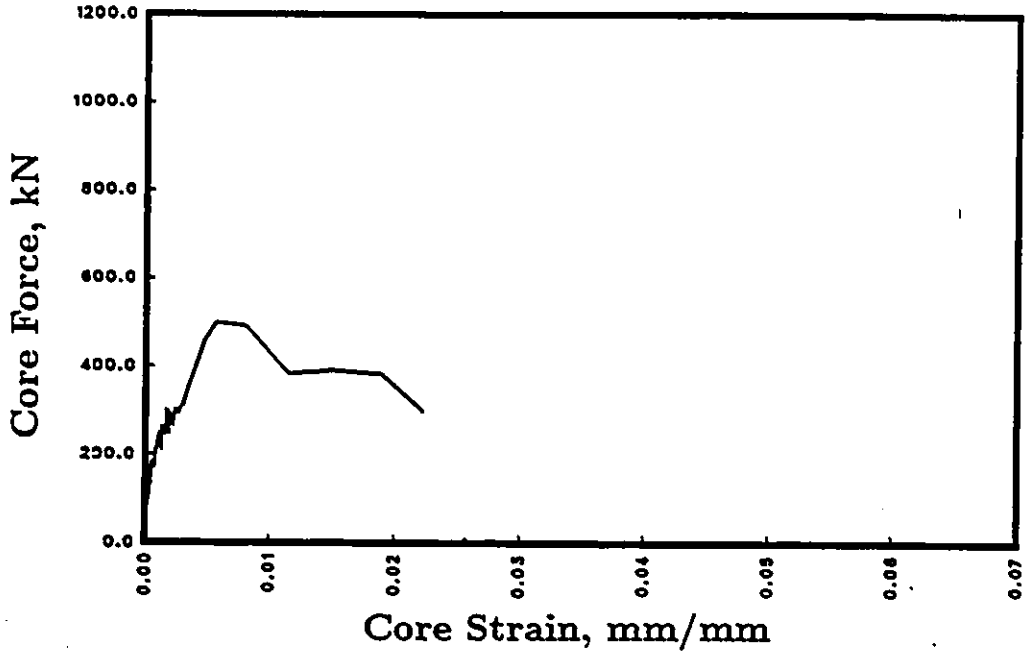

Figure A.9: Core Force-Core Strain Relationship for C9-1

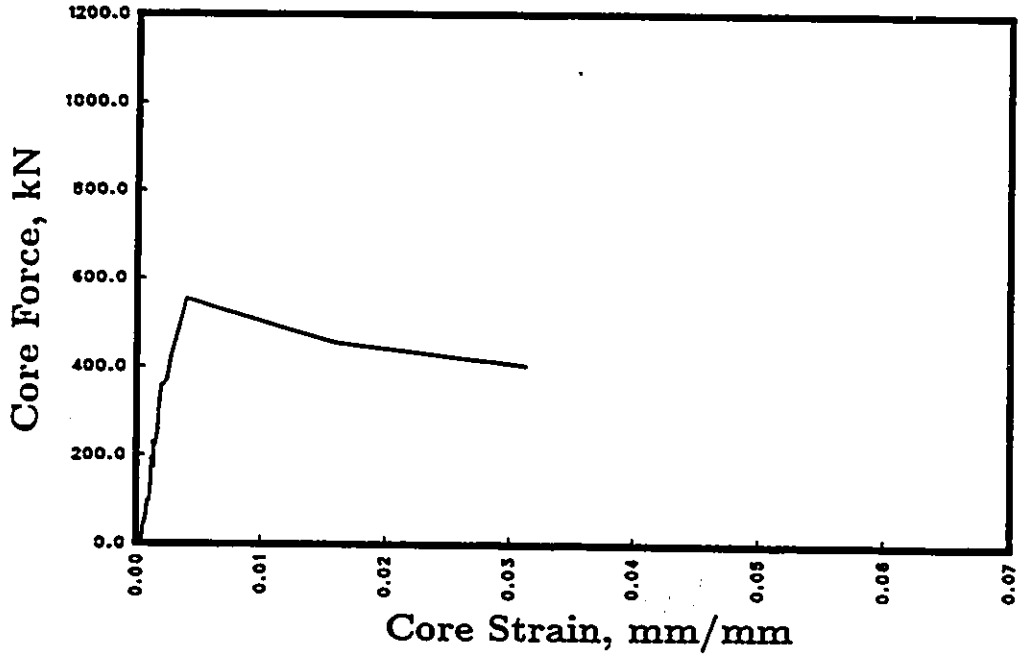

Figure A.10: Core Force-Core Strain Relationship for C10-2

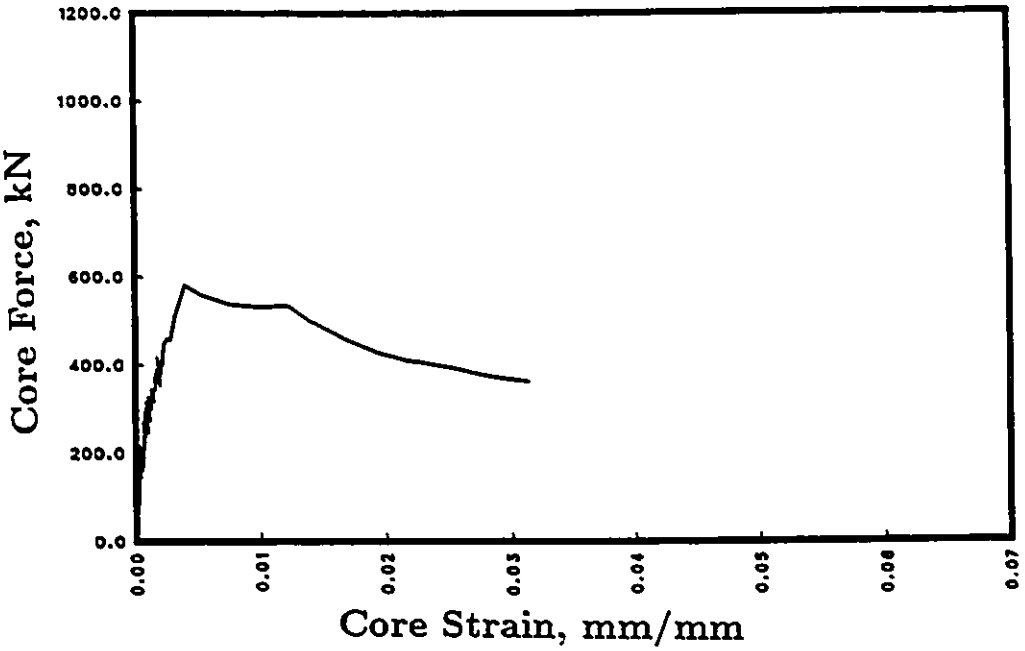

Figure A.11: Core Force-Core Strain Relationship for C11-2

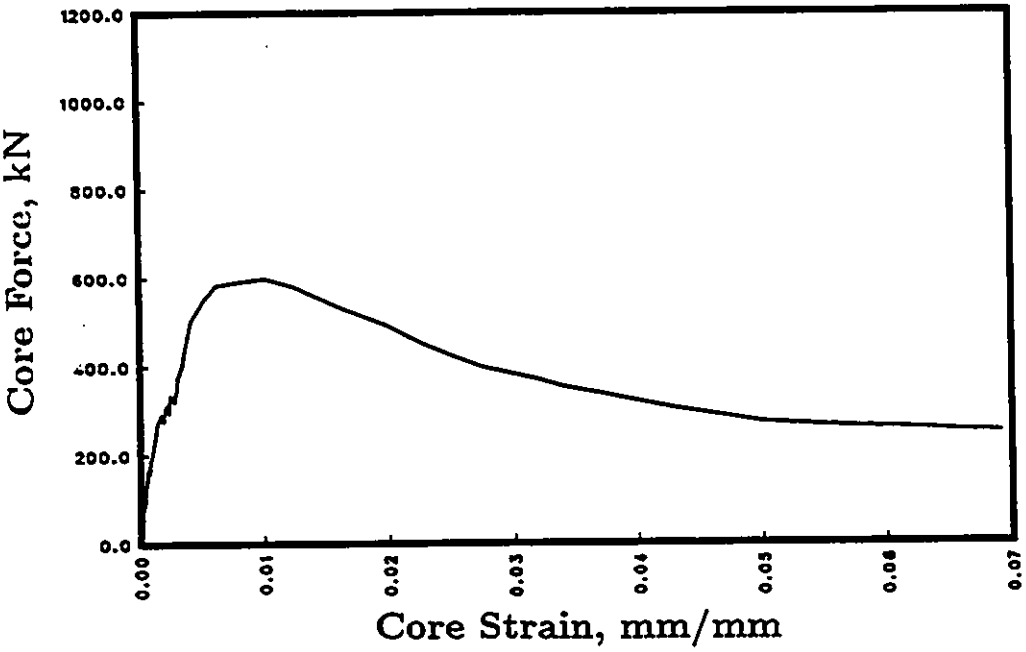

Figure A.12: Core Force-Core Strain Relationship for C12-2

.APPENDIX B

RECTANGULAR STRESS BLOCK PARAMETERS FOR CONFINED CONCRETE STREES-STRAIN RELATIONSHIP

It is a common practice to compute flexural strength of reinforced concrete members through plane section analysis using a rectangular stress-block for concrete. Building Codes [30.31] provide coefficients to convert actual parabolic stress distribution of compressed concrete to an equivalent rectangular stress distribution at ultimate. These coefficients are valid for unconfined concrete at ultimate condition where the ultimate capacity is assumed to take place at a maximum fiber strain of $0.003 mm/mm$. Therefore, an engineer has to integrate the actual parabolic stress-strain relationship for service load calculations and also for calculations involving confined concrete.

An equivalent rectangular stress block can be established for stress-strain relationships other than that commonly used in practice. Furthermore, rectangular stress blocks can also be established for service load conditions, prior to reaching ultimate. The essential requirements are the equivalence in force and lever arm of the compressed concrete. Coefficient α and γ can be derived to obtain forces and moments by using a rectangular stress block that will be equivalent to using the actual stress-strain relationship. The following expressions can be used to determine these parameters:

$$C = \alpha f'_c bc = \int_0^{\epsilon_{cc}} f_c d\epsilon_c \tag{B.1}$$

Then:

$$\alpha = \frac{\int_0^{\epsilon_{cc}} f_c d\epsilon_c}{f'_c bc} \tag{B.2}$$

and

$$M = \gamma C \tag{B.3}$$

$$\gamma = 1 - \frac{\int_0^{\epsilon_{cc}} \epsilon_c f_c d\epsilon_c}{\epsilon_c \int_0^{\epsilon_{cc}} f_c d\epsilon_c} \tag{B.4}$$

It is clear form the above expressions that both α and γ are functions of the extreme fiber strain ϵ_{cc}. These parameters have been derived for the analytical stress-strain relationship proposed by Saatcioglu and Razvi [19].

The parameters tabulated in Tables B.1 to B.40 provide convenient means of predicting sectional response manually for any concrete extreme fiber strain.

Table B.1: Stress Block Parameter α for $\epsilon_c \leq \epsilon_1$

ϵ_c	ϵ_1								
	0.0020	0.0025	0.0030	0.0035	0.0040	0.0045	0.0050	0.0055	0.0060
	Strength Enhacement Factor K								
	0.00	0.05	0.10	0.15	0.20	0.25	0.30	0.35	0.40
0.0005	0.229	0.214	0.208	0.208	0.211	0.215	0.221	0.227	0.234
0.0010	0.417	0.376	0.354	0.341	0.335	0.333	0.333	0.336	0.339
0.0015	0.562	0.506	0.471	0.448	0.434	0.425	0.421	0.419	0.419
0.0020	0.667	0.608	0.566	0.536	0.516	0.502	0.493	0.487	0.483
0.0025		0.684	0.642	0.609	0.584	0.566	0.554	0.545	0.539
0.0030			0.700	0.668	0.641	0.621	0.606	0.595	0.586
0.0035				0.714	0.689	0.668	0.651	0.638	0.628
0.0040					0.727	0.707	0.722	0.675	0.664
0.0045						0.739	0.722	0.708	0.696
0.0050							0.750	0.736	0.724
0.0055								0.760	0.748
0.0060									0.769
0.0065									
0.0070									
0.0775									
0.0080									
0.0085									
0.0090									
0.0095									
0.0100									

Table B.2: Stress Block Parameter α for $\epsilon_c \leq \epsilon_1$ Cont.

ϵ_c	ϵ_1							
	0.0065	0.0070	0.0075	0.0080	0.0085	0.0090	0.0095	0.0100
	Strength Enhacement Factor K							
	0.45	0.50	0.55	0.60	0.65	0.70	0.75	0.80
0.0005	0.242	0.249	0.257	0.265	0.273	0.281	0.288	0.296
0.0010	0.344	0.349	0.354	0.360	0.366	0.372	0.378	0.385
0.0015	0.420	0.422	0.425	0.429	0.433	0.437	0.442	0.447
0.0020	0.482	0.482	0.483	0.484	0.487	0.489	0.493	0.486
0.0025	0.535	0.532	0.531	0.531	0.532	0.533	0.535	0.537
0.0030	0.580	0.576	0.573	0.572	0.571	0.571	0.572	0.573
0.0035	0.620	0.614	0.610	0.607	0.605	0.604	0.604	0.604
0.0040	0.655	0.648	0.643	0.639	0.636	0.634	0.632	0.632
0.0045	0.686	0.678	0.672	0.667	0.663	0.660	0.658	0.657
0.0050	0.714	0.705	0.698	0.692	0.688	0.684	0.682	0.679
0.0055	0.738	0.729	0.722	0.715	0.710	0.706	0.703	0.760
0.0060	0.759	0.750	0.742	0.736	0.730	0.726	0.722	0.719
0.0065	0.777	0.769	0.761	0.755	0.749	0.744	0.740	0.736
0.0070		0.785	0.778	0.771	0.765	0.760	0.756	0.752
0.0775			0.793	0.786	0.780	0.775	0.771	0.767
0.0080				0.800	0.794	0.789	0.784	0.780
0.0085					0.806	0.801	0.796	0.792
0.0090						0.812	0.807	0.803
0.0095							0.818	0.814
0.0100								0.823

Table B.3: Stress Block Parameter γ for $\epsilon_c \leq \epsilon_1$

ϵ_c	ϵ_1								
	0.0020	0.0025	0.0030	0.0035	0.0040	0.0045	0.0050	0.0055	0.0060
	Strength Enhacement Factor K								
	0.00	0.05	0.10	0.15	0.20	0.25	0.30	0.35	0.40
0.0005	0.341	0.349	0.357	0.365	0.371	0.377	0.383	0.388	0.393
0.0010	0.350	0.356	0.362	0.369	0.374	0.380	0.385	0.390	0.395
0.0015	0.361	0.363	0.368	0.373	0.378	0.383	0.388	0.392	0.396
0.0020	0.375	0.372	0.374	0.378	0.382	0.386	0.390	0.394	0.398
0.0025		0.383	0.381	0.383	0.386	0.389	0.393	0.397	0.400
0.0030			0.390	0.389	0.390	0.393	0.396	0.399	0.402
0.0035				0.396	0.395	0.397	0.399	0.402	0.404
0.0040					0.401	0.401	0.402	0.404	0.407
0.0045						0.406	0.406	0.408	0.409
0.0050							0.410	0.411	0.412
0.0055								0.414	0.415
0.0060									0.418
0.0065									
0.0070									
0.0775									
0.0080									
0.0085									
0.0090									
0.0095									
0.0100									

Table B.4: Stress Block Parameter γ for $\epsilon_c \leq \epsilon_1$ Cont.

ϵ_c	ϵ_1							
	0.0065	0.0070	0.0075	0.0080	0.0085	0.0090	0.0095	0.0100
	Strength Enhacement Factor K							
	0.45	0.50	0.55	0.60	0.65	0.70	0.75	0.80
0.0005	0.397	0.401	0.405	0.408	0.412	0.415	0.417	0.420
0.0010	0.399	0.403	0.406	0.409	0.413	0.415	0.418	0.421
0.0015	0.400	0.404	0.407	0.411	0.414	0.416	0.419	0.422
0.0020	0.402	0.405	0.409	0.412	0.415	0.417	0.420	0.422
0.0025	0.404	0.407	0.410	0.413	0.416	0.418	0.421	0.423
0.0030	0.405	0.408	0.411	0.414	0.417	0.419	0.422	0.424
0.0035	0.407	0.410	0.413	0.415	0.418	0.420	0.423	0.425
0.0040	0.409	0.412	0.414	0.417	0.419	0.421	0.424	0.426
0.0045	0.411	0.414	0.416	0.418	0.420	0.422	0.425	0.427
0.0050	0.414	0.416	0.418	0.420	0.422	0.424	0.426	0.427
0.0055	0.416	0.418	0.419	0.421	0.423	0.425	0.427	0.428
0.0060	0.419	0.420	0.421	0.423	0.424	0.426	0.428	0.429
0.0065	0.421	0.422	0.423	0.424	0.426	0.427	0.429	0.430
0.0070		0.424	0.425	0.426	0.427	0.429	0.430	0.432
0.0775			0.427	0.428	0.429	0.430	0.431	0.433
0.0080				0.430	0.431	0.432	0.433	0.434
0.0085					0.432	0.433	0.434	0.435
0.0090						0.435	0.435	0.436
0.0095							0.437	0.438
0.0100								0.439

Table B.5 : Stress Block Parameter α for $\epsilon_c \geq \epsilon_1$

ϵ_c	$\epsilon_1 = 0.002$ and $K = 0.0$							
	Z							
	10	20	30	40	50	60	70	80
0.002	0.667	0.667	0.667	0.667	0.667	0.667	0.667	0.667
0.003	0.776	0.774	0.773	0.771	0.769	0.768	0.766	0.764
0.004	0.828	0.823	0.818	0.813	0.808	0.803	0.798	0.793
0.005	0.858	0.849	0.840	0.831	0.822	0.813	0.804	0.795
0.006	0.876	0.862	0.849	0.836	0.822	0.809	0.796	0.782
0.007	0.887	0.869	0.851	0.833	0.815	0.798	0.780	0.762
0.008	0.894	0.872	0.849	0.827	0.804	0.782	0.759	0.737
0.009	0.899	0.871	0.844	0.817	0.790	0.763	0.735	0.708
0.010	0.901	0.869	0.837	0.805	0.773	0.741	0.709	0.677
0.011	0.903	0.866	0.829	0.792	0.755	0.718	0.682	0.645
0.012	0.903	0.861	0.819	0.778	0.736	0.694	0.653	0.611
0.013	0.902	0.856	0.809	0.763	0.716	0.669	0.623	0.576
0.014	0.901	0.850	0.798	0.747	0.695	0.644	0.592	0.541
0.015	0.899	0.843	0.787	0.730	0.674	0.618	0.561	
0.016	0.897	0.836	0.775	0.713	0.652	0.591	0.530	
0.017	0.895	0.828	0.762	0.696	0.630	0.564		
0.018	0.892	0.821	0.750	0.679	0.607	0.536		
0.019	0.889	0.813	0.737	0.661	0.585			
0.020	0.886	0.805	0.724	0.643	0.562			

Table B.6 : Stress Block Parameter α for $\epsilon_c \geq \epsilon_1$ Cont.

ϵ_c	$\epsilon_1 = 0.002$ and $K = 0.0$							
	Z							
	90	100	150	200	250	300	350	400
0.002	0.667	0.667	0.667	0.667	0.667	0.667	0.667	0.667
0.003	0.763	0.761	0.753	0.744	0.736	0.728	0.719	0.711
0.004	0.788	0.783	0.758	0.733	0.708	0.683	0.658	0.633
0.005	0.786	0.777	0.732	0.687	0.642	0.597	0.552	
0.006	0.769	0.756	0.689	0.622	0.556			
0.007	0.744	0.726	0.637	0.548				
0.008	0.714	0.692	0.579					
0.009	0.681	0.654						
0.010	0.645	0.613						
0.011	0.608	0.571						
0.012	0.569	0.528						
0.013	0.530							
0.014								
0.015								
0.016								
0.017								
0.018								
0.019								
0.020								

Table B.7 : Stress Block Parameter α for $\epsilon_c \geq \epsilon_1$

ϵ_c	$\epsilon_1 = 0.0030$ and $K = 0.10$							
	Z							
	10	20	30	40	50	60	70	80
0.0030	0.700	0.700	0.700	0.700	0.700	0.700	0.700	0.700
0.0040	0.774	0.773	0.771	0.770	0.769	0.768	0.766	0.765
0.0050	0.816	0.812	0.808	0.804	0.800	0.796	0.792	0.788
0.0060	0.843	0.835	0.828	0.820	0.813	0.805	0.798	0.790
0.0070	0.860	0.849	0.837	0.826	0.814	0.803	0.791	0.780
0.0080	0.872	0.856	0.841	0.825	0.809	0.794	0.778	0.763
0.0090	0.880	0.860	0.884	0.820	0.800	0.780	0.760	0.740
0.0100	0.886	0.861	0.837	0.812	0.788	0.763	0.739	0.714
0.0110	0.889	0.860	0.831	0.802	0.773	0.744	0.715	0.685
0.0120	0.891	0.858	0.824	0.790	0.756	0.723	0.689	0.655
0.0130	0.892	0.854	0.815	0.777	0.738	0.700	0.662	0.623
0.0140	0.893	0.849	0.806	0.763	0.720	0.676	0.633	0.590
0.0150	0.892	0.844	0.796	0.748	0.700	0.652	0.604	0.556
0.0160	0.891	0.838	0.785	0.733	0.680	0.627	0.574	
0.0170	0.889	0.832	0.774	0.716	0.659	0.601	0.544	
0.0180	0.888	0.825	0.763	0.700	0.638	0.575		
0.0190	0.885	0.818	0.751	0.683	0.616	0.548		
0.0200	0.883	0.811	0.738	0.666	0.594			

Table B.8 : Stress Block Parameter α for $\epsilon_c \geq \epsilon_1$ Cont.

ϵ_c	$\epsilon_1 = 0.0030$ and $K = 0.10$							
	Z							
	90	100	150	200	250	300	350	400
0.0030	0.700	0.700	0.700	0.700	0.700	0.700	0.700	0.700
0.0040	0.764	0.763	0.756	0.750	0.744	0.738	0.731	0.725
0.0050	0.784	0.780	0.760	0.740	0.720	0.700	0.680	0.660
0.0060	0.783	0.775	0.738	0.700	0.663	0.625	0.588	
0.0070	0.769	0.757	0.700	0.643	0.586			
0.0080	0.747	0.731	0.653	0.575				
0.0090	0.720	0.700	0.600					
0.0100	0.690	0.665						
0.0110	0.656	0.627						
0.0120	0.621	0.588						
0.0130	0.585	0.546						
0.0140	0.547							
0.0150								
0.0160								
0.0170								
0.0180								
0.0190								
0.0200								

Table B.9: Stress Block Parameter α for $\epsilon_c \geq \epsilon_1$

ϵ_c	$\epsilon_1 = 0.0040$ and $K = 0.20$							
	Z							
	10	20	30	40	50	60	70	80
0.0040	0.727	0.727	0.727	0.727	0.727	0.727	0.727	0.727
0.0050	0.781	0.780	0.779	0.778	0.777	0.776	0.775	0.774
0.0060	0.815	0.812	0.808	0.805	0.802	0.798	0.795	0.792
0.0070	0.838	0.831	0.825	0.818	0.812	0.806	0.799	0.793
0.0080	0.854	0.844	0.834	0.824	0.814	0.804	0.794	0.784
0.0090	0.865	0.851	0.837	0.823	0.809	0.795	0.782	0.768
0.0100	0.873	0.855	0.837	0.819	0.801	0.783	0.765	0.747
0.0110	0.879	0.856	0.834	0.812	0.789	0.767	0.745	0.723
0.0120	0.882	0.856	0.829	0.802	0.776	0.749	0.722	0.696
0.0130	0.885	0.854	0.823	0.791	0.760	0.729	0.698	0.667
0.0140	0.886	0.851	0.815	0.779	0.744	0.708	0.672	0.636
0.0150	0.887	0.847	0.806	0.766	0.726	0.685	0.645	0.605
0.0160	0.887	0.842	0.797	0.752	0.707	0.662	0.617	0.572
0.0170	0.886	0.836	0.787	0.737	0.687	0.638	0.588	
0.0180	0.885	0.831	0.776	0.722	0.667	0.613	0.558	
0.0190	0.883	0.824	0.765	0.706	0.647	0.587		
0.0200	0.881	0.817	0.753	0.689	0.625	0.561		

Table B.10: Stress Block Parameter α for $\epsilon_c \geq \epsilon_1$ Cont.

ϵ_c	$\epsilon_1 = 0.0040$ and $K = 0.20$							
	Z							
	90	100	150	200	250	300	350	400
0.0040	0.727	0.727	0.727	0.727	0.727	0.727	0.727	0.727
0.0050	0.773	0.772	0.767	0.762	0.757	0.752	0.747	0.742
0.0060	0.788	0.785	0.768	0.752	0.735	0.718	0.702	0.685
0.0070	0.786	0.780	0.748	0.716	0.683	0.651		
0.0080	0.774	0.764	0.714	0.664	0.614			
0.0090	0.754	0.740	0.670	0.601				
0.0100	0.729	0.711	0.621					
0.0110	0.700	0.678						
0.0120	0.669	0.642						
0.0130	0.636	0.605						
0.0140	0.601	0.565						
0.0150	0.564							
0.0160								
0.0170								
0.0180								
0.0190								
0.0200								

Table B.11: Stress Block Parameter α for $\epsilon_c \geq \epsilon_1$

ϵ_c	$\epsilon_1 = 0.0050$ and $K = 0.30$							
	Z							
	10	20	30	40	50	60	70	80
0.0050	0.750	0.750	0.750	0.750	0.750	0.750	0.750	0.750
0.0060	0.791	0.790	0.789	0.788	0.787	0.787	0.786	0.785
0.0070	0.819	0.816	0.813	0.810	0.807	0.804	0.801	0.799
0.0080	0.838	0.832	0.827	0.821	0.816	0.810	0.804	0.799
0.0090	0.852	0.843	0.834	0.826	0.817	0.808	0.799	0.790
0.0100	0.862	0.850	0.837	0.825	0.812	0.800	0.787	0.775
0.0110	0.870	0.854	0.837	0.821	0.805	0.788	0.772	0.755
0.0120	0.875	0.855	0.835	0.814	0.794	0.773	0.753	0.732
0.0130	0.879	0.855	0.830	0.805	0.781	0.756	0.732	0.707
0.0140	0.882	0.853	0.824	0.795	0.766	0.737	0.708	0.679
0.0150	0.883	0.850	0.817	0.783	0.750	0.717	0.683	0.650
0.0160	0.884	0.846	0.808	0.771	0.733	0.695	0.657	0.619
0.0170	0.884	0.842	0.799	0.757	0.715	0.672	0.630	0.588
0.0180	0.884	0.837	0.790	0.743	0.696	0.649	0.602	
0.0190	0.883	0.831	0.779	0.728	0.676	0.625	0.573	
0.0200	0.881	0.825	0.769	0.712	0.656	0.600		

Table B.12: Stress Block Parameter α for $\epsilon_c \geq \epsilon_1$ Cont.

ϵ_c	$\epsilon_1 = 0.0050$ and $K = 0.30$							
	Z							
	90	100	150	200	250	300	350	400
0.0050	0.750	0.750	0.750	0.750	0.750	0.750	0.750	0.750
0.0060	0.784	0.783	0.779	0.775	0.771	0.767	0.762	0.758
0.0070	0.796	0.793	0.779	0.764	0.750	0.736	0.721	0.707
0.0080	0.793	0.787	0.759	0.731	0.703	0.675	0.647	
0.0090	0.781	0.772	0.728	0.683	0.639			
0.0100	0.762	0.750	0.687	0.625				
0.0110	0.739	0.723	0.641					
0.0120	0.712	0.692						
0.0130	0.682	0.658						
0.0140	0.650	0.621						
0.0150	0.617	0.583						
0.0160	0.582							
0.0170								
0.0180								
0.0190								
0.0200								

Table B.13: Stress Block Parameter α for $\epsilon_c \geq \epsilon_1$

ϵ_c	$\epsilon_1 = 0.0060$ and $K = 0.40$							
	Z							
	10	20	30	40	50	60	70	80
0.0060	0.769	0.769	0.766	0.769	0.769	0.769	0.769	0.769
0.0070	0.801	0.801	0.800	0.799	0.798	0.798	0.797	0.796
0.0080	0.824	0.822	0.819	0.817	0.814	0.812	0.809	0.807
0.0090	0.841	0.836	0.831	0.826	0.821	0.816	0.811	0.806
0.0100	0.853	0.845	0.835	0.829	0.821	0.813	0.805	0.797
0.0110	0.863	0.851	0.839	0.829	0.817	0.806	0.794	0.783
0.0120	0.870	0.855	0.840	0.825	0.810	0.795	0.780	0.765
0.0130	0.875	0.856	0.838	0.818	0.799	0.780	0.761	0.743
0.0140	0.878	0.855	0.835	0.810	0.787	0.764	0.741	0.718
0.0150	0.881	0.854	0.830	0.800	0.773	0.746	0.719	0.692
0.0160	0.882	0.851	0.823	0.788	0.757	0.726	0.695	0.663
0.0170	0.883	0.847	0.812	0.776	0.741	0.705	0.669	0.634
0.0180	0.883	0.843	0.803	0.763	0.723	0.683	0.643	0.603
0.0190	0.883	0.838	0.794	0.749	0.705	0.660	0.616	
0.0200	0.882	0.833	0.784	0.735	0.686	0.637	0.588	

Table B.14: Stress Block Parameter α for $\epsilon_c \geq \epsilon_1$ Cont.

ϵ_c	$\epsilon_1 = 0.0060$ and $K = 0.40$							
	Z							
	90	100	150	200	250	300	350	400
0.0060	0.769	0.769	0.769	0.769	0.769	0.769	0.769	0.769
0.0070	0.796	0.795	0.791	0.788	0.784	0.781	0.777	0.773
0.0080	0.804	0.802	0.789	0.777	0.764	0.752	0.739	0.727
0.0090	0.801	0.796	0.771	0.746	0.721	0.696		
0.0100	0.789	0.781	0.741	0.701	0.661			
0.0110	0.772	0.760	0.704	0.647				
0.0120	0.750	0.735	0.660					
0.0130	0.724	0.705						
0.0140	0.695	0.672						
0.0150	0.665	0.638						
0.0160	0.632	0.601						
0.0170	0.598							
0.0180								
0.0190								
0.0200								

Table B.15: Stress Block Parameter α for $\epsilon_c \geq \epsilon_1$

ϵ_c	$\epsilon_1 = 0.0070$ and $K = 0.50$							
	Z							
	10	20	30	40	50	60	70	80
0.0070	0.785	0.785	0.785	0.785	0.785	0.785	0.785	0.785
0.0080	0.812	0.811	0.810	0.810	0.809	0.808	0.808	0.807
0.0090	0.831	0.829	0.826	0.824	0.822	0.820	0.818	0.815
0.0100	0.845	0.841	0.836	0.832	0.827	0.823	0.818	0.814
0.0110	0.856	0.849	0.842	0.834	0.827	0.820	0.813	0.805
0.0120	0.864	0.854	0.844	0.833	0.823	0.812	0.802	0.791
0.0130	0.871	0.857	0.843	0.829	0.815	0.801	0.788	0.774
0.0140	0.875	0.858	0.840	0.823	0.805	0.788	0.770	0.753
0.0150	0.879	0.857	0.836	0.815	0.793	0.772	0.751	0.729
0.0160	0.881	0.855	0.830	0.805	0.780	0.754	0.729	0.704
0.0170	0.882	0.853	0.823	0.794	0.765	0.735	0.706	0.676
0.0180	0.883	0.849	0.816	0.782	0.748	0.715	0.681	0.648
0.0190	0.883	0.845	0.807	0.769	0.731	0.694	0.656	0.618
0.0200	0.883	0.840	0.798	0.756	0.714	0.671	0.629	

Table B.16: Stress Block Parameter α for $\epsilon_c \geq \epsilon_1$ Cont.

ϵ_c	$\epsilon_1 = 0.0070$ and $K = 0.50$							
	Z							
	90	100	150	200	250	300	350	400
0.0070	0.785	0.785	0.785	0.785	0.785	0.785	0.785	0.785
0.0080	0.807	0.806	0.803	0.800	0.797	0.793	0.790	0.787
0.0090	0.813	0.811	0.800	0.789	0.778	0.766	0.755	0.744
0.0100	0.809	0.805	0.782	0.760	0.737	0.715	0.692	
0.0110	0.798	0.791	0.754	0.718	0.682			
0.0120	0.781	0.771	0.719	0.666				
0.0130	0.760	0.746	0.677					
0.0140	0.735	0.718						
0.0150	0.708	0.687						
0.0160	0.678	0.653						
0.0170	0.647	0.618						
0.0180	0.614							
0.0190								
0.0200								

Table B.17: Stress Block Parameter α for $\epsilon_c \geq \epsilon_1$

ϵ_c	$\epsilon_1 = 0.0080$ and $K = 0.60$							
	Z							
	10	20	30	40	50	60	70	80
0.0080	0.800	0.800	0.800	0.800	0.800	0.800	0.800	0.800
0.0090	0.821	0.821	0.820	0.820	0.819	0.818	0.818	0.817
0.0100	0.838	0.836	0.834	0.832	0.830	0.828	0.826	0.824
0.0110	0.850	0.846	0.842	0.838	0.834	0.830	0.826	0.821
0.0120	0.860	0.853	0.846	0.840	0.833	0.826	0.820	0.813
0.0130	0.867	0.857	0.848	0.838	0.829	0.819	0.809	0.800
0.0140	0.873	0.860	0.847	0.834	0.821	0.808	0.795	0.783
0.0150	0.877	0.860	0.844	0.828	0.811	0.795	0.779	0.762
0.0160	0.880	0.860	0.840	0.820	0.800	0.780	0.760	0.740
0.0170	0.882	0.858	0.834	0.810	0.787	0.763	0.739	0.715
0.0180	0.883	0.855	0.828	0.800	0.772	0.744	0.716	0.689
0.0190	0.884	0.852	0.820	0.788	0.756	0.725	0.693	0.661
0.0200	0.884	0.848	0.812	0.776	0.740	0.704	0.668	0.632

Table B.18: Stress Block Parameter α for $\epsilon_c \geq \epsilon_1$ Cont.

ϵ_c	$\epsilon_1 = 0.0080$ and $K = 0.60$							
	Z							
	90	100	150	200	250	300	350	400
0.0080	0.800	0.800	0.800	0.800	0.800	0.800	0.800	0.800
0.0090	0.817	0.816	0.813	0.811	0.808	0.805	0.802	0.800
0.0100	0.822	0.820	0.810	0.800	0.790	0.780	0.770	0.760
0.0110	0.817	0.813	0.793	0.772	0.752	0.731		
0.0120	0.806	0.800	0.766	0.733	0.700			
0.0130	0.790	0.780	0.732	0.684				
0.0140	0.770	0.757	0.693					
0.0150	0.746	0.730						
0.0160	0.720	0.700						
0.0170	0.691	0.667						
0.0180	0.661	0.633						
0.0190	0.629							
0.0200								

Table B.19: Stress Block Parameter α for $\epsilon_c \geq \epsilon_1$

ϵ_c	$\epsilon_1 = 0.0090$ and $K = 0.70$							
	Z							
	10	20	30	40	50	60	70	80
0.0090	0.812	0.812	0.812	0.812	0.812	0.812	0.812	0.812
0.0100	0.830	0.830	0.829	0.829	0.828	0.828	0.827	0.827
0.0110	0.844	0.842	0.841	0.839	0.837	0.835	0.833	0.832
0.0120	0.855	0.851	0.848	0.844	0.840	0.836	0.833	0.829
0.0130	0.864	0.857	0.851	0.845	0.839	0.833	0.827	0.821
0.0140	0.870	0.861	0.852	0.843	0.834	0.826	0.817	0.808
0.0150	0.875	0.863	0.851	0.839	0.827	0.815	0.803	0.791
0.0160	0.879	0.864	0.848	0.833	0.818	0.802	0.787	0.772
0.0170	0.882	0.863	0.844	0.825	0.806	0.787	0.769	0.750
0.0180	0.883	0.861	0.838	0.816	0.793	0.771	0.748	0.726
0.0190	0.885	0.858	0.832	0.806	0.779	0.753	0.727	0.700
0.0200	0.885	0.855	0.825	0.794	0.764	0.734	0.704	0.673

Table B.20 : Stress Block Parameter α for $\epsilon_c \geq \epsilon_1$ Cont.

ϵ_c	$\epsilon_1 = 0.0090$ and $K = 0.70$							
	Z							
	90	100	150	200	250	300	350	400
0.0090	0.812	0.812	0.812	0.812	0.812	0.812	0.812	0.812
0.0100	0.826	0.826	0.823	0.821	0.818	0.816	0.813	0.811
0.0110	0.830	0.828	0.819	0.810	0.801	0.792	0.782	0.773
0.0120	0.825	0.821	0.803	0.784	0.765	0.746	0.728	
0.0130	0.814	0.808	0.777	0.747	0.716			
0.0140	0.799	0.790	0.745	0.701				
0.0150	0.779	0.767	0.707					
0.0160	0.756	0.741						
0.0170	0.731	0.712						
0.0180	0.703	0.681						
0.0190	0.674	0.648						
0.0200	0.643							

Table B.21: Stress Block Parameter α for $\epsilon_c \geq \epsilon_1$

ϵ_c	$\epsilon_1 = 0.0100$ and $K = 0.80$							
	Z							
	10	20	30	40	50	60	70	80
0.0100	0.823	0.823	0.823	0.823	0.823	0.823	0.823	0.823
0.0110	0.838	0.838	0.838	0.837	0.837	0.836	0.836	0.835
0.0120	0.851	0.849	0.847	0.846	0.844	0.842	0.841	0.839
0.0130	0.860	0.857	0.853	0.850	0.846	0.843	0.839	0.836
0.0140	0.868	0.862	0.856	0.851	0.845	0.839	0.833	0.828
0.0150	0.874	0.865	0.857	0.849	0.840	0.832	0.824	0.815
0.0160	0.878	0.867	0.856	0.844	0.833	0.822	0.811	0.799
0.0170	0.881	0.867	0.853	0.838	0.824	0.809	0.795	0.780
0.0180	0.884	0.866	0.848	0.830	0.813	0.795	0.777	0.759
0.0190	0.885	0.864	0.843	0.821	0.800	0.779	0.758	0.736
0.0200	0.886	0.861	0.836	0.811	0.786	0.761	0.736	0.711

Table B.22: Stress Block Parameter α for $\epsilon_c \geq \epsilon_1$ Cont.

ϵ_c	$\epsilon_1 = 0.0100$ and $K = 0.80$							
	Z							
	90	100	150	200	250	300	350	400
0.0100	0.823	0.823	0.823	0.823	0.823	0.823	0.823	0.823
0.0110	0.835	0.834	0.832	0.830	0.828	0.825	0.823	0.821
0.0120	0.837	0.836	0.827	0.819	0.811	0.802	0.794	0.786
0.0130	0.833	0.829	0.812	0.794	0.777	0.760	0.743	
0.0140	0.822	0.816	0.788	0.759	0.731			
0.0150	0.807	0.799	0.757	0.715				
0.0160	0.788	0.777	0.721					
0.0170	0.766	0.752						
0.0180	0.742	0.724						
0.0190	0.715	0.694						
0.0200	0.686	0.661						

Table B.23: Stress Block Parameter γ for $\epsilon_c \geq \epsilon_1$

ϵ_c	$\epsilon_1 = 0.002$ and $K = 0.0$							
	Z							
	10	20	30	40	50	60	70	80
0.0020	0.375	0.375	0.375	0.375	0.375	0.375	0.375	0.375
0.0030	0.405	0.406	0.407	0.407	0.408	0.409	0.409	0.410
0.0040	0.427	0.428	0.430	0.431	0.433	0.435	0.436	0.438
0.0050	0.441	0.444	0.446	0.449	0.452	0.454	0.457	0.460
0.0060	0.451	0.455	0.459	0.462	0.466	0.470	0.474	0.479
0.0070	0.459	0.464	0.469	0.473	0.479	0.484	0.490	0.496
0.0080	0.466	0.471	0.477	0.483	0.490	0.497	0.504	0.512
0.0090	0.471	0.477	0.484	0.492	0.500	0.508	0.518	0.528
0.0100	0.475	0.483	0.491	0.500	0.509	0.520	0.531	0.544
0.0110	0.479	0.488	0.497	0.507	0.519	0.532	0.546	0.561
0.0120	0.482	0.492	0.503	0.515	0.528	0.543	0.560	0.580
0.0130	0.485	0.496	0.508	0.522	0.538	0.556	0.576	0.600
0.0140	0.488	0.500	0.514	0.529	0.547	0.568	0.593	0.622
0.0150	0.490	0.504	0.519	0.537	0.557	0.582	0.611	
0.0160	0.492	0.507	0.524	0.544	0.568	0.597	0.632	
0.0170	0.495	0.511	0.529	0.552	0.579	0.612		
0.0180	0.497	0.514	0.535	0.560	0.590	0.629		
0.0190	0.499	0.517	0.540	0.568	0.603			
0.0200	0.500	0.521	0.545	0.576	0.616			

Table B.24 : Stress Block Parameter γ for $\epsilon_c \geq \epsilon_1$ Cont.

ϵ_c	$\epsilon_1 = 0.002$ and $K = 0.0$							
	Z							
	90	100	150	200	250	300	350	400
0.0020	0.375	0.375	0.375	0.375	0.375	0.375	0.375	0.375
0.0030	0.411	0.411	0.415	0.418	0.421	0.425	0.429	0.432
0.0040	0.440	0.441	0.451	0.460	0.471	0.482	0.494	0.507
0.0050	0.463	0.466	0.482	0.501	0.522	0.546	0.575	
0.0060	0.483	0.488	0.513	0.545	0.583			
0.0070	0.502	0.508	0.546	0.596				
0.0080	0.520	0.529	0.583					
0.0090	0.538	0.550						
0.0100	0.558	0.573						
0.0110	0.579	0.598						
0.0120	0.602	0.627						
0.0130	0.628							
0.0140								
0.0150								
0.0160								
0.0170								
0.0180								
0.0190								
0.0200								

Table B.25 : Stress Block Parameter γ for $\epsilon_c \geq \epsilon_1$

ϵ_c	$\epsilon_1 = 0.003$ and $K = 0.10$							
	Z							
	10	20	30	40	50	60	70	80
0.0030	0.390	0.390	0.390	0.390	0.390	0.390	0.390	0.390
0.0040	0.408	0.409	0.409	0.410	0.410	0.411	0.411	0.412
0.0050	0.424	0.425	0.426	0.428	0.429	0.431	0.432	0.434
0.0060	0.436	0.438	0.440	0.443	0.445	0.448	0.451	0.453
0.0070	0.445	0.448	0.452	0.455	0.459	0.463	0.467	0.471
0.0080	0.452	0.457	0.462	0.466	0.471	0.476	0.482	0.487
0.0090	0.459	0.464	0.470	0.476	0.482	0.489	0.496	0.503
0.0100	0.464	0.471	0.477	0.485	0.493	0.501	0.510	0.519
0.0110	0.469	0.476	0.484	0.493	0.503	0.513	0.524	0.536
0.0120	0.472	0.481	0.491	0.501	0.512	0.524	0.538	0.553
0.0130	0.476	0.486	0.497	0.509	0.522	0.536	0.553	0.571
0.0140	0.479	0.490	0.503	0.516	0.531	0.549	0.568	0.591
0.0150	0.482	0.494	0.550	0.524	0.541	0.562	0.585	0.612
0.0160	0.485	0.498	0.514	0.531	0.551	0.575	0.603	
0.0170	0.487	0.502	0.519	0.539	0.562	0.589	0.623	
0.0180	0.490	0.506	0.525	0.547	0.573	0.605		
0.0190	0.492	0.509	0.530	0.554	0.584	0.622		
0.0200	0.494	0.513	0.535	0.563	0.597			

Table B.26: Stress Block Parameter γ for $\epsilon_c \geq \epsilon_1$ Cont.

ϵ_c	$\epsilon_1 = 0.003$ and $K = 0.10$							
	Z							
	90	100	150	200	250	300	350	400
0.0030	0.390	0.390	0.390	0.390	0.390	0.390	0.390	0.390
0.0040	0.412	0.413	0.416	0.418	0.421	0.424	0.427	0.430
0.0050	0.435	0.437	0.445	0.453	0.462	0.472	0.482	0.492
0.0060	0.456	0.459	0.474	0.490	0.509	0.529	0.552	
0.0070	0.475	0.479	0.503	0.531	0.564	0.604		
0.0080	0.493	0.499	0.534	0.578				
0.0090	0.511	0.519	0.569					
0.0100	0.530	0.540						
0.0110	0.549	0.563						
0.0120	0.569	0.588						
0.0130	0.592	0.615						
0.0140	0.617							
0.0150								
0.0160								
0.0170								
0.0180								
0.0190								
0.0200								

Table B.27: Stress Block Parameter γ for $\epsilon_c \geq \epsilon_1$

ϵ_c	$\epsilon_1 = 0.004$ and $K = 0.20$							
	Z							
	10	20	30	40	50	60	70	80
0.0040	0.401	0.401	0.401	0.401	0.401	0.401	0.401	0.401
0.0050	0.414	0.414	0.414	0.415	0.415	0.416	0.416	0.417
0.0060	0.425	0.426	0.428	0.429	0.430	0.432	0.433	0.434
0.0070	0.435	0.437	0.439	0.442	0.444	0.446	0.449	0.451
0.0080	0.443	0.446	0.450	0.453	0.456	0.460	0.464	0.468
0.0090	0.450	0.454	0.458	0.463	0.468	0.473	0.478	0.483
0.0100	0.456	0.461	0.466	0.472	0.478	0.485	0.492	0.499
0.0110	0.461	0.467	0.474	0.481	0.489	0.497	0.505	0.514
0.0120	0.465	0.473	0.481	0.489	0.498	0.508	0.519	0.530
0.0130	0.469	0.478	0.487	0.497	0.508	0.520	0.533	0.547
0.0140	0.473	0.482	0.493	0.505	0.518	0.532	0.547	0.565
0.0150	0.476	0.487	0.499	0.512	0.527	0.544	0.563	0.584
0.0160	0.479	0.491	0.505	0.520	0.537	0.557	0.579	0.605
0.0170	0.482	0.495	0.510	0.527	0.547	0.570	0.597	
0.0180	0.484	0.499	0.516	0.535	0.558	0.584	0.616	
0.0190	0.487	0.503	0.521	0.543	0.568	0.599		
0.0200								

Table B.28: Stress Block Parameter γ for $\epsilon_c \geq \epsilon_1$ Cont.

ϵ_c	$\epsilon_1 = 0.004$ and $K = 0.20$							
	Z							
	90	100	150	200	250	300	350	400
0.0040	0.401	0.401	0.401	0.401	0.401	0.401	0.401	0.401
0.0050	0.417	0.418	0.420	0.422	0.425	0.427	0.429	0.432
0.0060	0.436	0.437	0.444	0.452	0.459	0.467	0.476	0.485
0.0070	0.454	0.456	0.470	0.485	0.501	0.518	0.538	
0.0080	0.471	0.475	0.497	0.522	0.551			
0.0090	0.489	0.494	0.526	0.566				
0.0100	0.506	0.514	0.559					
0.0110	0.524	0.534						
0.0120	0.542	0.556						
0.0130	0.562	0.579						
0.0140	0.584	0.606						
0.0150	0.608							
0.0160								
0.0170								
0.0180								
0.0190								
0.0200								

Table B.29: Stress Block Parameter γ for $\epsilon_c \geq \epsilon_1$

ϵ_c	$\epsilon_1 = 0.005$ and $K = 0.30$							
	Z							
	10	20	30	40	50	60	70	80
0.0050	0.410	0.410	0.410	0.410	0.410	0.410	0.410	0.410
0.0060	0.419	0.420	0.420	0.421	0.421	0.421	0.422	0.422
0.0070	0.428	0.429	0.431	0.432	0.433	0.434	0.435	0.437
0.0080	0.436	0.438	0.440	0.443	0.445	0.447	0.449	0.452
0.0090	0.443	0.446	0.449	0.453	0.456	0.459	0.463	0.466
0.0100	0.449	0.453	0.458	0.462	0.466	0.471	0.476	0.481
0.0110	0.454	0.460	0.465	0.471	0.477	0.483	0.489	0.496
0.0120	0.459	0.465	0.472	0.479	0.486	0.494	0.502	0.511
0.0130	0.463	0.471	0.479	0.487	0.496	0.505	0.515	0.526
0.0140	0.467	0.476	0.485	0.495	0.505	0.517	0.529	0.542
0.0150	0.471	0.480	0.491	0.502	0.515	0.528	0.543	0.560
0.0160	0.474	0.485	0.497	0.510	0.524	0.540	0.558	0.578
0.0170	0.477	0.489	0.502	0.517	0.534	0.553	0.574	0.599
0.0180	0.480	0.493	0.508	0.525	0.544	0.566	0.591	
0.0190	0.482	0.497	0.513	0.532	0.554	0.580	0.610	
0.0200	0.485	0.501	0.519	0.540	0.565	0.595		

Table B.30: Stress Block Parameter γ for $\epsilon_c \geq \epsilon_1$ Cont.

ϵ_c	$\epsilon_1 = 0.005$ and $K = 0.30$							
	Z							
	90	100	150	200	250	300	350	400
0.0050	0.410	0.410	0.410	0.410	0.410	0.410	0.410	0.410
0.0060	0.423	0.423	0.425	0.427	0.429	0.431	0.433	0.435
0.0070	0.438	0.439	0.445	0.452	0.459	0.466	0.473	0.481
0.0080	0.454	0.456	0.468	0.482	0.496	0.511	0.528	
0.0090	0.470	0.474	0.494	0.516	0.542			
0.0100	0.486	0.491	0.521	0.556				
0.0110	0.503	0.510	0.552					
0.0120	0.520	0.529						
0.0130	0.538	0.550						
0.0140	0.557	0.573						
0.0150	0.578	0.598						
0.0160	0.601							
0.0170								
0.0180								
0.0190								
0.0200								

Table B.31: Stress Block Parameter γ for $\epsilon_c \geq \epsilon_1$

ϵ_c	$\epsilon_1 = 0.006$ and $K = 0.40$							
	Z							
	10	20	30	40	50	60	70	80
0.0060	0.418	0.418	0.418	0.418	0.418	0.418	0.418	0.418
0.0070	0.425	0.425	0.426	0.426	0.426	0.427	0.427	0.427
0.0080	0.432	0.433	0.434	0.435	0.436	0.437	0.438	0.440
0.0090	0.438	0.440	0.442	0.444	0.446	0.448	0.451	0.453
0.0100	0.444	0.447	0.450	0.453	0.456	0.460	0.463	0.466
0.0110	0.450	0.454	0.458	0.462	0.466	0.471	0.475	0.480
0.0120	0.454	0.459	0.465	0.470	0.476	0.482	0.488	0.494
0.0130	0.459	0.465	0.471	0.478	0.485	0.492	0.500	0.508
0.0140	0.463	0.470	0.478	0.486	0.494	0.503	0.513	0.523
0.0150	0.466	0.475	0.484	0.493	0.503	0.514	0.526	0.539
0.0160	0.470	0.479	0.490	0.501	0.513	0.526	0.540	0.556
0.0170	0.473	0.483	0.495	0.508	0.522	0.538	0.555	0.574
0.0180	0.476	0.488	0.501	0.515	0.532	0.550	0.570	0.593
0.0190	0.478	0.492	0.506	0.523	0.541	0.563	0.587	
0.0200	0.481	0.495	0.512	0.530	0.552	0.576	0.605	

Table B.32: Stress Block Parameter γ for $\epsilon_c \geq \epsilon_1$ Cont.

ϵ_c	$\epsilon_1 = 0.006$ and $K = 0.40$							
	Z							
	90	100	150	200	250	300	350	400
0.0060	0.418	0.418	0.418	0.418	0.418	0.418	0.418	0.418
0.0070	0.428	0.428	0.430	0.431	0.433	0.435	0.437	0.439
0.0080	0.441	0.442	0.447	0.453	0.459	0.466	0.472	0.479
0.0090	0.455	0.457	0.468	0.480	0.493	0.507	0.521	
0.0100	0.470	0.473	0.491	0.512	0.535			
0.0110	0.485	0.490	0.517	0.549				
0.0120	0.500	0.507	0.546					
0.0130	0.517	0.526						
0.0140	0.534	0.546						
0.0150	0.553	0.568						
0.0160	0.573	0.592						
0.0170	0.595							
0.0180								
0.0190								
0.0200								

Table B.33: Stress Block Parameter γ for $\epsilon_c \geq \epsilon_1$

ϵ_c	$\epsilon_1 = 0.007$ and $K = 0.50$							
	Z							
	10	20	30	40	50	60	70	80
0.0070	0.424	0.424	0.424	0.424	0.424	0.424	0.424	0.424
0.0080	0.430	0.430	0.431	0.431	0.431	0.431	0.432	0.432
0.0090	0.436	0.437	0.438	0.439	0.440	0.440	0.441	0.442
0.0100	0.441	0.443	0.445	0.447	0.448	0.450	0.452	0.454
0.0110	0.446	0.449	0.452	0.455	0.458	0.461	0.464	0.467
0.0120	0.451	0.455	0.459	0.463	0.467	0.471	0.475	0.480
0.0130	0.455	0.460	0.465	0.470	0.476	0.481	0.487	0.493
0.0140	0.459	0.465	0.471	0.478	0.484	0.492	0.499	0.507
0.0150	0.463	0.470	0.477	0.485	0.493	0.502	0.511	0.521
0.0160	0.466	0.474	0.483	0.492	0.502	0.513	0.524	0.536
0.0170	0.469	0.479	0.489	0.500	0.511	0.524	0.538	0.552
0.0180	0.472	0.483	0.494	0.507	0.520	0.535	0.552	0.570
0.0190	0.475	0.487	0.500	0.514	0.530	0.547	0.567	0.589
0.0200	0.478	0.491	0.505	0.521	0.539	0.560	0.583	

Table B.34: Stress Block Parameter γ for $\epsilon_c \geq \epsilon_1$ Cont.

ϵ_c	$\epsilon_1 = 0.007$ and $K = 0.50$							
	Z							
	90	100	150	200	250	300	350	400
0.0070	0.424	0.424	0.424	0.424	0.424	0.424	0.424	0.424
0.0080	0.432	0.433	0.434	0.436	0.437	0.439	0.440	0.442
0.0090	0.444	0.445	0.450	0.455	0.460	0.466	0.472	0.478
0.0100	0.456	0.458	0.469	0.479	0.491	0.503	0.516	
0.0110	0.470	0.473	0.490	0.509	0.529			
0.0120	0.484	0.489	0.514	0.543				
0.0130	0.499	0.505	0.541					
0.0140	0.515	0.523						
0.0150	0.531	0.542						
0.0160	0.549	0.563						
0.0170	0.569							
0.0180	0.590							
0.0190								
0.0200								

Table B.35 : Stress Block Parameter γ for $\epsilon_c \geq \epsilon_1$

ϵ_c	$\epsilon_1 = 0.005$ and $K = 0.60$							
	Z							
	10	20	30	40	50	60	70	80
0.0050	0.430	0.430	0.430	0.430	0.430	0.430	0.430	0.430
0.0060	0.434	0.435	0.435	0.435	0.435	0.436	0.436	0.436
0.0070	0.439	0.440	0.441	0.442	0.443	0.444	0.445	0.445
0.0080	0.444	0.445	0.447	0.449	0.451	0.452	0.454	0.456
0.0090	0.448	0.451	0.453	0.456	0.459	0.462	0.465	0.467
0.0100	0.452	0.456	0.460	0.463	0.467	0.471	0.475	0.480
0.0110	0.456	0.461	0.466	0.471	0.476	0.481	0.487	0.492
0.0120	0.460	0.466	0.472	0.478	0.484	0.491	0.498	0.505
0.0130	0.463	0.470	0.477	0.485	0.493	0.501	0.510	0.519
0.0140	0.466	0.474	0.483	0.492	0.501	0.512	0.522	0.534
0.0150	0.469	0.479	0.488	0.499	0.510	0.522	0.535	0.550
0.0160	0.472	0.483	0.494	0.506	0.519	0.534	0.549	0.566
0.0170	0.475	0.487	0.499	0.513	0.528	0.545	0.564	0.584

Table B.36: Stress Block Parameter γ for $\epsilon_c \geq \epsilon_1$ Cont.

ϵ_c	$\epsilon_1 = 0.005$ and $K = 0.60$							
	Z							
	90	100	150	200	250	300	350	400
0.0080	0.430	0.430	0.430	0.430	0.430	0.430	0.430	0.430
0.0090	0.437	0.437	0.438	0.440	0.441	0.442	0.444	0.445
0.0100	0.446	0.447	0.452	0.457	0.462	0.467	0.472	0.477
0.0110	0.458	0.460	0.469	0.479	0.490	0.501	0.513	
0.0120	0.470	0.473	0.489	0.506	0.525			
0.0130	0.484	0.488	0.512	0.539				
0.0140	0.498	0.504	0.538					
0.0150	0.513	0.521						
0.0160	0.529	0.539						
0.0170	0.546	0.559						
0.0180	0.565	0.582						
0.0190	0.585							
0.0200								

Table B.37 : Stress Block Parameter γ for $\epsilon_c \geq \epsilon_1$

ϵ_c	$\epsilon_1 = 0.009$ and $K = 0.70$							
	Z							
	10	20	30	40	50	60	70	80
0.0090	0.435	0.435	0.435	0.435	0.435	0.435	0.435	0.435
0.0100	0.438	0.439	0.439	0.439	0.439	0.440	0.440	0.440
0.0110	0.442	0.443	0.444	0.445	0.446	0.446	0.447	0.448
0.0120	0.446	0.448	0.450	0.451	0.453	0.454	0.456	0.458
0.0130	0.450	0.453	0.455	0.458	0.460	0.463	0.466	0.468
0.0140	0.454	0.457	0.461	0.465	0.468	0.472	0.476	0.480
0.0150	0.457	0.462	0.467	0.471	0.476	0.481	0.486	0.492
0.0160	0.461	0.466	0.472	0.478	0.484	0.491	0.498	0.504
0.0170	0.464	0.471	0.478	0.485	0.493	0.501	0.509	0.518
0.0180	0.467	0.475	0.483	0.492	0.501	0.511	0.521	0.532
0.0190	0.470	0.479	0.488	0.499	0.509	0.521	0.534	0.547
0.0200	0.472	0.483	0.494	0.505	0.518	0.532	0.547	0.563

Table B.38: Stress Block Parameter γ for $\epsilon_c \geq \epsilon_1$ Cont.

ϵ_c	$\epsilon_1 = 0.009$ and $K = 0.70$							
	Z							
	90	100	150	200	250	300	350	400
0.0090	0.435	0.435	0.435	0.435	0.435	0.435	0.435	0.435
0.0100	0.440	0.441	0.442	0.443	0.444	0.446	0.447	0.448
0.0110	0.449	0.450	0.454	0.459	0.463	0.468	0.472	0.477
0.0120	0.460	0.461	0.470	0.479	0.489	0.499	0.510	
0.0130	0.471	0.474	0.489	0.505	0.522			
0.0140	0.484	0.488	0.510	0.535				
0.0150	0.497	0.503	0.534					
0.0160	0.512	0.519						
0.0170	0.527	0.537						
0.0180	0.544	0.556						
0.0190	0.562	0.577						
0.0200	0.581							

Table B.39 : Stress Block Parameter γ for $\epsilon_c \geq \epsilon_1$

ϵ_c	$\epsilon_1 = 0.0100$ and $K = 0.80$							
	Z							
	10	20	30	40	50	60	70	80
0.0100	0.439	0.439	0.439	0.439	0.439	0.439	0.439	0.439
0.0110	0.442	0.442	0.442	0.443	0.443	0.443	0.443	0.444
0.0120	0.445	0.446	0.447	0.448	0.448	0.449	0.450	0.451
0.0130	0.449	0.450	0.452	0.453	0.455	0.456	0.458	0.460
0.0140	0.452	0.455	0.457	0.459	0.462	0.464	0.467	0.470
0.0150	0.456	0.459	0.462	0.466	0.469	0.473	0.476	0.480
0.0160	0.459	0.463	0.468	0.472	0.477	0.482	0.487	0.492
0.0170	0.462	0.467	0.473	0.479	0.485	0.491	0.497	0.504
0.0180	0.465	0.471	0.478	0.452	0.492	0.500	0.508	0.517
0.0190	0.468	0.475	0.483	0.492	0.501	0.510	0.520	0.530
0.0200	0.470	0.479	0.488	0.498	0.509	0.520	0.532	0.545

Table B.40: Stress Block Parameter γ for $\epsilon_c \geq \epsilon_1$ Cont.

ϵ_c	$\epsilon_1 = 0.0100$ and $K = 0.80$							
	Z							
	90	100	150	200	250	300	350	400
0.0100	0.439	0.439	0.439	0.439	0.439	0.439	0.439	0.439
0.0110	0.444	0.444	0.445	0.446	0.447	0.449	0.450	0.451
0.0120	0.452	0.452	0.456	0.460	0.465	0.469	0.473	0.478
0.0130	0.461	0.463	0.471	0.480	0.489	0.498	0.508	
0.0140	0.472	0.475	0.489	0.503	0.519			
0.0150	0.484	0.488	0.509	0.532				
0.0160	0.497	0.502	0.532					
0.0170	0.511	0.518						
0.0180	0.525	0.535						
0.0190	0.541	0.553						
0.0200	0.559	0.573						

APPENDIX C

Moment-Curvature Relationships for Constant Axial Load

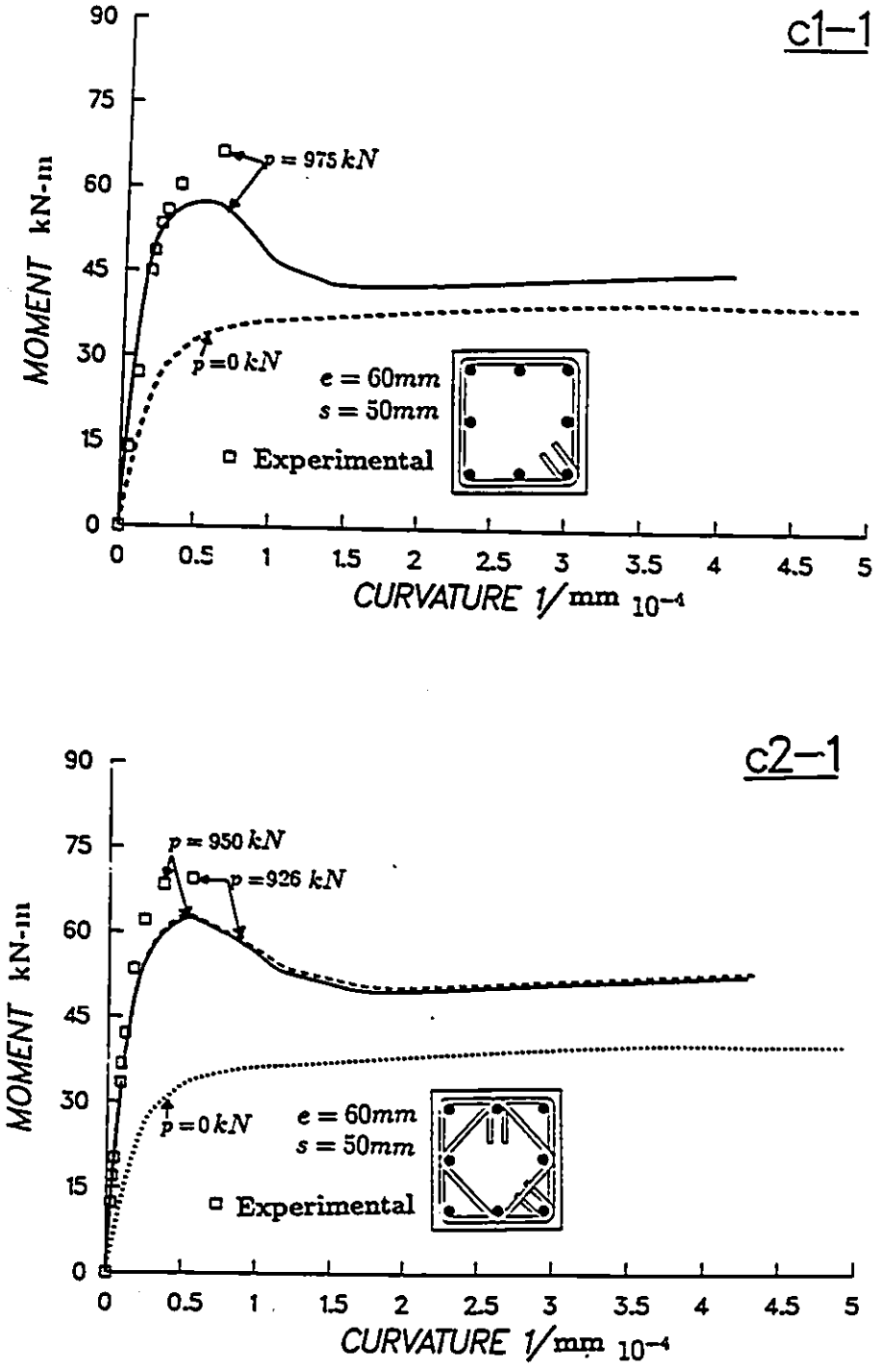

Figure C.1 : Moment-Curvature Relationship for Constant Load , Sheikh and Uzumeri [23]

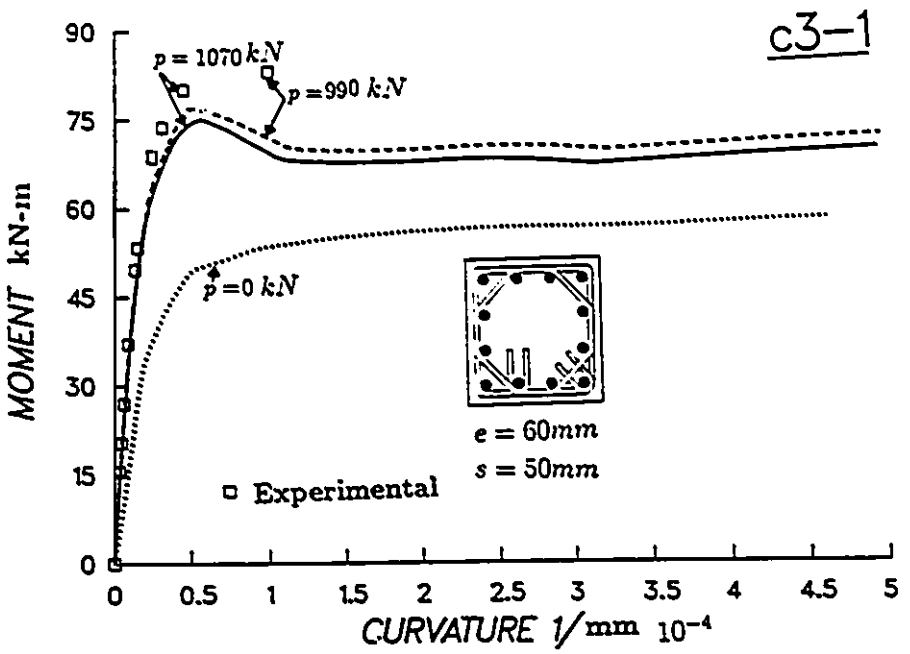

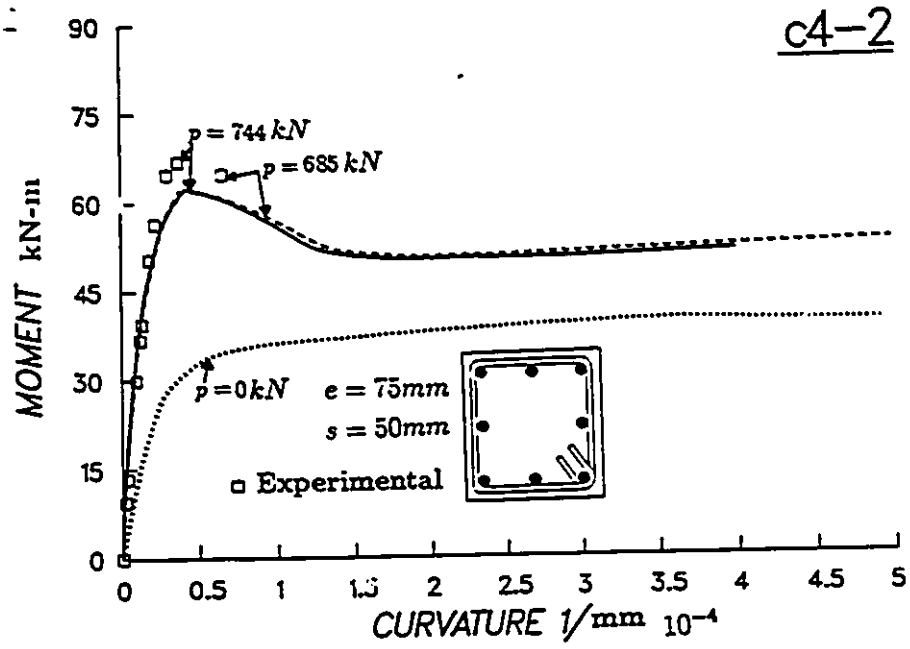

Figure C.2 :Moment-Curvature Relationship for Constant Load , Sheikh and Uzumeri [23]

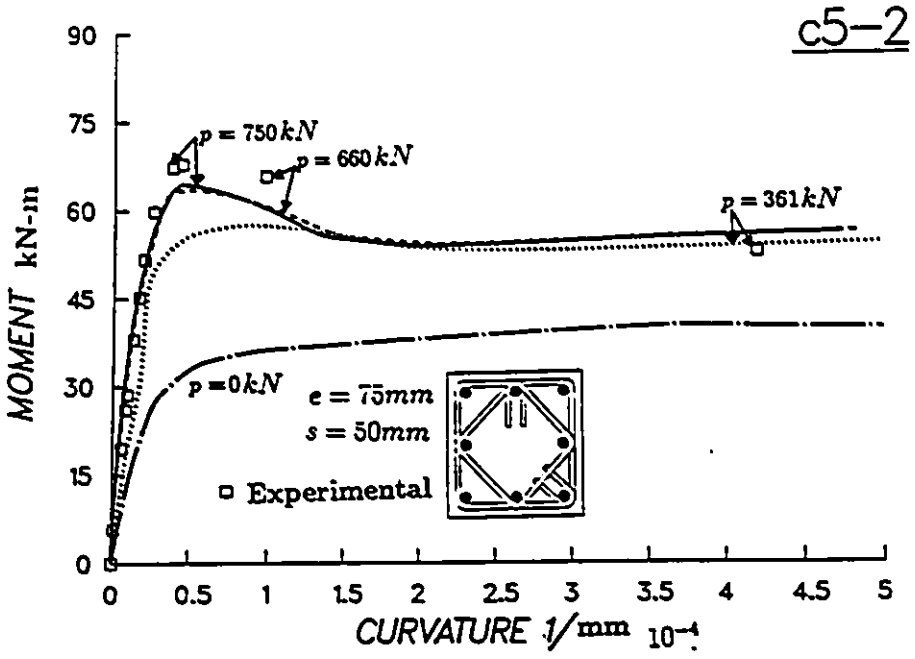

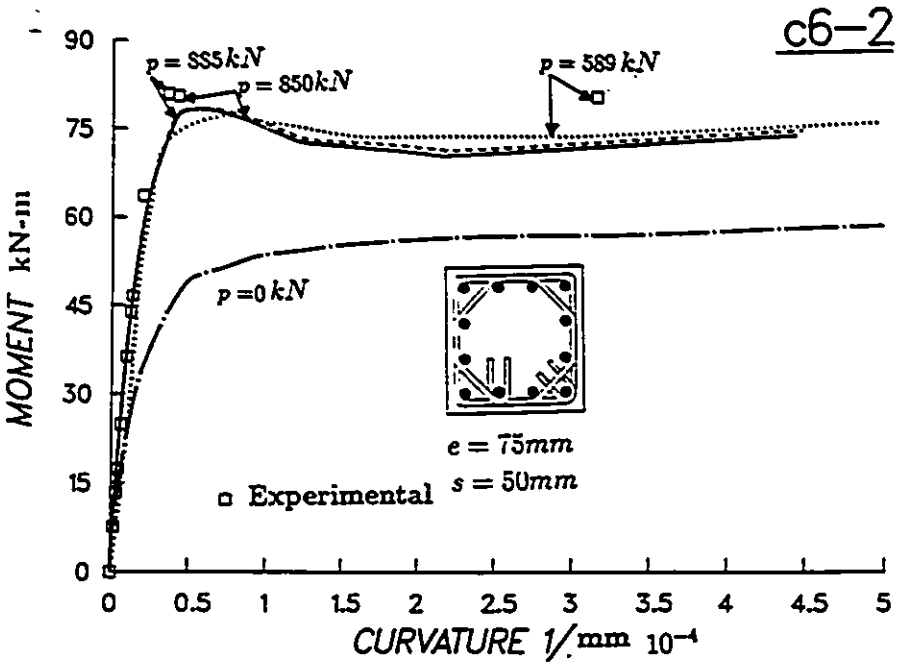

Figure C .3:Moment-Curvature Relationship for Constant Load , Sheikh and Uzumeri [23]

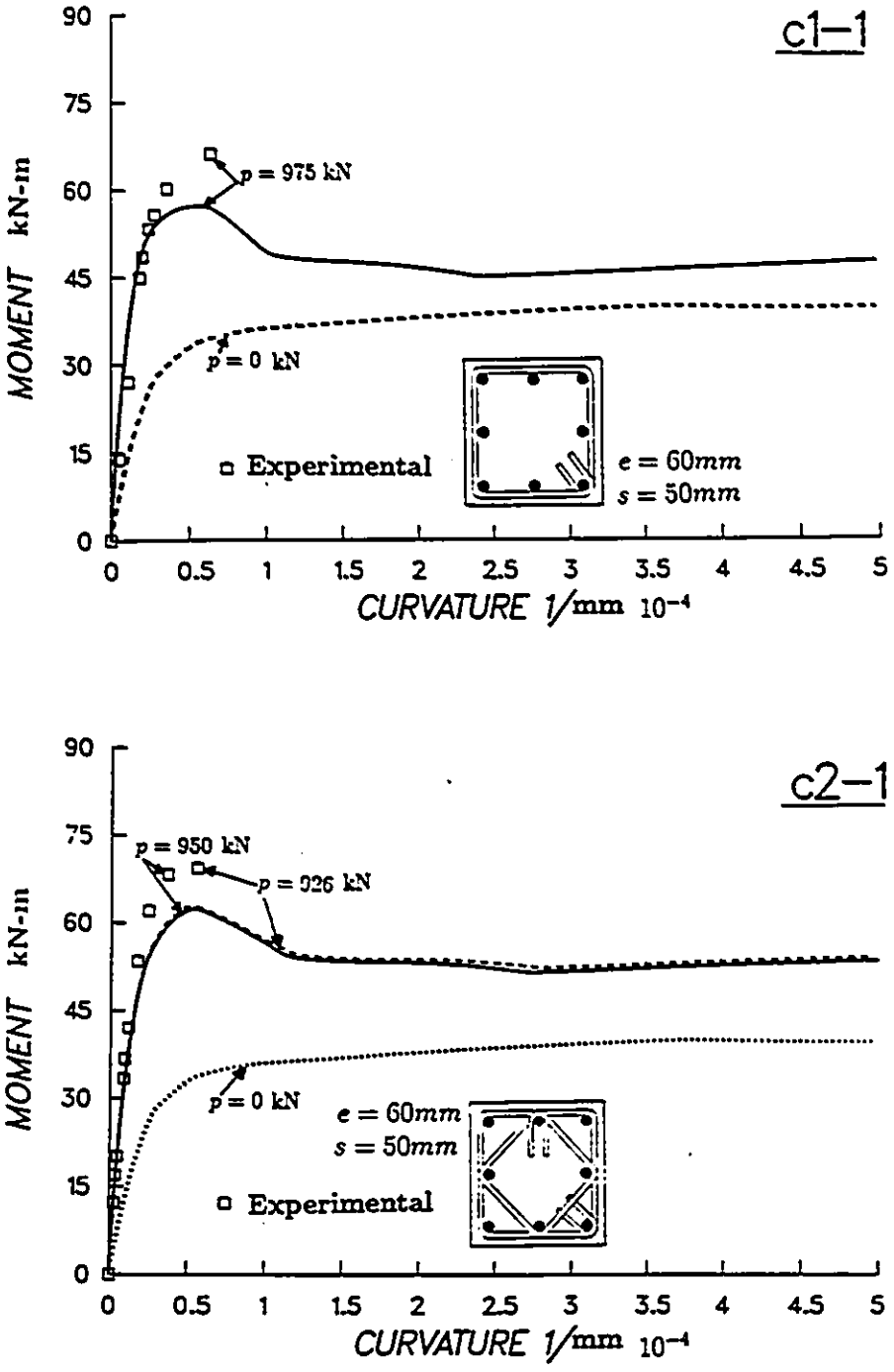

Figure C.4 : Moment-Curvature Relationship for Constant Load , Sheikh and Yeh [25]

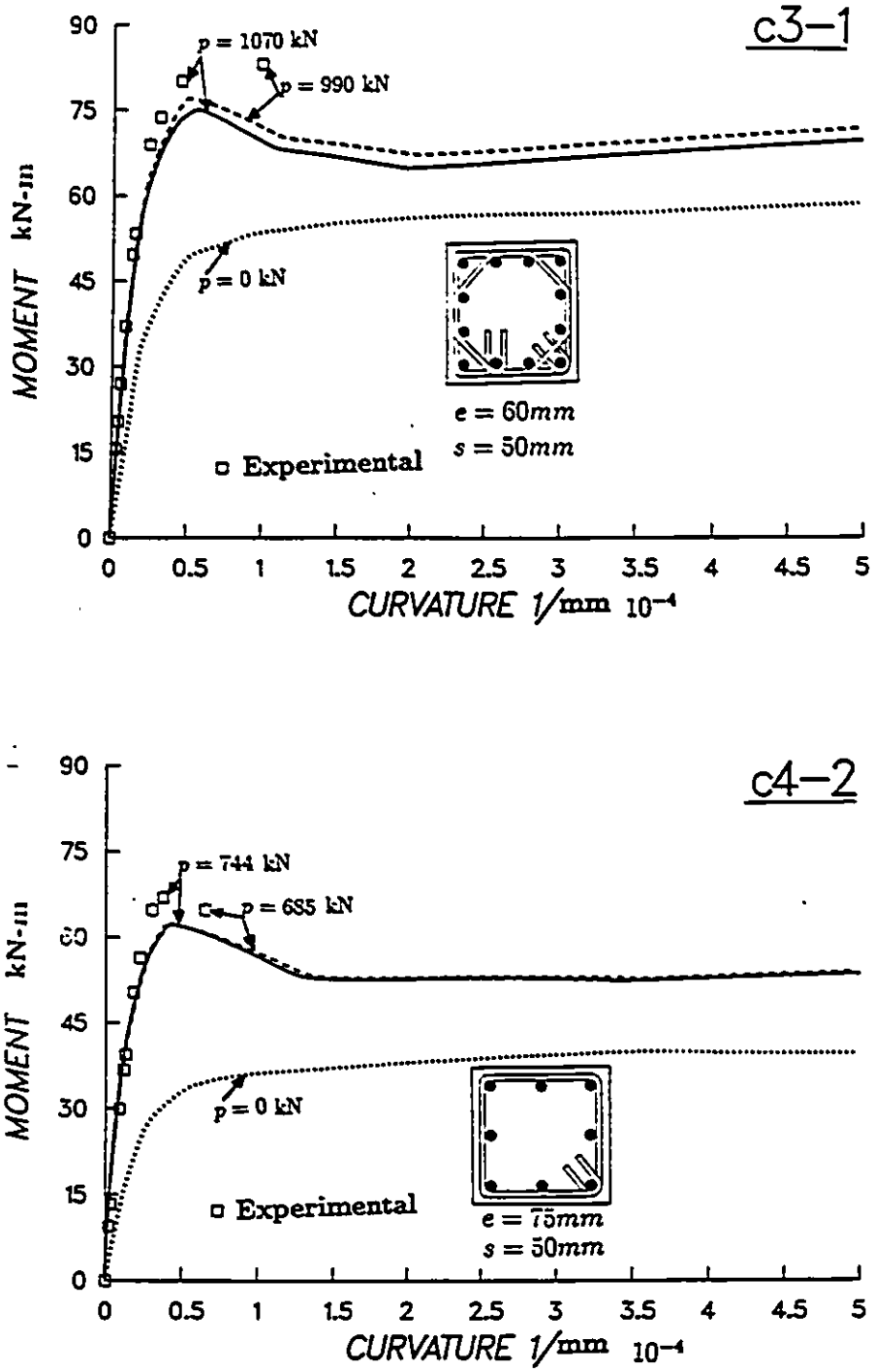

Figure C.5 : Moment-Curvature Relationship for Constant Load , Sheikh and Yeh [25]

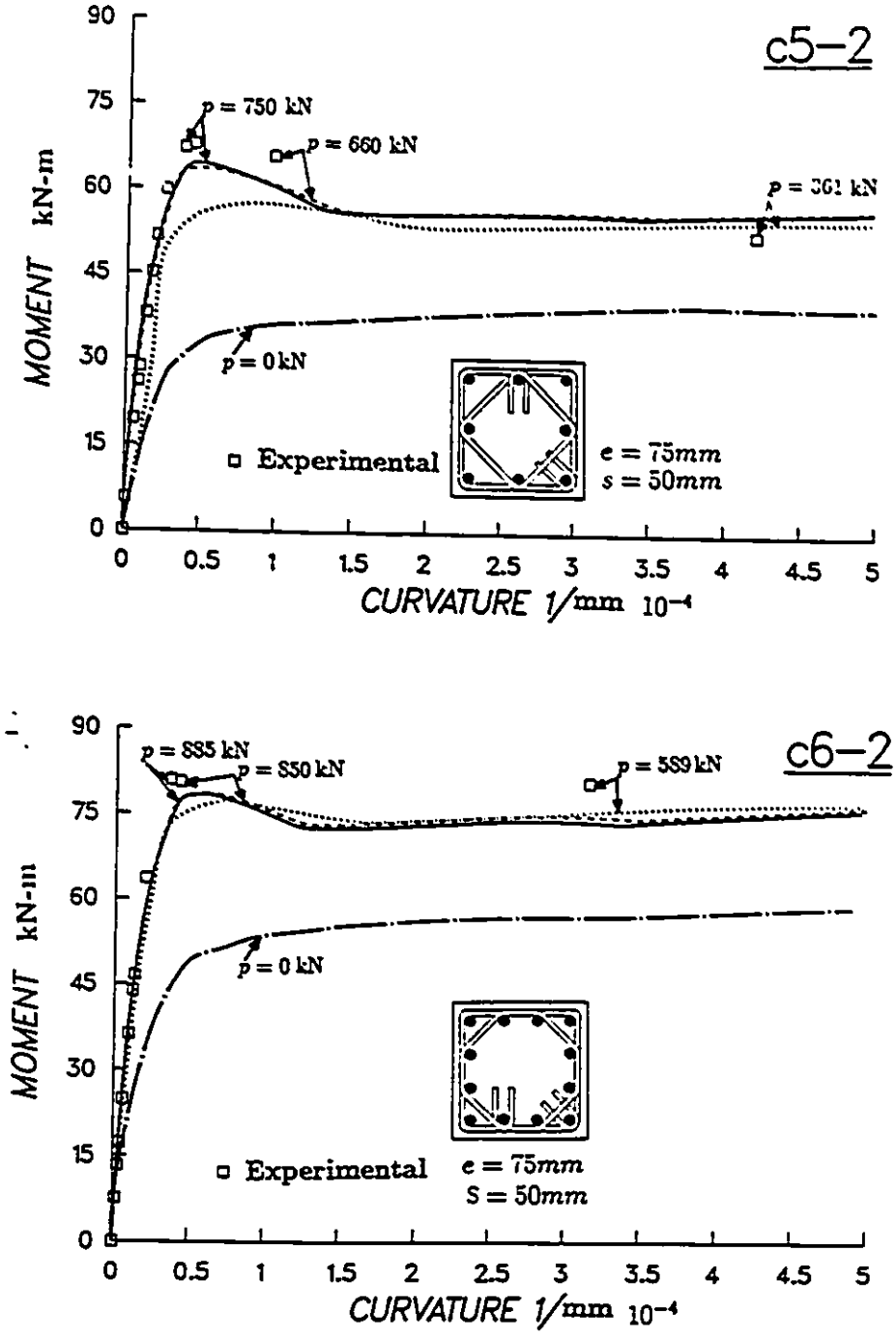

Figure C.6 :Moment-Curvature Relationship for Constant Load , Sheikh and Yeh [25]

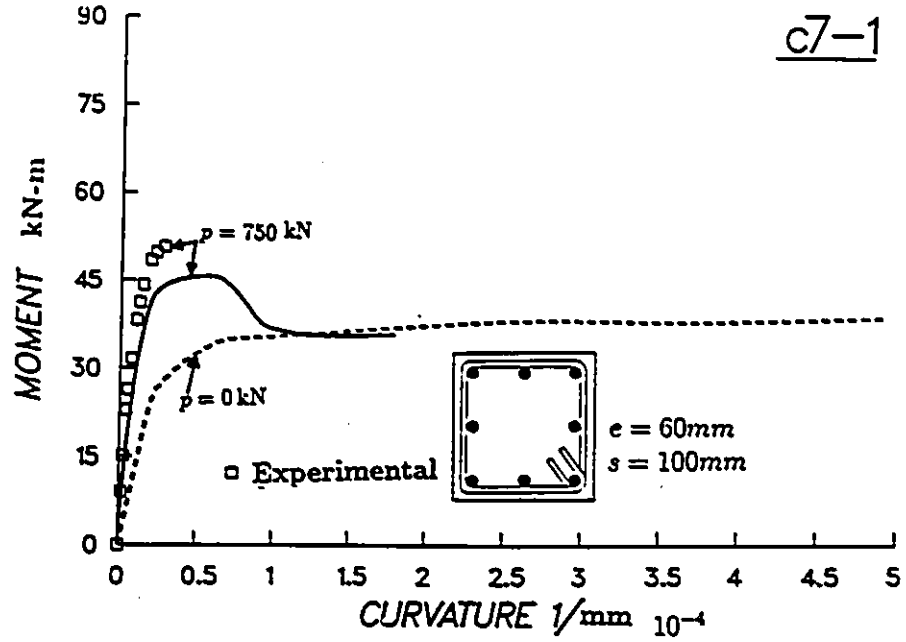

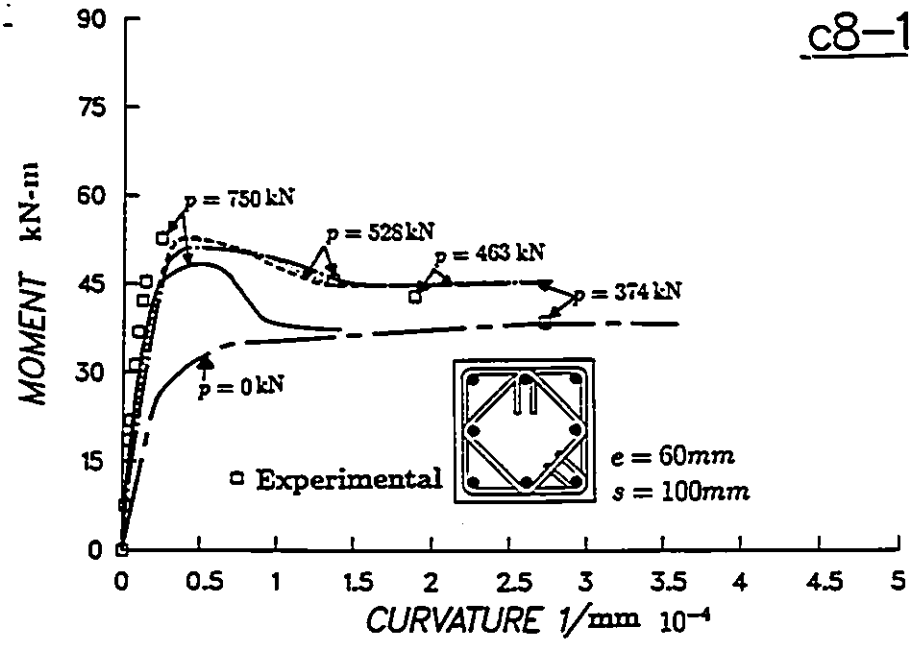

Figure C-7 :Moment-Curvature Relationship for Constant Load , Sheikh and Yeh [25]

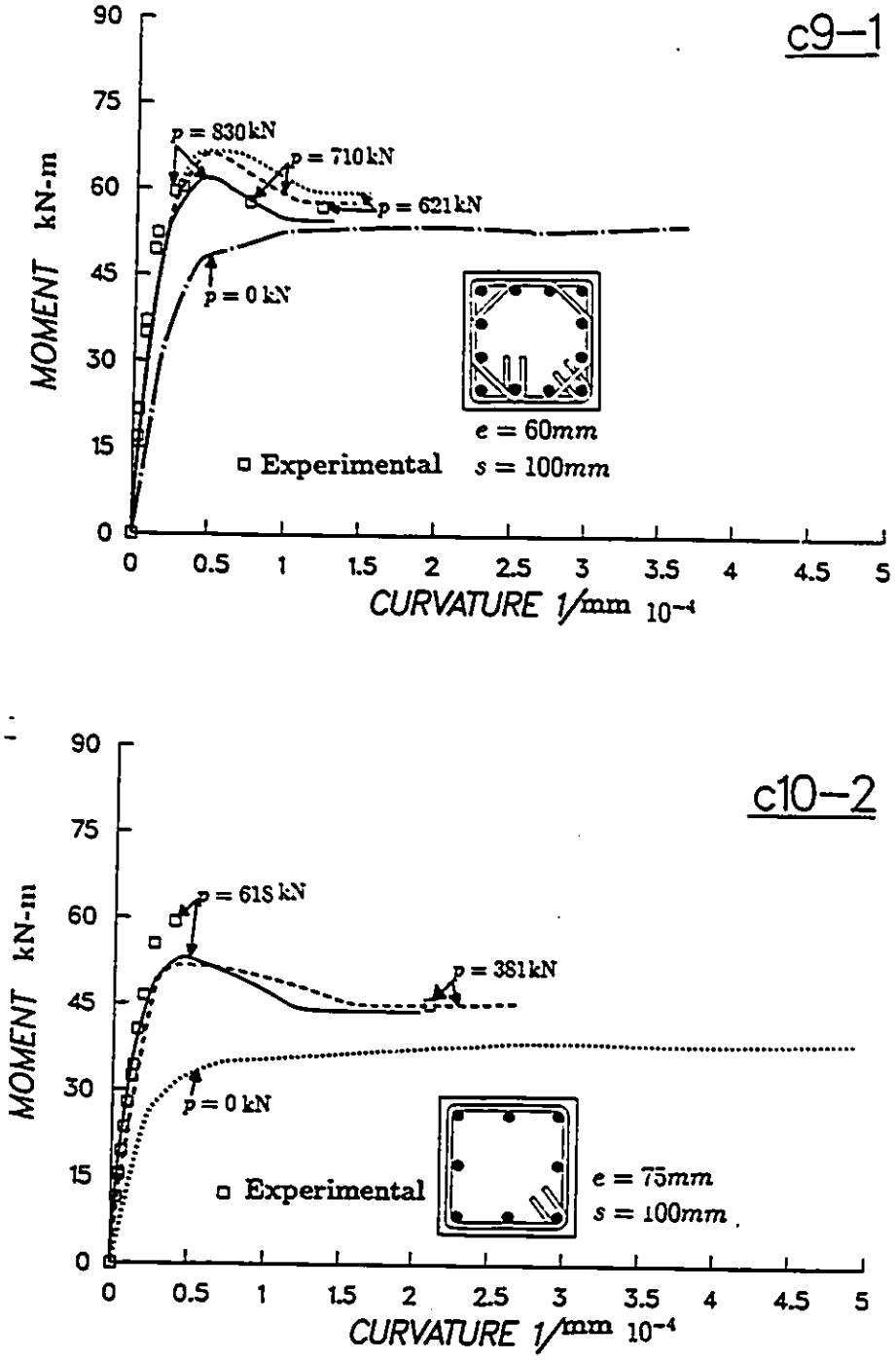

Figure C.8 :Moment-Curvature Relationship for Constant Load , Sheikh and Yeh [25]

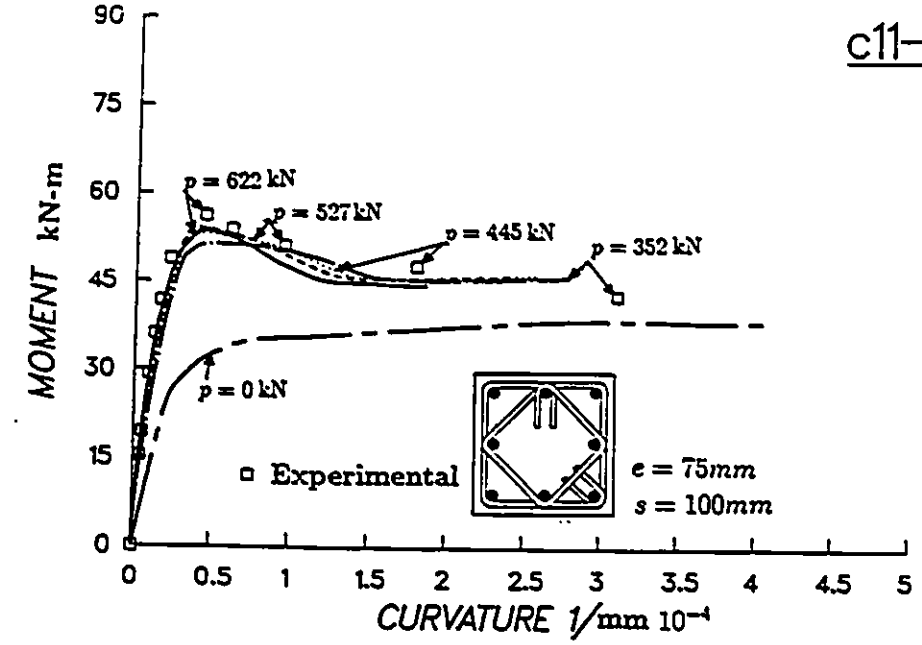

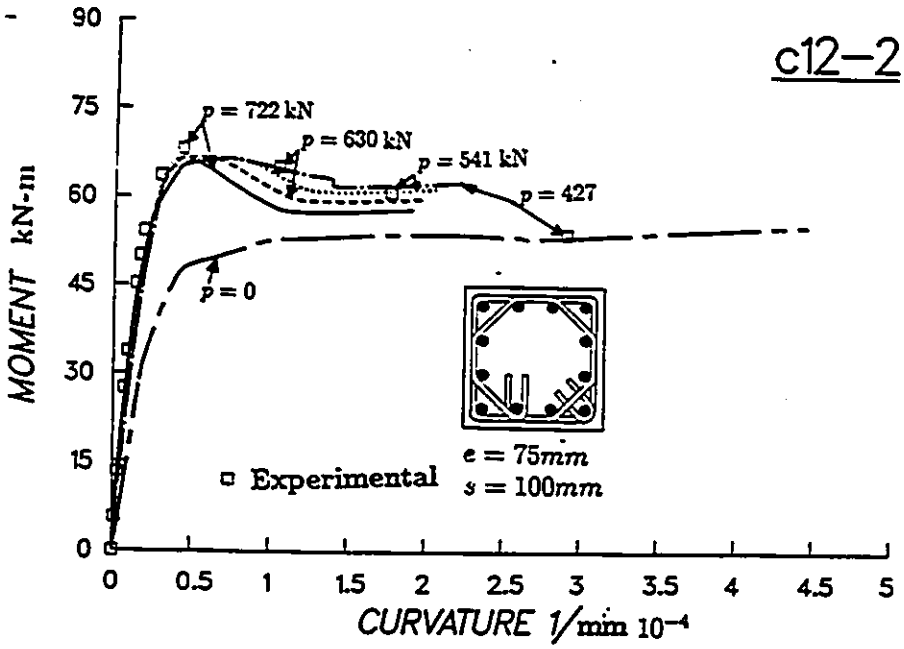

Figure C.9 :Moment-Curvature Relationship for Constant Load , Sheikh and Yeh [25]

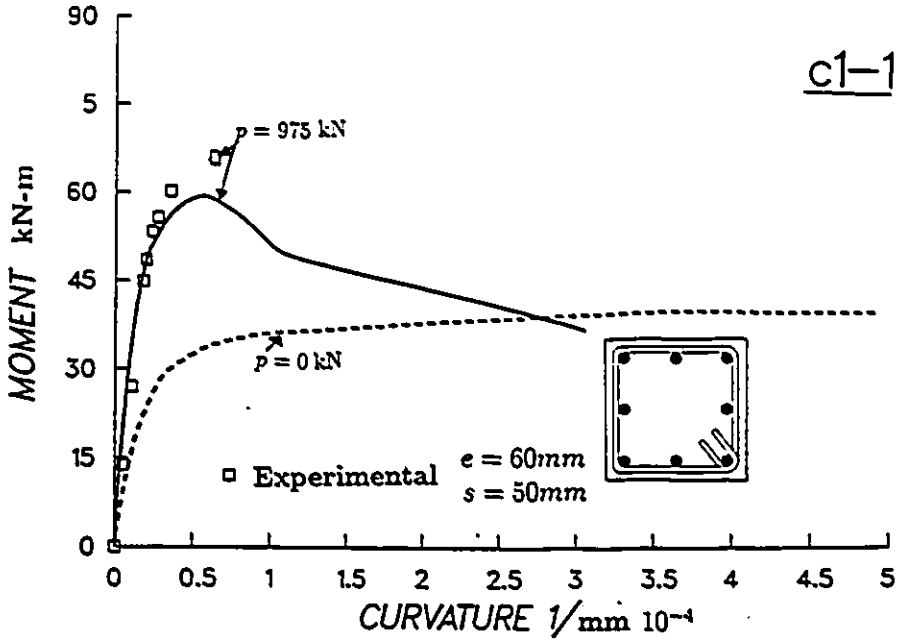

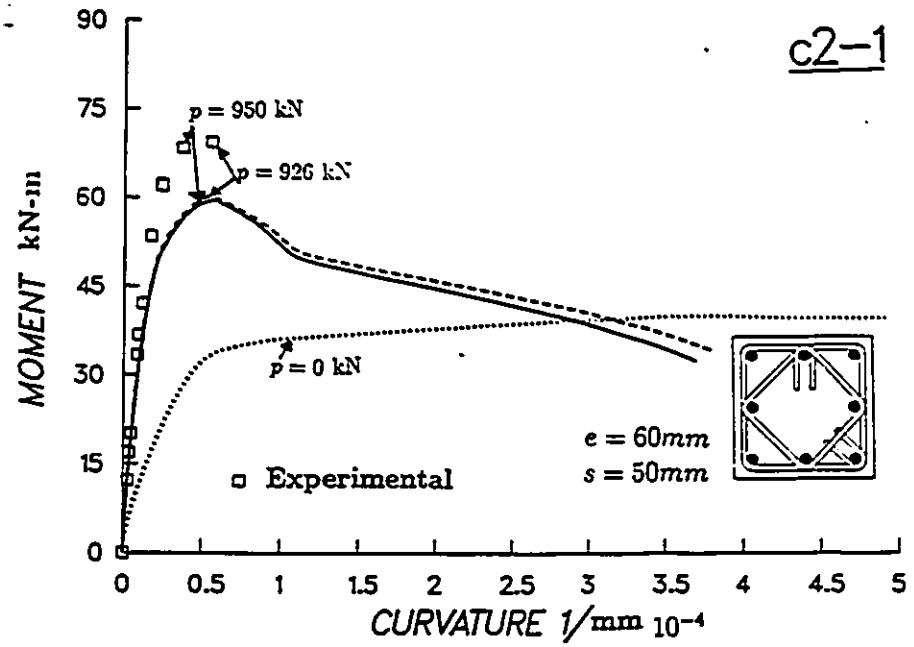

Figure C.10:Moment-Curvature Relationship for Constant Load , Saatcioglu and Razvi [19]

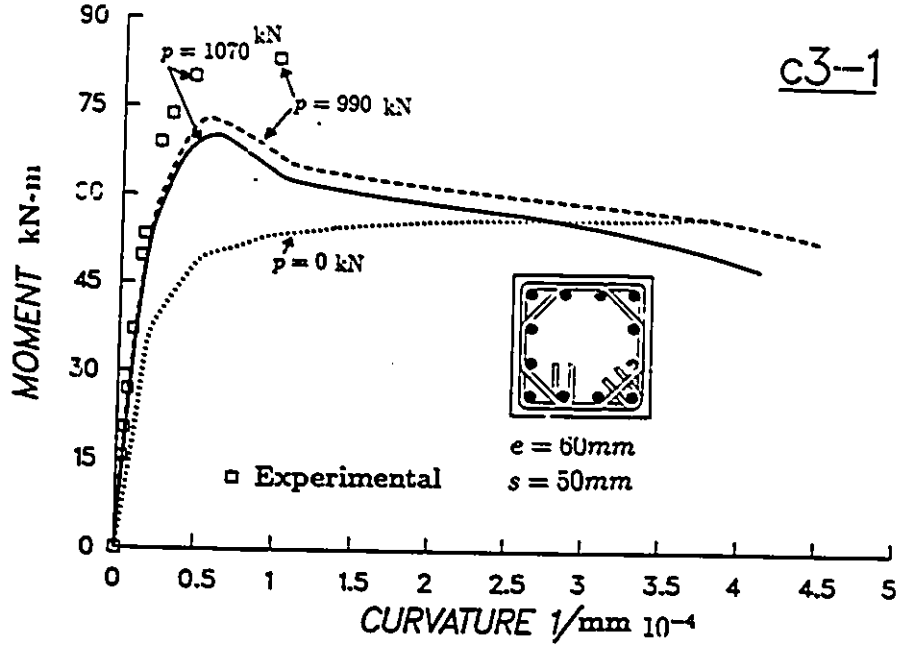

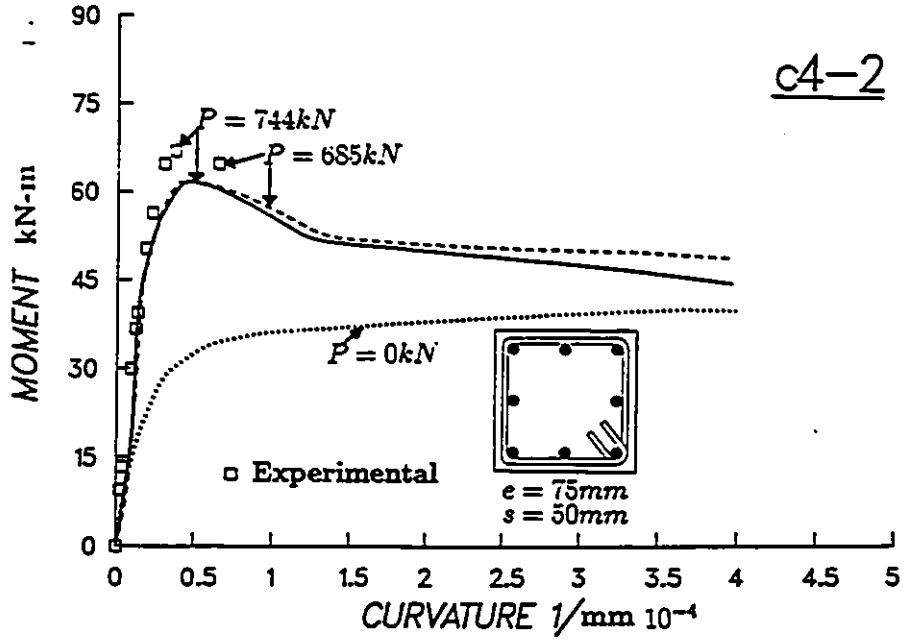

Figure C.11: Moment-Curvature Relationship for Constant Load , Saatcioglu and Razvi [19]

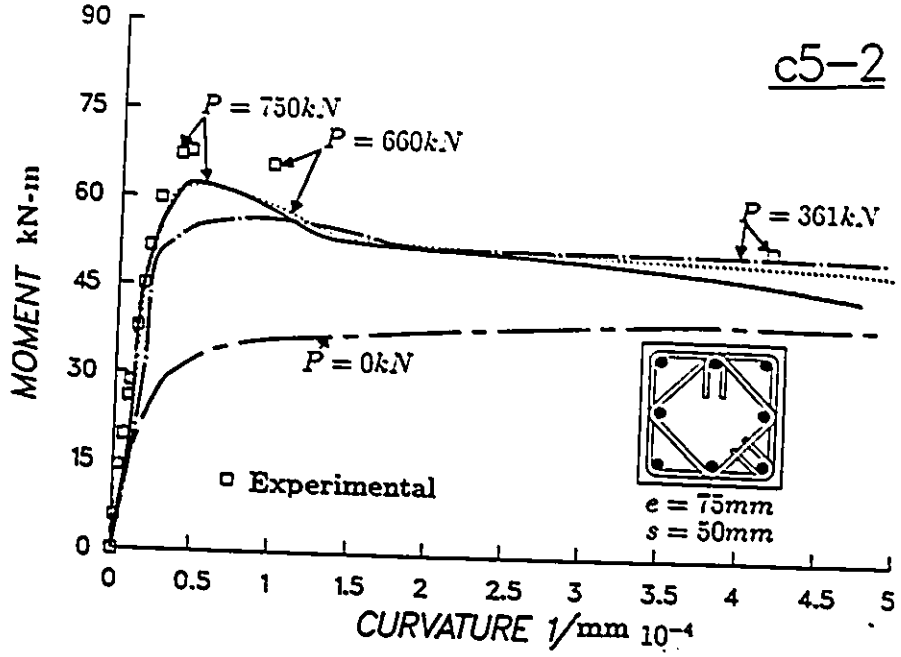

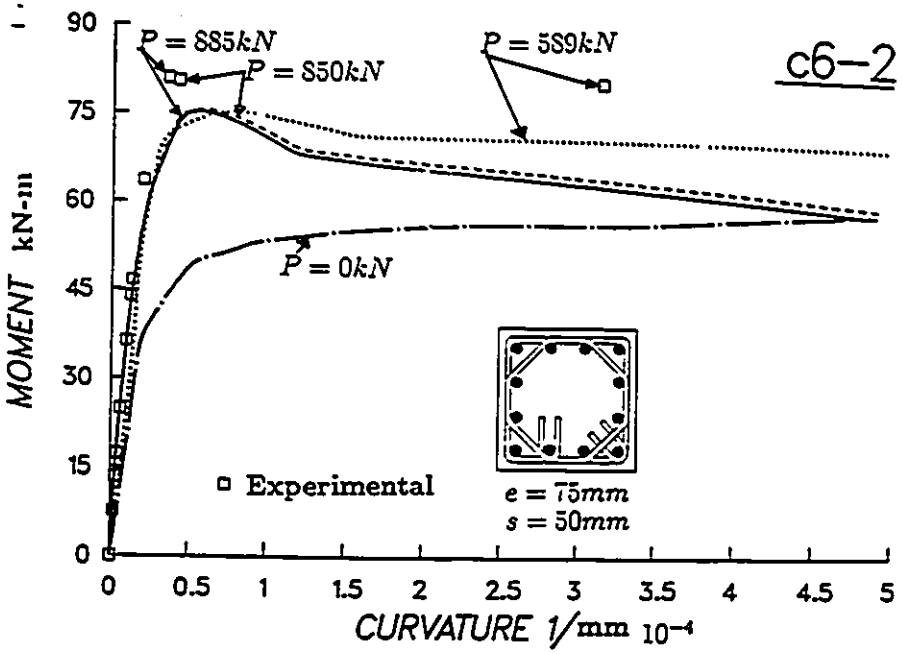

FigureC.12:Moment-Curvature Relationship for Constant Load , Saatcioglu and Razvi [19]

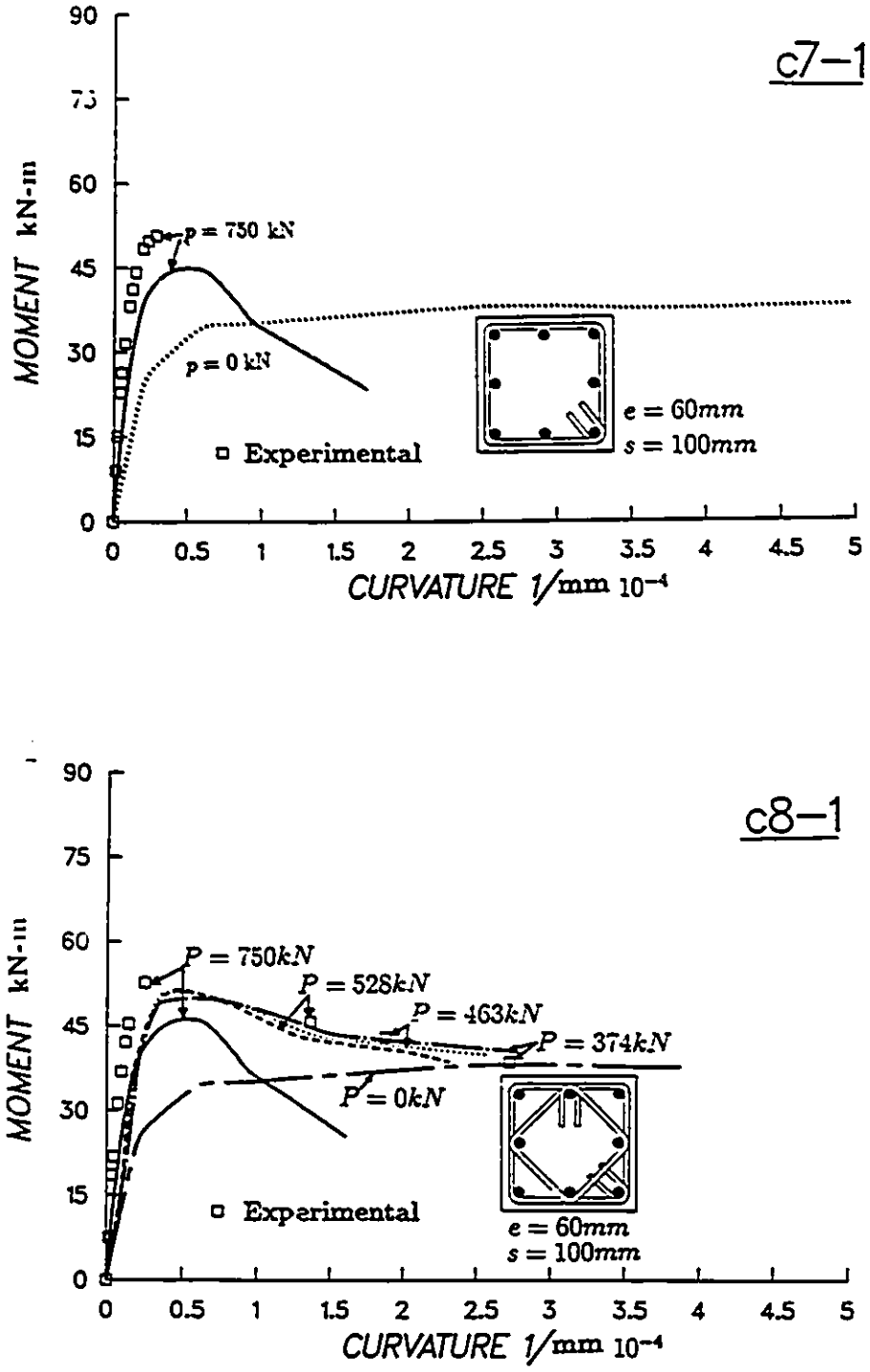

FigureC 13:Moment-Curvature Relationship for Constant Load , Saatcioglu and Razvi [19]

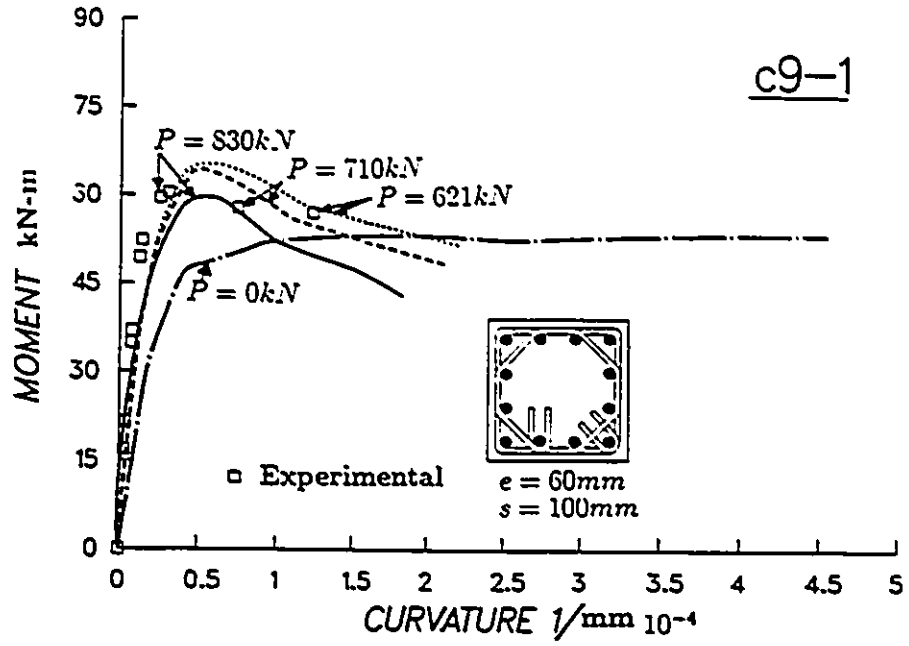

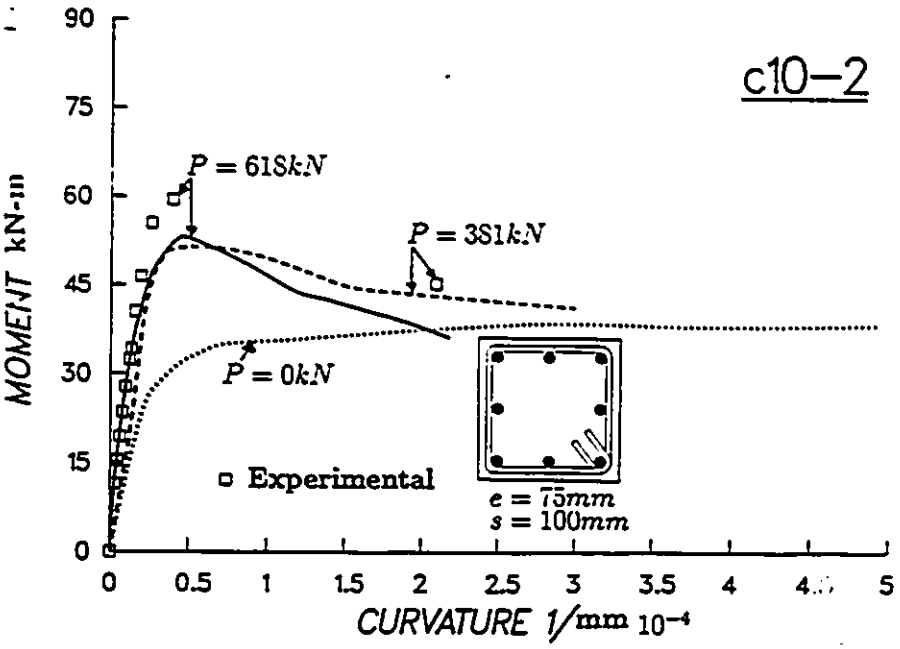

Figure C.14:Moment-Curvature Relationship for Constant Load , Saatcioglu and Razvi [19]

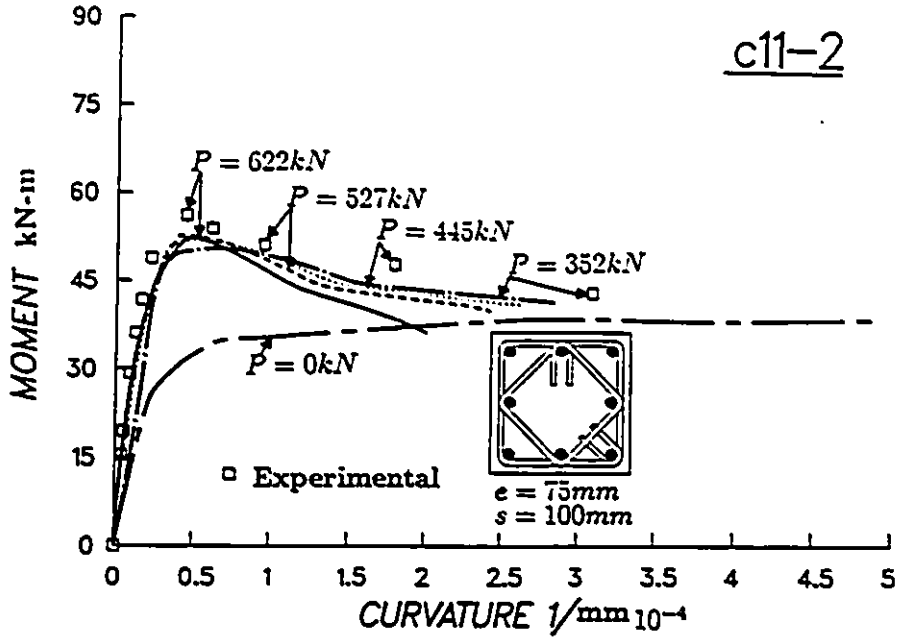

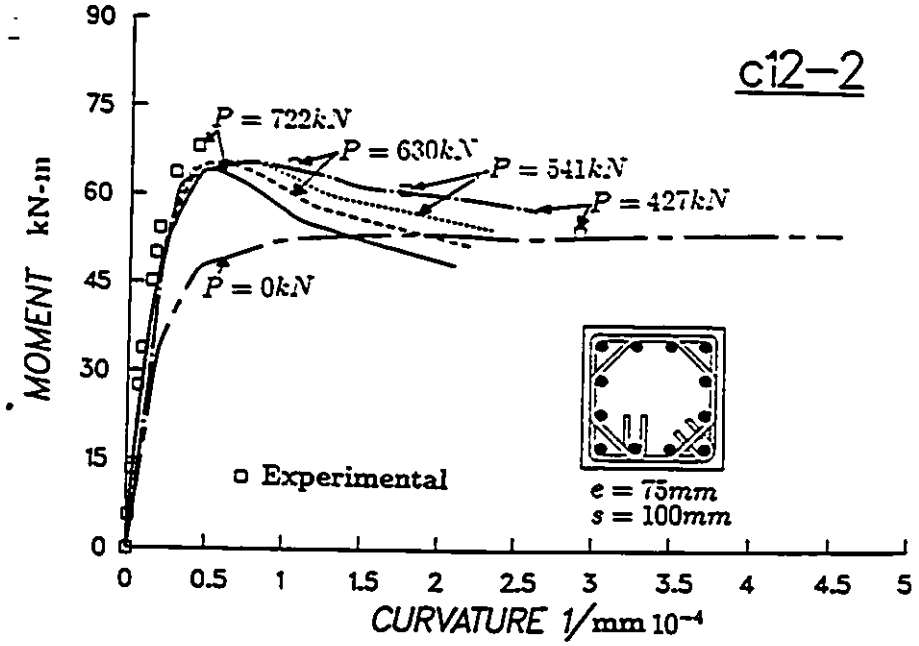

Figure C.15:Moment-Curvature Relationship for Constant Load , Saatcioglu and Razvi [19]